

DISSERTATION

DISSECTING SPECIFIC COMPONENTS OF THE OPIOID SYSTEM: FROM RECEPTOR
TO CIRCUIT

Submitted by

Marissa Joan Metz

Department of Biomedical Sciences

In partial fulfillment of the requirements

For the Degree of Doctor of Philosophy

Colorado State University

Fort Collins, Colorado

Fall 2021

Doctoral Committee:

Advisor: Shane T. Hentges

Michael M. Tamkun

Jozsef Vigh

Charles S. Henry

Copyright by Marissa Joan Metz 2021

All Rights Reserved

ABSTRACT

DISSECTING SPECIFIC COMPONENTS OF THE OPIOID SYSTEM: FROM RECEPTOR TO CIRCUIT

For thousands of years, humans have been using various forms of opioid drugs as analgesics, recreational drugs, and more. The power of these opioid drugs rests in the availability of opioid receptors expressed within the human brain and body. Opioid receptors sense opioid agonists and confer various actions in the cell through inhibitory g-proteins. One type of opioid receptor, the mu-opioid receptor (MOR), is especially important for sensing both currently used analgesic drugs and opioids of abuse. Thus the MOR is of focus in the following chapters. Understanding particular signaling states of MORs is important because each function of the MOR corresponds to specific cellular and behavioral effects. In Chapter 2, an attempt was made to better observe MOR activities through direct observation of mobility states within the cell membrane. Experiments were performed to examine if specific mobility states of the MOR within the cell membrane correspond to specific functional states of the MOR. Particular mobility states did not always correspond to single functional states, but the variation in mobility states observed at baseline hinted at the potential for a rich variety of functional states before agonist was applied. Therefore, the experiments in Chapter 3 investigated if the functional state of MORs could be shifted towards more active, or sensitized receptors. Using a clinically relevant antagonist treatment, low dose naltrexone (LDN), the response of MORs to subsequent agonist treatment was tested using electrophysiology and found to be no different from MOR responses in cells from animals not treated with LDN. Further, the activity of cells producing

endogenous opioids in the brain, proopiomelanocortin (POMC) neurons, was investigated to understand if LDN could alter endogenous opioid systems. This was not the case, however, and LDN actions appeared to be independent of enhancement of MOR activity or endorphin production from POMC neurons in the brain. Therefore, Chapter 4 focused on how the circuitry of POMC neurons is set up to handle many different functions. Dual retrograde tracing was used to examine whether individual POMC neurons project to more than one location, with the expectation that POMC neurons might form subpopulations based on the region they project to. This hypothesis was largely supported, as very few individual POMC neurons projected to more than one of the examined target regions. These findings help in understanding the organization of neurons that make β -endorphin and other peptides. Overall, the work presented in this dissertation reveals the complexity and heterogeneity of the opioid system from receptor to circuit. While the application of LDN does not appear to affect this complex system within POMC neurons, the circuitry of POMC neurons themselves lends promise to manipulating opioid processes with more precision in the future.

ACKNOWLEDGEMENTS

Shane—This journey for me has run the gamut from being a frozen, shy young pup of a graduate student to a mouthy but more confident academic, and you have been able to pick out the good parts of me in between all of that. I have always known you would have my back and that you believed I could do this, and you have kept me going through the triumphs and the lows. Thank you for showing me the joy of being an academic scientist.

Mike, Bob, Chuck, and Jozsef—As science goes, the path of my dissertation work did not always go as planned but thank you for offering your support and guidance through the years, despite the twists and turns.

Connie—Without you, I would still be in the basement on the confocal for another two years. I am so grateful for your scientific help, and I also look up to you as a model of class and staying in touch with the art of life and joy outside of work. Thank you for all of your gifts.

Andrew—Your consistent, high quality work coupled with the fact that you also are an incredibly interesting and fun person to be around is a credit to you not only as an academic but as a genuinely wonderful human. Thanks the inspiration and also for always knowing what to say to keep me moving forward.

Caitlin—Any dark times of my PhD journey have been brightened by the fact that I have made you as a friend. I am so grateful for the late-night texts, the junk food rewards, and every single cat picture. I will value your friendship for the rest of my life.

Matt—You, more than anyone, had a front row seat to my growth, including the good and the ugly parts. Somehow, you always dig out and reveal the best parts of me, even when you are exhausted yourself. I am so grateful for your love and support. Also, thank you for bringing AJ into my life, without whom 2020 and beyond would have been so much lonelier. You are the best teammate ever.

Mom, Dad, and Anita—Half of the time I am sure you had no idea what was going on, but you have been proud of me all the same. Thank you for your unwavering support, for reminding me of my roots, and for always being proud of me.

TABLE OF CONTENTS

ABSTRACT.....	ii
ACKNOWLEDGEMENTS.....	iv
CHAPTER 1—INTRODUCTION.....	1
Opioid types and their history.....	1
Pathways of action in the body.....	2
Opioid receptors.....	2
Analgesia.....	7
Reward.....	10
Side effects.....	12
Dissertation scope.....	13
References.....	13
CHAPTER 2—DIRECT MONITORING OF MOR ACTIVITY STATES USING SINGLE PARTICLE TRACKING.....	18
Preamble.....	18
Background.....	18
Signaling processes of the MOR.....	18
Measures of MOR activity.....	18
Single particle tracking for direct study of individual MORs.....	20
Published work.....	20
Summary.....	20
Introduction.....	21
Results.....	25
Discussion.....	41
Materials and Methods.....	45
References.....	49
Acknowledgments.....	53
CHAPTER 3—MODULATION OF ENDOGENOUS ENDORPHIN SYSTEMS USING LOW DOSE NALTREXONE.....	54
Preamble.....	54
Background.....	54
Potential for sensitization of the MOR by low dose naltrexone.....	54
Published Work.....	55
Summary.....	55
Significance Statement.....	56
Introduction.....	57
Methods.....	58
Results.....	65
Discussion.....	77
References.....	80
CHAPTER 4—EXPLORING THE ORGANIZATION OF THE ENDOGENOUS β - ENDORPHIN SYSTEM.....	85
Preamble.....	85

Background	85
Submitted Work	86
Summary.....	86
Introduction	87
Methods	88
Results	94
Discussion.....	103
References	106
CHAPTER 5—CONCLUSION	110
Exogenous versus endogenous opioid signaling.....	110
The many effects of opioid signaling.....	112
The future of opioid analgesics	114
References	117
APPENDIX.....	121

CHAPTER 1—INTRODUCTION

Opioid types and their history

Naturally-derived opioids, in the form of poppy (*Papaver somniferum*) heads, were one of the first active medications available to humans, and various formulations from the poppy plant have been used for thousands of years as analgesics, recreational drugs, and more. Medical texts from ancient Egypt reveal that the raw product of the poppy pod was being processed into more potent opium for a variety of ailments thousands of years ago. Both medical and recreational use of opium continued in the form of smoking, eating, and mixing with alcohol to drink until even more potent opioid forms were created (Booth, 1998; Rosso, 2010).

The first more potent opioid agonist discovered was morphine, a natural alkaloid of opium, which was first purified in the early 1800s in Germany by Freidrich Sertürner and quickly became a mainstay in every physician’s pharmacopeia. Morphine revolutionized pain medicine and saved lives, seeming nothing short of miraculous, given the abundance of nonfunctional placebos up until modern times. However, the reinforcing and respiratory depressive effects of opioids were also responsible for the loss of many lives. In the case of the United States Civil War, extremely casual use of morphine saved lives by combatting dysentery and relieving extreme pain, but the same soldiers whose lives were saved by morphine retired from their service with an opioid addiction, which was dubbed the “Soldier’s Disease” because of its prevalence (Booth, 1998; Quinones, 1975). The opioid-related problems of the 19th century were in part spawned from the economic boon granted by its illicit sale. Illegal smuggling of opium into China by the British East India Trading Company resulted in over 4 million people harboring a substance abuse disorder in 1836 (Downing, 1838). Despite China’s pleading and threatening, Britain refused to give up this source of revenue from farms they controlled in India,

so from 1839 – 1842 and again from 1856 – 1860, Great Britain and China fought two “opium wars”, both of which China lost (Booth, 1998). In the meantime, the invention of the hypodermic needle and discovery of more potent opioid formulations increased recreational use worldwide. Heroin, first synthesized in 1874, was discovered and used briefly as a painkiller and as a cure for respiratory ailments such as asthma but was quickly controlled after its potency was discovered (Manges, 1898, 1900). Heroin continues to be a common recreational drug that is injected directly into the circulatory system for recreational use.

Within the last century, even more potent formulations of synthetic opioids have provided utility to the medical field in cases of severe pain. Fentanyl, synthesized in late 1960, remains one of the most potent analgesics used in medical clinics today (Stanley et al., 2008). However, fentanyl is also the culprit for many opioid-related deaths, as heroin laced with fentanyl is extremely potent and dangerous in such an unregulated market as the drug trade. Overall, our relationship with potent opioid analgesics is a double-edged sword: opioid analgesics remain a mainstay in medical treatment of severe pain, and yet the United States lives within an opioid crisis in which thousands of overdose deaths every year (Mattson et al., 2021).

Pathways of action in the body

The widespread use and subsequent societal impact of opioids would not exist if opioids did not have the ability to affect the human brain and body so profoundly. These effects can be attributed to the existence of opioid receptors expressed throughout the brain and body that sense exogenously applied or endogenously released opioids.

Opioid receptors

Opioid receptors were discovered within the mammalian brain using competitive radioligand binding experiments and the labeled antagonist naloxone along with various opioid agonists

(Dhawan et al., 1996). Eventually, it was discovered that different types of opioids bind different types of opioid receptors. Tolerance assays within the dog spinal cord suggested that at least two different opioid receptors, the mu (MOR) and kappa (KOR) receptors, are responsive to two different types of opioids (Martin et al., 1976). A third type of opioid receptor, the delta (DOR) opioid receptor, was later identified by differential responses to opioid agonists in the guinea pig ileum and the mouse vas deferens (Lord et al., 1977). Decades of research went on to show that the expression of the MOR, KOR, and DOR is widespread throughout the brain and that each subtype is involved directly or indirectly in the processes of analgesia, reward, and mood modulation (Dhawan et al., 1996). However, most clinically available drugs today target the MOR, and the MOR is required for opioid-induced reward (Fig 1)(Le Merrer et al., 2009). Further, and especially relevant to chapters 3 and 4, the MOR is the only opioid receptor known to exist somatically on hypothalamic cells that produce the endogenous opioid β -endorphin for the brain (Pennock & Hentges, 2011). Therefore, the following work will focus mainly on the actions of MORs.

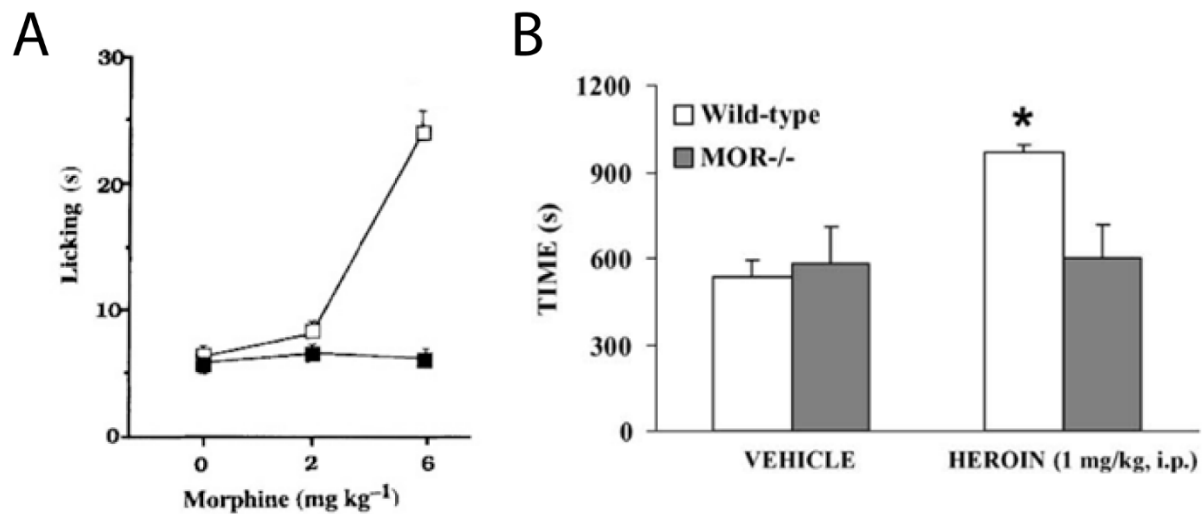


Figure 1. The MOR is targeted by currently used analgesic and recreational drugs. A) Morphine increases latency to paw lick in response to hot plate exposure in wild type mice.

(white squares) Latency to lick is abolished by MOR KO (MOR KO mice, black squares). Adapted by permission from Springer Nature: Nature (Matthes et al., 1996). B) Conditioned place preference for heroin is abolished in MOR KO mice, seen by a decrease in time spent in the paired side compared to wild type mice. Reprinted from *European Journal of Pharmacology*, Vol 446, Contarino et al., Lack of reward and locomotor stimulation induced by heroin in μ -opioid receptor-deficient mice, 103-109, Copyright 2002, with permission from Elsevier (Contarino et al., 2002).

All opioid receptors, including the MOR, are g-protein coupled receptors (GPCRs) coupled to inhibitory, or G α i, g-proteins. GPCRs are a large family of seven-transmembrane receptors that sense ligands in the extracellular environment and interact with many different intracellular partners to confer a wide breadth of effects within the cell (Prazeres & Martins, 2015). The ability of one receptor to couple with multiple intracellular partners allows for GPCRs to amplify their signal and to confer nuanced information about the extracellular environment beyond a simple yes/no ligand response (Keshelava et al., 2018). Coupling to these intracellular partners by the MOR begins when the MOR is bound by an agonist – such as β -endorphin or the opioid morphine – on its extracellular side and undergoes a conformational change on its intracellular side that allows for exchange of GDP for GTP on the G α i subunit bound to the MOR's C-terminal tail. This activates the α subunit and separates it from the β and γ subunits of the g-protein while remaining membrane-bound (Prazeres & Martins, 2015; Smrcka, 2008). The α subunit then inhibits the production of the second messenger cAMP by adenylyl cyclase, and the subsequent decrease in cAMP levels results in changes to transcription and protein activity throughout the cell (Huang et al., 1999). The β and γ subunits of the G α i complex typically signal within neurons as a heterodimer to inhibit calcium channels, activate potassium channels, and inhibit presynaptic release of neurotransmitter (Smrcka, 2008). Overall, these interactions of the MOR and its respective G α i complex work to dampen neuronal activity over the course of seconds to a few minutes after agonist administration (Fig 2).

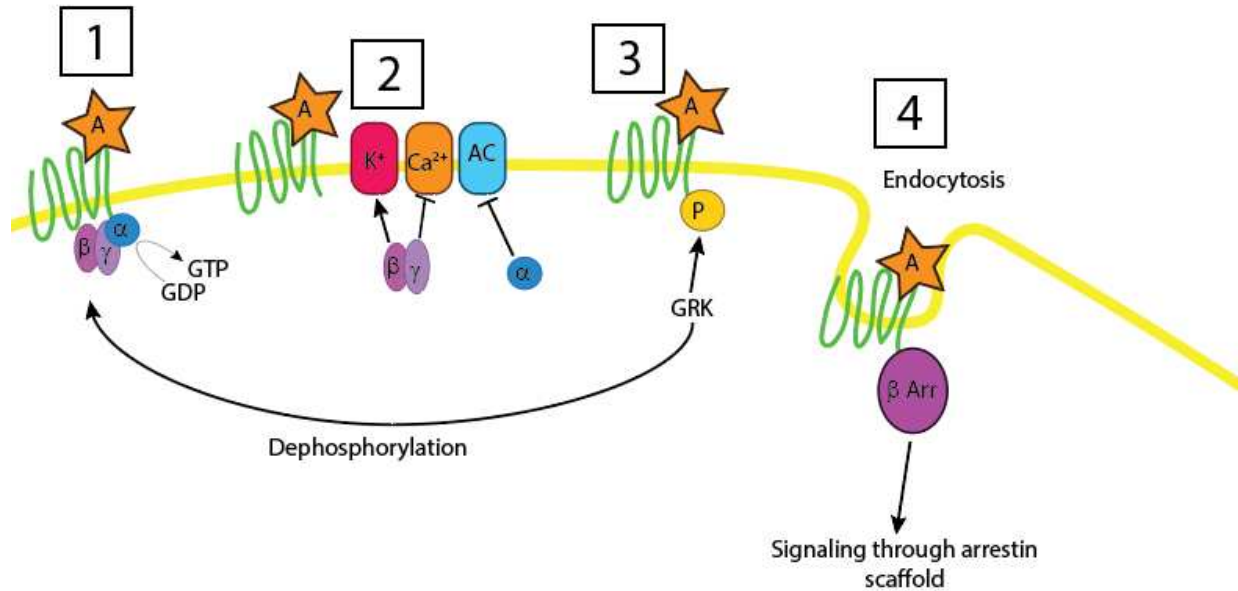


Figure 2. MOR signaling. MOR signaling begins with binding of an opioid agonist (A). 1) An exchange of GDP for GTP on the corresponding $G_i\alpha$ protein (α) releases the G_i complex from the receptor (α, β, γ). 2) The $G_i\alpha$ protein inhibits the activity of adenylyl cyclase (AC) to inhibit production of cyclic AMP, and the β and γ subunits inhibit Ca^{2+} channels and activate K^+ channels, allowing for outflow of K^+ . 3) Eventually, g-protein coupled receptor kinases (GRKs) phosphorylate (P) the MOR, which allows β -Arrestin (β -Arr) to bind and recruit MORs for endocytosis (4).

The acute activity induced by agonist binding to the MOR does not continue indefinitely even as opioids remain onboard. In fact, the initial conformational change induced by agonist binding renders the MOR vulnerable to signal termination. Activation of the MOR and subsequent uncoupling of G_i from the receptor exposes the C-terminal tail of the MOR to the cytosol. This provides access to the C-terminal by g-protein coupled receptor kinases, which phosphorylate the C-terminus and block the ability of the MOR to further interact with g-proteins. This inability to signal through g-proteins despite continued presence of agonist is called desensitization, which can be observed within cells within 5-10 minutes of agonist application (Williams et al., 2013).

Even acute desensitization may not be the end of MOR-induced intracellular changes, however. The phosphorylated C-terminus is recognized by the scaffolding protein β -arrestin, which binds to the MOR and recruits it to clathrin coated pits for internalization. After internalization, some signaling may continue, as numerous imaging and protein interaction studies show that MORs can signal from endosomes and the golgi apparatus (Eichel & von Zastrow, 2018). In recent years β -arrestin has also been shown to alter cellular signaling from the plasma membrane by encouraging the formation of signalosomes and kinase activation upon recruitment to GPCRs (Jean-Charles et al., 2017). Finally, dynamic and relatively weak binding of β -arrestin to the MOR can also allow for dephosphorylation of the C-terminal tail via phosphatases and subsequent resensitization, allowing for the MOR to regain its previous signaling ability (Arttamangkul et al., 2006).

The above described signaling states of the MOR contribute to overall behavioral effects of opioids in different ways. For example, acute desensitization appears to be a prerequisite for tolerance to opioids, or the need to administer higher doses in order to achieve the same effect. Transgenic mice harboring mutations in the C-terminal tail of the MOR (which renders the receptor resistant to desensitization and unable to bind β -arrestin) show a lack of tolerance, which is defined as the need to administer increasing doses of a drug to get the same effect (Kliwer et al., 2019). β -arrestin knockout (KO) studies confirm that the processes of acute desensitization and subsequent β -arrestin binding appear to be important for the development of behavioral tolerance (Bohn et al., 2002). G-protein signaling itself may also contribute to less desirable behavioral manifestations of chronic opioid use. Prolonged signaling of the MOR results in a resurgence of cAMP production, which ultimately induces enhanced neuronal excitability that exists in several brain regions upon cessation of continued MOR agonist

administration (Fry et al., 1980; Ingram et al., 1998; Johnson & Duggan, 1981; Russell et al., 1995). This increase in neuronal excitability contributes to paradoxical hyperalgesia, or heightened pain response, after chronic opioid use. Further, cAMP buildup contributes to withdrawal symptoms after cessation of prolonged opioid use, as KO of various portions of the AC-cAMP-PKA-CREB pathway decrease neuronal overexcitation and various withdrawal symptoms in rodents after cessation of prolonged morphine administration (Corder et al., 2013).

It is clear that specific signaling states of the MOR are important to the development of cellular and behavioral effects induced by opioids. Therefore, better understanding of MOR signaling states, as explored in chapter 2, could help contribute to better understanding of opioid effects on the brain in the future. The main effects of opioids on the brain and body are described below.

Analgesia

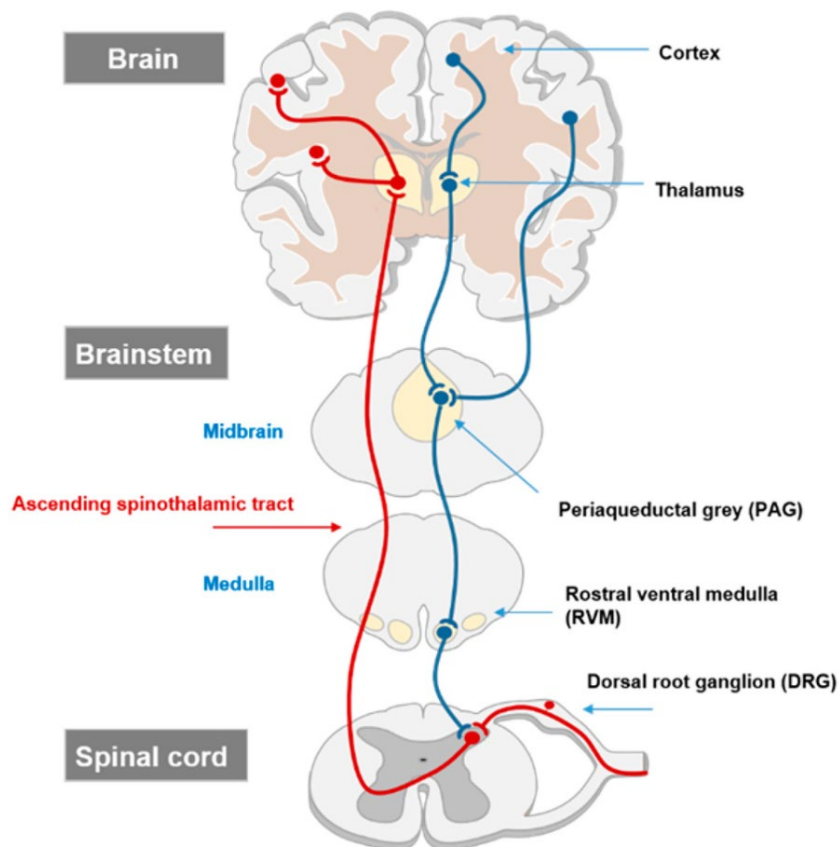


Figure 3. Ascending and descending pain pathways. Primary nociceptors send ascending pain signals up to the somatosensory cortex by passing through the dorsal horn, brainstem, and thalamus. Ascending inhibition of the pain signal occurs through converging inputs onto the PAG when then projects to the RVM. Projections from the RVM to the dorsal horn act to inhibit the sensation of pain. Adapted with permission from (Cioffi, 2018). Copyright 2018 American Chemical Society.

In modern times, the legal use of exogenous opioids is largely for analgesia, or pain relief.

Analgesic effects conferred by opioids are due to MOR-induced inhibition of pain-related signals in the brain and spinal cord. In the spinal cord, opioid-induced inhibition is due to the presynaptic expression of the MOR on A δ and C-type primary nociceptors and well as on the soma of neurons within the dorsal horn (Heinke et al., 2011). In a normally functioning system, the perception of pain occurs when potentially damaging stimuli (heat, cold, or mechanical) activates the primary nociceptors, so that they send a signal to neurons in the dorsal horn. Dorsal horn neurons then send afferents up the spinal cord and signal to regions in the brainstem, thalamus, and primary somatosensory cortex (Fig 3). When exogenous opioids are applied, or when endogenous opioids are released from the pituitary, opioids bind to MORs and inhibit the transmission of the pain signal within the dorsal horn, preventing the signal from reaching the brain (Garland, 2012).

MOR expression is also widespread within the brain itself, and several nuclei that express MORs are responsible for the top-down inhibition of pain (Fig 4). One of the major regions for top-down inhibition of pain is the periaqueductal gray (PAG), especially its ventrolateral portion. Upon painful stimulation, various cortical and subcortical brain regions converge onto the PAG. One of these converging regions contains the proopiomelanocortin (POMC) neurons of the hypothalamus that produce the endogenous opioid β -endorphin. POMC neurons are activated and release β -endorphin into the PAG, activating MORs and inhibiting neurons within this area.

Some question remains as to how the PAG next signals to its downstream partner the rostral ventral medulla (RVM). Disinhibition of GABAergic interneurons likely plays a role in activating RVM-projecting PAG neurons, but both inhibitory and excitatory signals from the PAG converge on to RVM. Therefore, top-down signaling from the PAG to the RVM is complex and still under active investigation. Ultimately, however, RVM neurons project down to the dorsal horn of the spinal cord to modulate the pain signal in the periphery (Bagley & Ingram, 2020).

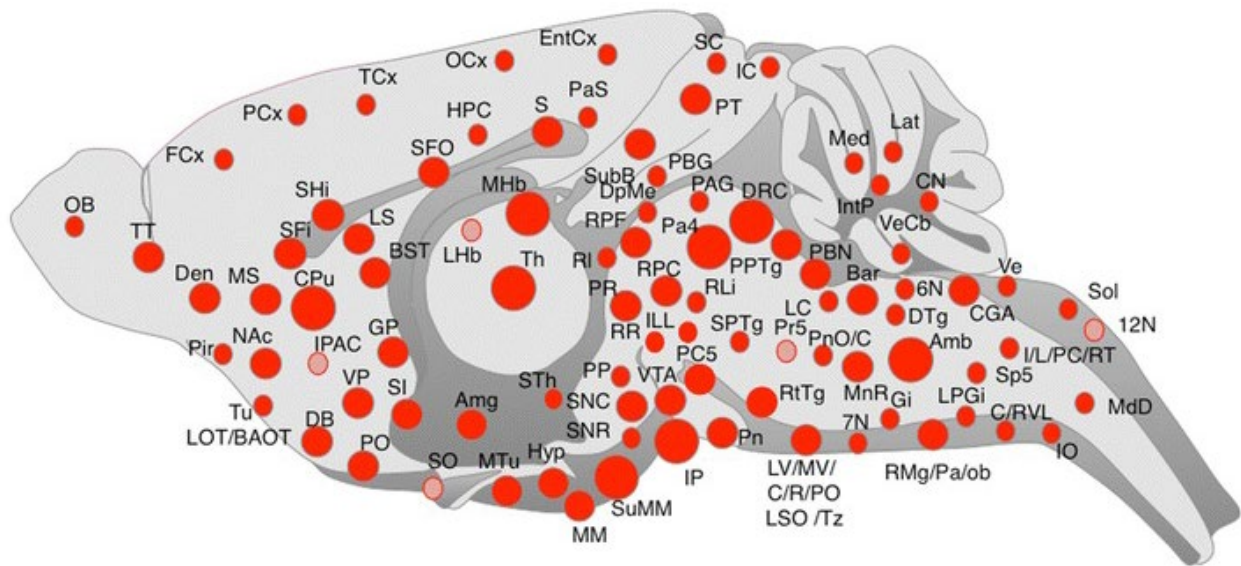


Figure 4. Opioid receptor expression is extremely widespread throughout the brain. The widespread pattern of opioid receptors accounts for the many functions conferred by the application of exogenous opioids. Red circles represent MOR expression in the rodent brain. Larger size corresponds to higher expression within a region, and light red circles have very low expression. MORs can be observed in regions relevant to Chapter 1 in the PAG, cortex, VTA, NAcc, and brainstem. Adapted with permission (Erbs et al., 2015).

The pain signal initiated at the primary nociceptors is reciprocally modulated by regions in the brain involved with motivational and emotional processing. Emotional and attentional centers of the brain provide inputs to state-dependently affect pain perception and evaluation. For example, it is known that inducing negative emotion using unpleasant odors can intensify the experience of pain, even though subjective pain measures remain the same. On the contrary, heightened

autonomic activation through stress can actually diminish feelings of pain, such as when soldiers from the battlefield do not report pain though objective measures indicate nociceptive responses (Porreca & Navratilova, 2017). In the context of opioid use, the expectation of pain relief also dramatically influences self-reported pain measures, with greater expected relief in response to drug correlated with more diminished feelings of pain (Wiech & Tracey, 2009). Several brain regions interact to contribute to this pain response, but the anterior cingulate cortex (ACC) is especially important for contributing to emotional components of pain. Lesion studies in the ACC show that this region is important for pain-induced aversion. For example, excitotoxin-induced lesion of the rostral ACC abolished conditioned place aversion for formalin injection in the rat hind paw. (Johansen et al., 2001) The ACC also houses MORs, and addition of exogenous opioids or induction of endogenous opioid release inhibits this region, thus inhibiting aversive feelings associated with pain. Along with a decrease in aversive feelings, the relief of pain also appears to induce feelings of reward shown by a combination of subjective measures and fMRI imaging data which reveal increases in activity of reward-related brain regions during self-reported relief of pain (Porreca & Navratilova, 2017). These effects are likely due to direct activation of MORs within reward-related systems of the brain.

Reward

Seminal experiments by Olds and Milner (Olds & Milner, 1954) showed that electrical stimulation of certain parts of the brain cause approach behavior and positive reinforcement in rats. Further studies showed that dopamine appears to be a key player in the reward system, and that the VTA and substantia nigra (SN) were the most abundant sources in the brain for this neurotransmitter (Lammel et al., 2014). Later studies revealed that VTA dopamine signaling was not as much responsible for the feeling of reward, but rather the motivation and salience (or

prominence) of reward. The nucleus accumbens (NAcc) was shown to receive heavy input from dopaminergic VTA neurons and is now known to be important for the action related to reward salience signals received from the VTA and other locations. The VTA-NAcc circuit has received the most attention due to its integral role in the development of drug abuse, but other regions have been implicated in the modulation of reward and aversion, including the habenula, serotonergic systems of the raphe nucleus, the amygdala, the cortex, and the hypothalamus (Hu, 2016).

The MOR is heavily expressed in reward-related regions of the brain, and chronic opioid use can substantially alter MOR expression patterns and reward-related circuit interactions. Expression of MORs in the NAcc and intracerebral injection studies of opioid agonists into this region show that opioid signaling here is involved in feelings of “liking” a reward (Fig 5). In the VTA, MORs are largely expressed on GABAergic interneurons, and thus addition of MOR agonists disinhibits dopamine signaling. Endogenous opioids themselves also play a role in reward, as acquisition of dependence to certain drugs of abuse requires β -endorphin (Le Merrer et al., 2009). Drugs of abuse are known to alter expression patterns of the MOR as well as release of β -endorphin, and chronic drug use dysregulates the reward system, perpetuating processes of dependence (Darcq

& Kieffer, 2018; De Waele & Gianoulakis, 1994; Gianoulakis et al., 1981; Van Bockstaele et al., 2006; Zhang et al., 2018).

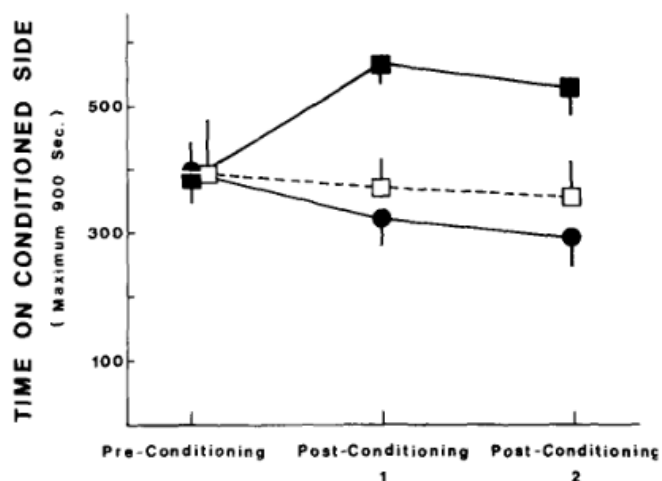


Figure 5. Microinjections of opioids into the VTA are rewarding. Conditioned place preference experiments showed that injection of morphine into the VTA (black boxes) increased time spent on the morphine-paired side of the testing compartment. In contrast, morphine + naloxone (white boxes) and saline (black circles) did not induce conditioned place preference in cannulated rats. Reprinted from *Pharmacology Biochemistry and Behavior*, Vol 12, Phillips, A. G., & LePiane, F. G., Reinforcing effects of morphine microinjection into the ventral tegmental area, 90460-90468, Copyright (1980), with permission from Elsevier. (Phillips & LePiane, 1980)

Side effects

Aside from the addictive potential of exogenous opioids, flooding the brain and body with opioids also can have more immediate negative consequences. In the clinic, constipation is a negative side effect of opioid analgesic administration. This is due to extensive expression of MORs in the gastrointestinal system in humans, specifically between the small and large intestine on neurons of the enteric nervous system and on central inputs from the vagus and pelvic nerves. Activation of MORs in these regions inhibits gastrointestinal motility. When an abundance of exogenous opioids is present chronically, this can inhibit expulsion of waste and cause constipation (Thomas, 2008).

A more lethal side effect of opioid administration is respiratory depression. This is typically the cause of death upon opioid overdose. Opioid-induced respiratory depression appears to occur due to the expression of MORs within nuclei of the medulla (Varga et al., 2020). These receptors retain high levels of activity despite a tendency for decreased responsivity of MORs in other brain regions after chronic opioid use, and therefore the danger of fatal respiratory depression increases with escalating doses associated with opioid addiction (Levitt & Williams, 2018). An increasing trend for recreational heroin to be laced with fentanyl has further exacerbated overdose deaths, as the potency of fentanyl is extremely high and it is difficult to detect in street versions of recreational opioids (O'Donnell et al., 2017).

Dissertation scope

As described above, the effects of administered and exogenous opioids can vary depending upon the location of MOR expression as well as the duration of opioid exposure, and each signaling state of the MOR is important for the development of acute and chronic behavioral effects of opioids. Chapter 2 will focus on understanding how direct observation of the MOR at various time points and in response to various ligands may help in understanding these specific signaling states. We conclude that specific mobility states of the MOR are not sufficient to indicate exact signaling state, however MOR signaling states appear to exist in many forms even before drug application occurs. Therefore, in Chapter 3 we focus on understanding if sensitizing more of the MOR population is possible through the use of a clinically relevant treatment, low dose naltrexone (LDN). Further, we investigate if LDN increases activity of endogenous opioid signaling through increases in activity of POMC neurons. Finally, Chapter 4 examines how the hypothalamic POMC system is wired in relation to the wide variety of regions responsible for opioid-related functions. Chapter 5 concludes that the opioid system is complex, but that specific

organization of the endogenous system may provide opportunity for more targeted modulation of opioid-related processes.

References

- Arttamangkul, S., Torrecilla, M., Kobayashi, K., Okano, H., & Williams, J. T. (2006). Separation of mu-opioid receptor desensitization and internalization: endogenous receptors in primary neuronal cultures. *J Neurosci*, 26(15), 4118-4125. doi:10.1523/jneurosci.0303-06.2006
- Bagley, E. E., & Ingram, S. L. (2020). Endogenous opioid peptides in the descending pain modulatory circuit. *Neuropharmacology*, 173, 108131. doi:10.1016/j.neuropharm.2020.108131
- Bohn, L. M., Lefkowitz, R. J., & Caron, M. G. (2002). Differential mechanisms of morphine antinociceptive tolerance revealed in (beta)arrestin-2 knock-out mice. *J Neurosci*, 22(23), 10494-10500. doi:10.1523/jneurosci.22-23-10494.2002
- Booth, M. (1998). *Opium: A history*: St. Martin's Press.
- Cioffi, C. L. (2018). Modulation of Glycine-Mediated Spinal Neurotransmission for the Treatment of Chronic Pain. *Journal of Medicinal Chemistry*, 61(7), 2652-2679. doi:10.1021/acs.jmedchem.7b00956
- Contarino, A., Picetti, R., Matthes, H. W., Koob, G. F., Kieffer, B. L., & Gold, L. H. (2002). Lack of reward and locomotor stimulation induced by heroin in mu-opioid receptor-deficient mice. *Eur J Pharmacol*, 446(1-3), 103-109. doi:10.1016/s0014-2999(02)01812-5
- Corder, G., Doolen, S., Donahue, R. R., Winter, M. K., Jutras, B. L., He, Y., . . . Taylor, B. K. (2013). Constitutive μ -opioid receptor activity leads to long-term endogenous analgesia and dependence. *Science*, 341(6152), 1394-1399. doi:10.1126/science.1239403
- Darcq, E., & Kieffer, B. L. (2018). Opioid receptors: drivers to addiction? *Nat Rev Neurosci*, 19(8), 499-514. doi:10.1038/s41583-018-0028-x
- De Waele, J. P., & Gianoulakis, C. (1994). Enhanced activity of the brain beta-endorphin system by free-choice ethanol drinking in C57BL/6 but not DBA/2 mice. *Eur J Pharmacol*, 258(1-2), 119-129. doi:10.1016/0014-2999(94)90064-7
- Dhawan, B. N., Cesselin, F., Raghbir, R., Reisine, T., Bradley, P. B., Portoghese, P. S., & Hamon, M. (1996). International Union of Pharmacology. XII. Classification of opioid receptors. *Pharmacol Rev*, 48(4), 567-592.
- Downing, C. (1838). *The Fan-qui in China: 1836-1837*. London.
- Eichel, K., & von Zastrow, M. (2018). Subcellular Organization of GPCR Signaling. *Trends Pharmacol Sci*, 39(2), 200-208. doi:10.1016/j.tips.2017.11.009
- Erbs, E., Faget, L., Scherrer, G., Matifas, A., Filliol, D., Vonesch, J. L., . . . Massotte, D. (2015). A mu-delta opioid receptor brain atlas reveals neuronal co-occurrence in subcortical networks. *Brain Struct Funct*, 220(2), 677-702. doi:10.1007/s00429-014-0717-9
- Fry, J. P., Herz, A., & Zieglgänsberger, W. (1980). A demonstration of naloxone-precipitated opiate withdrawal on single neurones in the morphine-tolerant/dependent rat brain. *Br J Pharmacol*, 68(3), 585-592. doi:10.1111/j.1476-5381.1980.tb14574.x
- Garland, E. L. (2012). Pain processing in the human nervous system: a selective review of nociceptive and biobehavioral pathways. *Prim Care*, 39(3), 561-571. doi:10.1016/j.pop.2012.06.013

- Gianoulakis, C., Drouin, J. N., Seidah, N. G., Kalant, H., & Chrétien, M. (1981). Effect of chronic morphine treatment on beta-endorphin biosynthesis by the rat neurointermediate lobe. *Eur J Pharmacol*, 72(4), 313-321. doi:10.1016/0014-2999(81)90569-0
- Heinke, B., Gingl, E., & Sandkühler, J. (2011). Multiple Targets of μ -Opioid Receptor-Mediated Presynaptic Inhibition at Primary Afferent A δ - and C-Fibers. *The Journal of Neuroscience*, 31(4), 1313-1322. doi:10.1523/jneurosci.4060-10.2011
- Hu, H. (2016). Reward and Aversion. *Annu Rev Neurosci*, 39, 297-324. doi:10.1146/annurev-neuro-070815-014106
- Huang, C., Duncan, J. A., Gilman, A. G., & Mumby, S. M. (1999). Persistent membrane association of activated and depalmitoylated G protein alpha subunits. *Proc Natl Acad Sci U S A*, 96(2), 412-417. doi:10.1073/pnas.96.2.412
- Ingram, S. L., Vaughan, C. W., Bagley, E. E., Connor, M., & Christie, M. J. (1998). Enhanced opioid efficacy in opioid dependence is caused by an altered signal transduction pathway. *J Neurosci*, 18(24), 10269-10276. doi:10.1523/jneurosci.18-24-10269.1998
- Jean-Charles, P. Y., Kaur, S., & Shenoy, S. K. (2017). G Protein-Coupled Receptor Signaling Through β -Arrestin-Dependent Mechanisms. *J Cardiovasc Pharmacol*, 70(3), 142-158. doi:10.1097/fjc.0000000000000482
- Johansen, J. P., Fields, H. L., & Manning, B. H. (2001). The affective component of pain in rodents: Direct evidence for a contribution of the anterior cingulate cortex. *Proceedings of the National Academy of Sciences*, 98(14), 8077-8082. doi:10.1073/pnas.141218998
- Johnson, S. M., & Duggan, A. W. (1981). Tolerance and dependence of dorsal horn neurones of the cat: the role of the opiate receptors of the substantia gelatinosa. *Neuropharmacology*, 20(11), 1033-1038. doi:10.1016/0028-3908(81)90093-9
- Keshelava, A., Solis, G. P., Hersch, M., Koval, A., Kryuchkov, M., Bergmann, S., & Katanaev, V. L. (2018). High capacity in G protein-coupled receptor signaling. *Nature Communications*, 9(1), 876. doi:10.1038/s41467-018-02868-y
- Kliwer, A., Schmiedel, F., Sianati, S., Bailey, A., Bateman, J. T., Levitt, E. S., . . . Schulz, S. (2019). Phosphorylation-deficient G-protein-biased μ -opioid receptors improve analgesia and diminish tolerance but worsen opioid side effects. *Nature Communications*, 10(1), 367. doi:10.1038/s41467-018-08162-1
- Lammel, S., Lim, B. K., & Malenka, R. C. (2014). Reward and aversion in a heterogeneous midbrain dopamine system. *Neuropharmacology*, 76 Pt B(0 0), 351-359. doi:10.1016/j.neuropharm.2013.03.019
- Le Merrer, J., Becker, J. A., Befort, K., & Kieffer, B. L. (2009). Reward processing by the opioid system in the brain. *Physiol Rev*, 89(4), 1379-1412. doi:10.1152/physrev.00005.2009
- Levitt, E. S., & Williams, J. T. (2018). Desensitization and Tolerance of Mu Opioid Receptors on Pontine Kölliker-Fuse Neurons. *Mol Pharmacol*, 93(1), 8-13. doi:10.1124/mol.117.109603
- Lord, J. A., Waterfield, A. A., Hughes, J., & Kosterlitz, H. W. (1977). Endogenous opioid peptides: multiple agonists and receptors. *Nature*, 267(5611), 495-499. doi:10.1038/267495a0
- Manges, M. (1898). The treatment of coughs with heroin. *New York Medical Journal*, 68, 768-770.
- Manges, M. (1900). A Second Report on the Therapeutics of Heroine. *New York Medical Journal*, 71, 51-55.

- Martin, W. R., Eades, C. G., Thompson, J. A., Huppler, R. E., & Gilbert, P. E. (1976). The effects of morphine- and nalorphine- like drugs in the nondependent and morphine-dependent chronic spinal dog. *J Pharmacol Exp Ther*, 197(3), 517-532.
- Matthes, H. W., Maldonado, R., Simonin, F., Valverde, O., Slowe, S., Kitchen, I., . . . Kieffer, B. L. (1996). Loss of morphine-induced analgesia, reward effect and withdrawal symptoms in mice lacking the mu-opioid-receptor gene. *Nature*, 383(6603), 819-823. doi:10.1038/383819a0
- Mattson, C. L., Tanz, L. J., Quinn, K., Kariisa, M., Patel, P., & Davis, N. L. (2021). Trends and Geographic Patterns in Drug and Synthetic Opioid Overdose Deaths - United States, 2013-2019. *MMWR Morb Mortal Wkly Rep*, 70(6), 202-207. doi:10.15585/mmwr.mm7006a4
- O'Donnell, J. K., Gladden, R. M., & Seth, P. (2017). Trends in Deaths Involving Heroin and Synthetic Opioids Excluding Methadone, and Law Enforcement Drug Product Reports, by Census Region - United States, 2006-2015. *MMWR Morb Mortal Wkly Rep*, 66(34), 897-903. doi:10.15585/mmwr.mm6634a2
- Olds, J., & Milner, P. (1954). Positive reinforcement produced by electrical stimulation of septal area and other regions of rat brain. *Journal of Comparative and Physiological Psychology*, 47(6), 419-427. doi:10.1037/h0058775
- Pennock, R. L., & Hentges, S. T. (2011). Differential expression and sensitivity of presynaptic and postsynaptic opioid receptors regulating hypothalamic proopiomelanocortin neurons. *J Neurosci*, 31(1), 281-288. doi:10.1523/jneurosci.4654-10.2011
- Phillips, A. G., & LePiane, F. G. (1980). Reinforcing effects of morphine microinjection into the ventral tegmental area. *Pharmacol Biochem Behav*, 12(6), 965-968. doi:10.1016/0091-3057(80)90460-8
- Porreca, F., & Navratilova, E. (2017). Reward, motivation, and emotion of pain and its relief. *Pain*, 158 Suppl 1(Suppl 1), S43-s49. doi:10.1097/j.pain.0000000000000798
- Prazeres, D. M., & Martins, S. A. (2015). G protein-coupled receptors: an overview of signaling mechanisms and screening assays. *Methods Mol Biol*, 1272, 3-19. doi:10.1007/978-1-4939-2336-6_1
- Quinones, M. A. (1975). Drug abuse during the Civil War (1861-1865). *Int J Addict*, 10(6), 1007-1020. doi:10.3109/10826087509028357
- Rosso, A. (2010). Poppy and opium in ancient times: Remedy or narcotic? . *Biomedicine International*, 1(1), 81-87.
- Russell, J. A., Leng, G., & Bicknell, R. J. (1995). Opioid tolerance and dependence in the magnocellular oxytocin system: a physiological mechanism? *Exp Physiol*, 80(3), 307-340. doi:10.1113/expphysiol.1995.sp003850
- Smrcka, A. V. (2008). G protein $\beta\gamma$ subunits: central mediators of G protein-coupled receptor signaling. *Cell Mol Life Sci*, 65(14), 2191-2214. doi:10.1007/s00018-008-8006-5
- Stanley, T. H., Egan, T. D., & Van Aken, H. (2008). A Tribute to Dr. Paul A. J. Janssen: Entrepreneur Extraordinaire, Innovative Scientist, and Significant Contributor to Anesthesiology. *Anesthesia & Analgesia*, 106(2), 451-462. doi:10.1213/ane.0b013e3181605add
- Thomas, J. (2008). Opioid-induced bowel dysfunction. *J Pain Symptom Manage*, 35(1), 103-113. doi:10.1016/j.jpainsymman.2007.01.017
- Van Bockstaele, E. J., Rudoy, C., Mannelli, P., Oropeza, V., & Qian, Y. (2006). Elevated mu-opioid receptor expression in the nucleus of the solitary tract accompanies attenuated

- withdrawal signs after chronic low dose naltrexone in opiate-dependent rats. *J Neurosci Res*, 83(3), 508-514. doi:10.1002/jnr.20738
- Varga, A. G., Reid, B. T., Kieffer, B. L., & Levitt, E. S. (2020). Differential impact of two critical respiratory centres in opioid-induced respiratory depression in awake mice. *J Physiol*, 598(1), 189-205. doi:10.1113/jp278612
- Wiech, K., & Tracey, I. (2009). The influence of negative emotions on pain: behavioral effects and neural mechanisms. *Neuroimage*, 47(3), 987-994. doi:10.1016/j.neuroimage.2009.05.059
- Williams, J. T., Ingram, S. L., Henderson, G., Chavkin, C., von Zastrow, M., Schulz, S., . . . Christie, M. J. (2013). Regulation of μ -opioid receptors: desensitization, phosphorylation, internalization, and tolerance. *Pharmacol Rev*, 65(1), 223-254. doi:10.1124/pr.112.005942
- Zhang, Y., Liang, Y., Randesi, M., Yufarov, V., Zhao, C., & Kreek, M. J. (2018). Chronic Oxycodone Self-administration Altered Reward-related Genes in the Ventral and Dorsal Striatum of C57BL/6J Mice: An RNA-seq Analysis. *Neuroscience*, 393, 333-349. doi:10.1016/j.neuroscience.2018.07.032

CHAPTER 2—DIRECT MONITORING OF MOR ACTIVITY STATES USING SINGLE PARTICLE TRACKING

Preamble

A portion of the following material was published online May 13, 2019 in the journal *Scientific Reports* under the title “Temporal dependence of shifts in mu opioid receptor mobility at the cell surface after agonist binding observed by single-particle tracking” (Metz et al., 2019). A brief, unpublished background introduces the topic of single particle tracking the MOR. Following the background section, the published work is reproduced as it appeared in the original journal article.

Background

Signaling processes of the MOR

Much work has been performed to understand how the MOR population within a cell signals and how this signaling contributes to behavior. As described in Chapter 1, upon binding of an agonist, the MOR goes through a stereotyped pattern of activation, acute desensitization, and long-term regulation. Each of these processes corresponds to specific interaction of the MOR with signaling partners that includes G_i α , β , and γ , β -arrestin, and various kinases and phosphatases. These signaling partners then go on to activate or inhibit downstream cellular effectors including adenylyl cyclase, calcium channels, potassium channels, and neurotransmitter release machinery. The activity of these downstream effectors has typically been the readout used for MOR activity assays. Measurements of secondary effector output are typically performed on a whole-cell basis as described below.

Measures of MOR activity

Electrophysiology

One of the most sensitive assays for assessing MOR activity is electrophysiology. Readouts are effector-based, meaning they assess output of MOR signaling partners and depend upon the ability of the MOR to enhance activation of g-protein coupled potassium channels (GIRKs), inhibit activation of calcium channels, or inhibit neurotransmitter release. Experiments are often performed to ensure that effects observed by electrophysiology are not due to a change at the effector instead of a change at the receptor (Williams et al., 2013). However electrophysiology is still limited by the fact that it depends upon the output of a signal secondary to MOR activation by ligands.

Whole-cell-based imaging assays

Other studies of the MOR that use whole cell activity averages also have important caveats. For example, a longstanding goal within the field of opioid receptor biology is to find chemical compounds that bias MORs towards a particular signaling state. Biased signaling could help to avoid some undesirable aspects of long term MOR signaling. Tolerance, for example, might be decreased if β -arrestin based signaling were avoided. However, the assays used to screen potentially biased compounds require two distinct assays to assess bias (typically whole-cell cAMP accumulation assays for g-protein activity and enzyme complementation assays for β -arrestin recruitment; DeWire et al., 2013; Manglik et al., 2016; Schmid et al., 2017). Due to the inherent differences between these assays, extensive calculation must be performed post-data collection in an attempt to avoid erroneous conclusions about the bias of a particular agonist (Black and Leff, 1983). Despite this careful calculation, however, efficacy, or the ability of an agonist to induce activity in general, can often be mistaken for bias since g-protein and β -arrestin-based assays inherently differ in their degree of amplification (Gillis et al., 2020).

Clearly, then, the use of secondary effectors and cell-based assays to understand MOR activity carry important caveats in interpretation.

Single particle tracking for direct study of individual MORs

One attractive alternative to averaged, effector-based assays for assessing MOR activity is direct observation of individual MORs within the cell membrane. All proteins within a cell membrane are dynamic and move laterally within the membrane, whether due to undirected Brownian diffusion or due to deliberate interactions with signaling partners. Previous studies employing single particle tracking of the MOR reveal that the MOR moves about the membrane with varying diffusivity, which suggests that different mobility states could correspond to specific states of the receptor. If particular mobility states correspond to particular signaling states, a simpler and more accurate assessment of MOR activity and interaction with signaling partners could be made. The following published work examines the possibility that signaling state of the MOR corresponds to particular mobility states as observed via single particle tracking.

Published work

Temporal dependence of shifts in mu opioid receptor mobility at the cell surface after agonist binding observed by single-particle tracking

Summary

Agonist binding to the mu opioid receptor (MOR) results in conformational changes that allow recruitment of G-proteins, activation of downstream effectors and eventual desensitization and internalization, all of which could affect receptor mobility. The present study employed single particle tracking (SPT) of quantum dot labeled FLAG-tagged MORs to examine shifts in MOR mobility after agonist binding. FLAG-MORs on the plasma membrane were in both mobile and immobile states under basal conditions. Activation of FLAG-MORs with DAMGO caused an

acute increase in the fraction of mobile MORs, and free portions of mobile tracks were partially dependent on interactions with G-proteins. In contrast, 10-minute exposure to DAMGO or morphine increased the fraction of immobile FLAG-MORs. While the decrease in mobility with prolonged DAMGO exposure corresponded to an increase in colocalization with clathrin, the increase in colocalization was present in both mobile and immobile FLAG-MORs. Thus, no single mobility state of the receptor accounted for colocalization with clathrin. These findings demonstrate that SPT can be used to track agonist-dependent changes in MOR mobility over time, but that the mobility states observed likely arise from a diverse set of interactions and will be most informative when examined in concert with particular downstream effectors.

Introduction

The mu opioid receptor (MOR) is a G-protein coupled receptor (GPCR) responsible for many of the physiological effects of endogenous opioids, as well as clinically important exogenously administered opioids (e.g. morphine, codeine, fentanyl). Thus, this receptor has been the focus of many studies examining signaling through effectors such as adenylyl cyclase, G-protein coupled inwardly rectifying K⁺ channels, voltage-gated calcium and potassium channels. Additionally, beta-arrestin binding, desensitization and internalization of the MOR have been heavily studied as these processes likely underlie the reduced efficacy of MOR agonists with prolonged exposure (Williams et al., 2013). Recently, imaging-based studies of directly labeled MORs have provided an alternative to effector-dependent assays and have been used to examine MOR mobility (Carayon et al., 2014; Daumas et al., 2003; Halls et al., 2016; Melkes et al., 2016; Sauliere-Nzeh Ndong et al., 2010; Suzuki et al., 2005; Vukojevic et al., 2008) and subcellular localization (Haberstock-Debic et al., 2003; Halls et al., 2016; Stoeber et al., 2018; Tobin et al., 2018; Yu et al., 2010). Studies of MOR mobility utilizing fluorescence recovery after photobleaching

(FRAP) and fluorescence correlation spectroscopy (FCS) have shown that MORs can exist in a variety of mobility states on the membrane even under non-stimulated conditions as the MOR can exist in nanodomains with varying lipid content and protein density or be outside of discrete nanodomains (Rogacki et al., 2018; Tobin et al., 2018).

The mobility of GPCRs including MORs is regulated by agonist binding and several lines of evidence suggest that distinct signaling states occurring upon agonist binding may be correlated with select mobility states (Baker et al., 2007; Calizo and Scarlata, 2013; Carayon et al., 2014; Golebiewska et al., 2011; Roumy et al., 2007; Tobin et al., 2018; Vukojevic et al., 2008). Further, for the MOR, it appears that changes in lateral diffusion within the plasma membrane likely reflect interactions with different membrane proteins (Daumas et al., 2003; Halls et al., 2016). Electrophysiologic studies indicate that agonist binding to MORs causes a rapid G-protein-mediated activation or inhibition of effectors that often declines significantly, although not completely, with minutes (often in <5 min) as the receptors undergo homologous desensitization (reviewed in (Williams et al., 2013)). Altogether, it seems plausible that distinct mobility states reflect differing states of signaling and desensitization.

Here, we set out to use single-particle tracking (SPT) to assess how the mobility of the MOR changes over time during agonist application reasoning that we should be able to detect signaling and desensitized receptors based on distinct mobilities as the receptor interacts with differing membrane and intracellular molecules (perhaps discrete nanodomains) in these states. SPT was employed because this imaging and tracking approach allows examination of individual receptor behavior without reliance on effector-based readouts and allows the evaluation of heterogeneities and molecule-to-molecule variations without relying on *a priori* models as required in ensemble measurements, such as FRAP (Krapf, 2018; Manzo and Garcia-Parajo,

2015). Specific mobility states of individual receptors detected with SPT may correlate with distinct interactions with select effectors and other binding partners. SPT studies have shown that the MOR can be in various mobility states under basal conditions, although the specifics are unclear. One study tracking the MOR reported that most receptors are confined within mobile microdomains, while a smaller fraction of receptors exhibit slow, directed diffusion (Daumas et al., 2003). Another study reported short-term confinement within specific membrane compartments followed by diffusion of the receptor between these compartments (Suzuki et al., 2005). Neither of these studies examined the effect of agonist binding on mobility.

The present study was designed to determine if SPT could provide a reliable approach to detect agonist-induced changes in mobility of the MOR that might correspond to interactions with G-proteins and recruitment to clathrin coated pits (CCPs) subsequent to agonist binding. Tracking of the MOR was performed in AtT20 cells stably expressing a FLAG-epitope-tagged MOR construct (FLAG-MOR) (Borgland et al., 2003) conjugated with quantum dots (Qdots) via an anti-FLAG antibody. Signaling through MORs has been extensively characterized in AtT20 cells (Borgland et al., 2003; Celver et al., 2004; Knapman and Connor, 2015). MORs in AtT20 cells couple to endogenously-expressed GIRKs (Celver et al., 2004; Yousuf et al., 2015), P/Q-type VDCCs (Borgland et al., 2003), adenylyl cyclase (Thompson et al., 2016), and G-protein coupled receptor kinases (Celver et al., 2004; Dang and Christie, 2012) via pertussis-toxin sensitive $G\alpha_{i/o}$ proteins (Knapman et al., 2013). Further, AtT20 cells stably expressing FLAG-MORs exhibit consistent and moderate expression of the tagged receptor (~31,000 receptors/cell), do not express endogenous MOR and display activation, desensitization, and internalization phases similar to MORs in neurons (Borgland et al., 2003). Thus, AtT20 cells

stably transfected with Flag-MOR provide a good system for examining real-time dynamics of the MOR in the plasma membrane before and during agonist exposure.

Here, MOR mobility was investigated in response to two different drugs: morphine, a low efficacy agonist that induces very little internalization, and DAMGO, a high efficacy agonist known to induce internalization. Mobility in response to these drugs was investigated after 1 minute or 10 minutes of agonist exposure. These time points were selected because 1 minute of agonist exposure has been shown to induce receptor coupling to G-proteins and signaling through various effectors, whereas 10 minutes of agonist exposure can lead to receptor desensitization and internalization in an agonist-dependent manner (Borgland et al., 2003). Quantitative diffusion analysis of trajectories of Qdot 565-conjugated FLAG-MORs shows that receptors can be found in both immobile and mobile states under basal conditions. Activation of FLAG-MORs with DAMGO, but not morphine, caused an initial increase in the population of mobile receptors (at 1 minute of exposure), followed at later time points by a decrease in the mobile fraction (10 min agonist exposure). These findings show that activation of the FLAG-MOR does not result in a uniform decrease in the mobility of the receptors, but instead it dynamically changes the fraction of FLAG-MORs found within a range of either more mobile or immobile states depending upon time observed after agonist exposure and the agonist applied. Therefore, ensemble measurements of receptor mobility, such as average mean square displacement (MSD), may not capture the full extent of receptor activity, and single-particle tracking can better account for heterogeneity in signaling states. Further, investigation of receptors in the mobile state revealed transient confinement partially influenced by G-protein binding. However, inspection of tracks after 10 min of DAMGO exposure revealed that the mobility state was a poor proxy for colocalization with clathrin. Altogether, while single particle

tracking of the MOR alone provides much richer information about heterogeneities in mobility and can provide information about signaling state (such as G-protein coupling), it may not account for the full range of potential effectors a receptor is coupled to (such as clathrin colocalization).

Results

In order to visualize MORs, FLAG-MORs in AtT20 cells were labeled with Qdots. Cells were imaged under differential interference contrast (DIC) to assess cell morphology (Fig. 1A) and under fluorescence using spinning disk confocal to detect Qdots (Fig. 1B). Trajectories of labeled FLAG-MOR were obtained as shown in the example in Fig. 1C. FLAG-MOR mobility was investigated before agonist application and after 1 or 10 minutes of treatment with agonist (10 μ M). The time-averaged MSD $\overline{\delta^2(t_{lag})}$ of individual Qdot-MOR trajectories were computed for time lags t_{lag} up to 2.5 s for each experimental condition (Eq.1 in methods section). Fig. S1 shows a representative set of individual MSDs for trajectories in various conditions. Most trajectories exhibit sub-diffusive behavior, i.e., the MSD of individual trajectories is not linear in lag time but it scales as a power law $K_\alpha t_{lag}^\alpha$ with $\alpha < 1$ where α is the anomalous exponent and K_α is the generalized diffusion coefficient (Hofling and Franosch, 2013; Krapf, 2015; Metzler et al., 2014). Furthermore, a substantial number of trajectories have a flat MSD, indicating that these particles are either immobile or confined to small domains (Akin et al., 2016). In all cases, only particles that were observed for at least 3 s were analyzed.

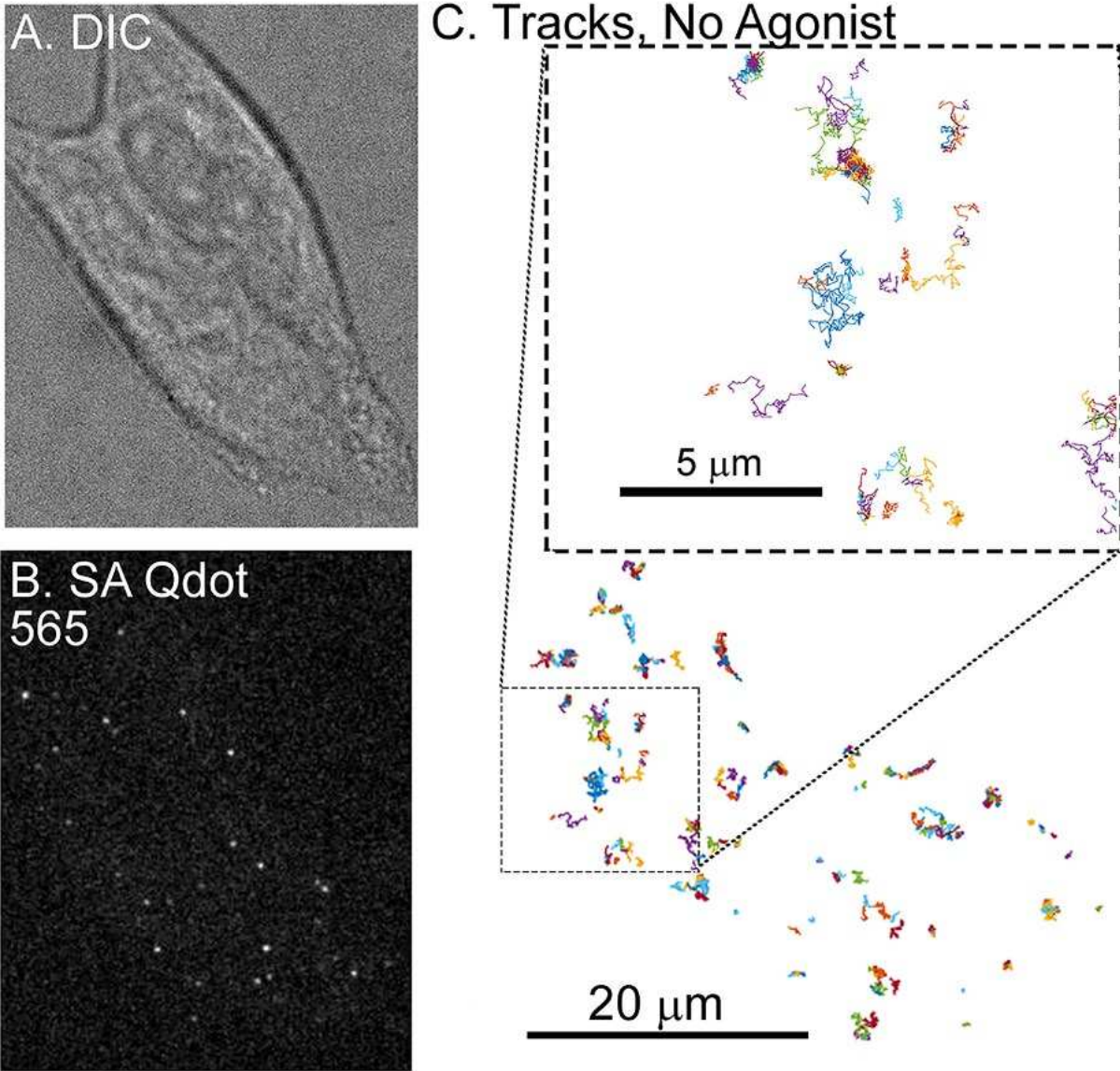


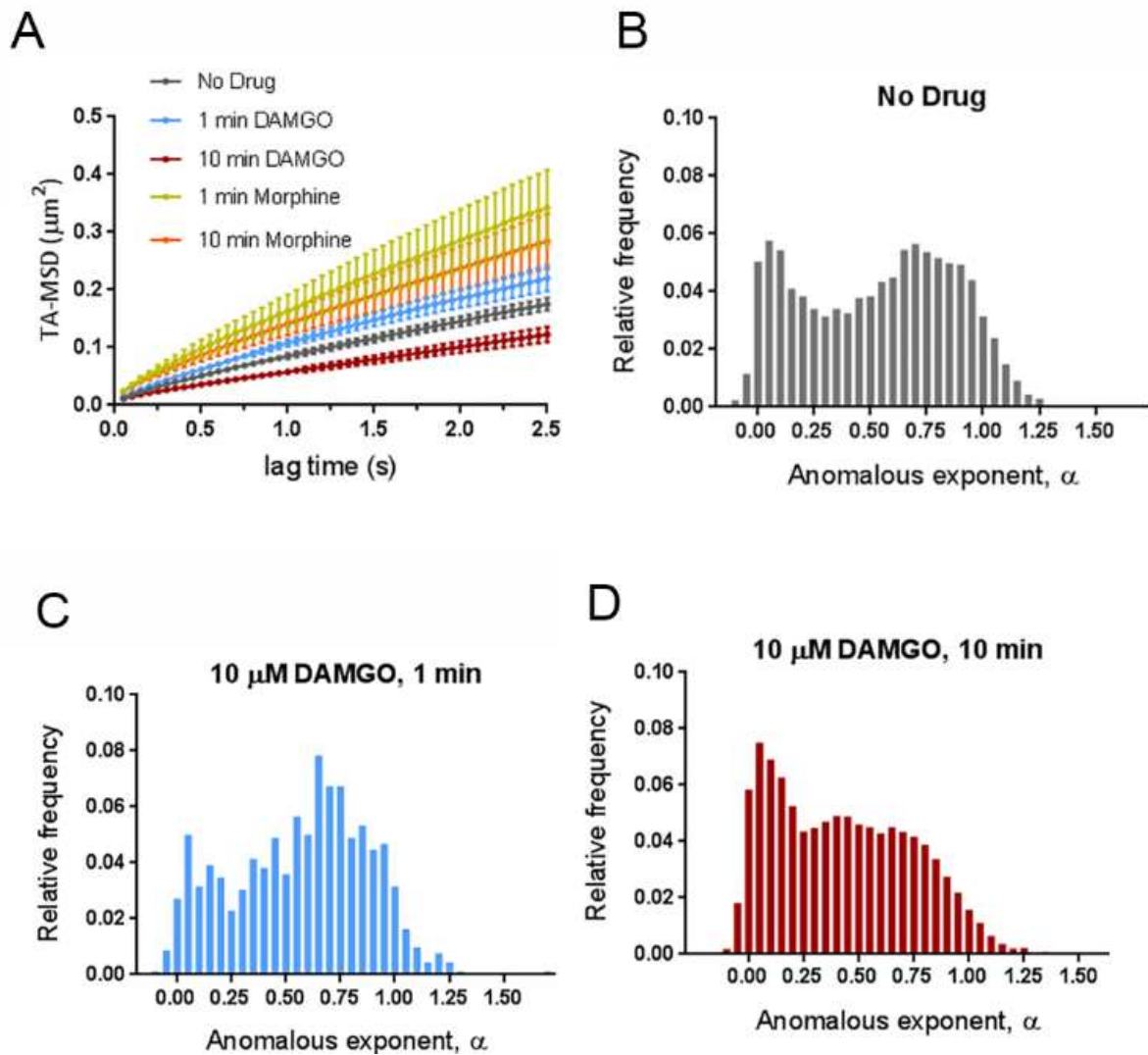
Figure 6. Single-particle tracking of FLAG-MORs in AtT20 cells. **A)** Representative DIC image of an AtT20 cell and **(B)** fluorescent image of SA Qdot 565 conjugated FLAG-MORs in the same cell. Labeling density in this image is typical for experiments carried out in this study. **C)** Trajectories of SA Qdot 565-conjugated FLAG-MORs imaged in the absence of drug from the cell shown in (A) and (B). All of the displayed trajectories were obtained from a single 1000-frame video segment. The upper square in (C) shows an enlarged image of trajectories from the area indicated by the lower dashed box. Both mobile and immobile trajectories can be seen in the inset, as well as confined and free portions of mobile trajectories.

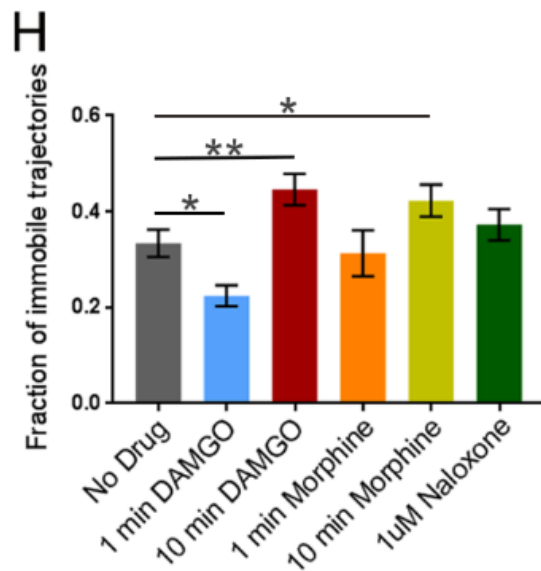
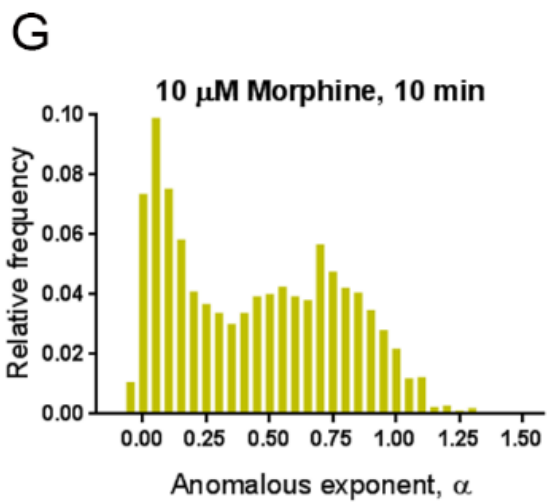
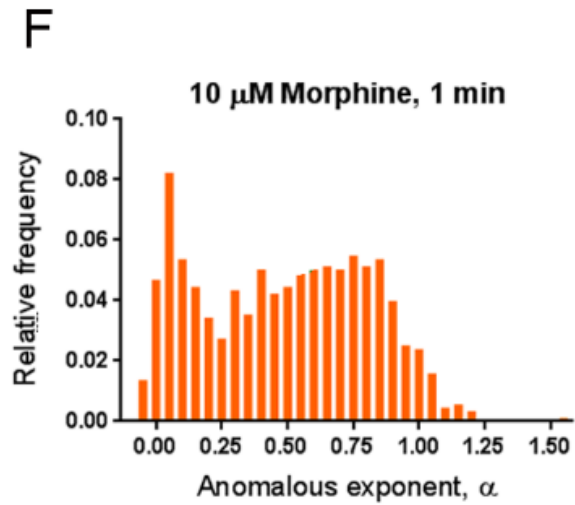
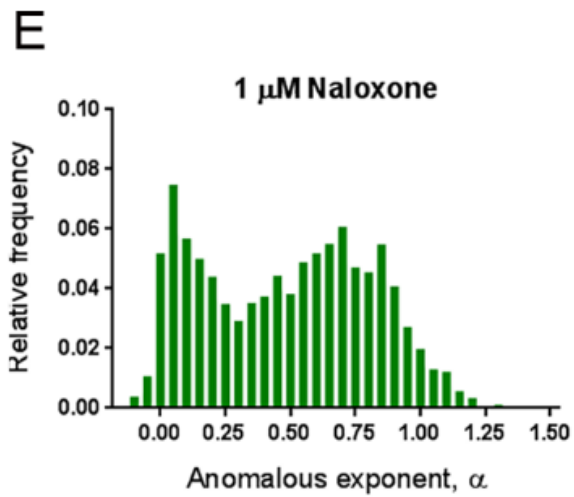
Clear differences were observed between the MSD under basal conditions and those in cells treated with DAMGO or morphine (Fig. 2A). Short DAMGO treatment (1 min) increased the anomalous exponent α of the average MSD from 0.49 ± 0.12 in the no-drug condition to 0.55 ± 0.02 . No change was observed from no drug in the anomalous exponent of the average MSD after 1 min morphine (0.48 ± 0.04 , $p = 0.88$). In contrast, longer DAMGO treatment (10 min) decreased the anomalous exponent of the average MSD to 0.38 ± 0.02 ($p = 0.014$ compared to no-drug), as did 10 min morphine treatment (0.40 ± 0.02 , $p = 0.02$). Further, the generalized diffusion coefficient, K_α , of the averaged MSD increased after the 1 min DAMGO exposure from $0.087 \pm 0.005 \mu\text{m}^2/\text{s}^{0.49}$ (no-drug condition) to $0.104 \pm 0.006 \mu\text{m}^2/\text{s}^{0.55}$ ($p = 0.034$). K_α also increased after 1 min morphine treatment ($0.16 \pm 0.03 \mu\text{m}^2/\text{s}^{0.48}$, $p = 0.002$) as well as after 10 min morphine treatment ($0.14 \pm 0.02 \mu\text{m}^2/\text{s}^{0.40}$, $p = 0.003$). Longer DAMGO exposure (10 min) decreased the generalized diffusion coefficient to $0.057 \pm 0.004 \mu\text{m}^2/\text{s}^{0.38}$ ($p = 0.0004$ compared to no-drug). Together, these results indicate that acute agonist exposure increases the average diffusivity of the receptor and this average diffusivity can either increase or decrease after prolonged agonist exposure.

Ensemble measurements, such as average MSD, however, may mask important characteristics in the data that can be revealed by measuring individual trajectories. Therefore, using the average MSD as a guide to underlying differences between drug conditions, we sought to investigate receptor dynamics at the individual particle level. Thus, the anomalous exponent α was computed for individual trajectories in each experimental condition. Very low anomalous exponents are indicative of particles that explore a more compact region and present a nearly flat MSD while larger exponents indicate that the trajectory explores a less compact region and present an MSD that increases with lag time (Weron et al., 2017). The histogram for the no-drug

condition shows a large scattering of α values, indicating marked heterogeneity in the diffusion behavior of FLAG-MORs (Fig. 2B). In particular, two populations are clearly visible, one with a narrow distribution centered at $\alpha = 0.09$ and another with a broader distribution centered at $\alpha = 0.71$. This was confirmed using silhouette criteria (Sikora et al., 2017) which also determines there are two classes within this distribution of α values. These populations can be separated by using a threshold in α . We selected a threshold $\alpha = 0.27$, based on the local minimum that is found in the histogram between the two populations. Other types of threshold selection, such as two Gaussian fitting and k means, show that the following results are similar, even if different thresholds are used (Fig. S3). Examination of the tracks within these two populations shows relatively more confinement in the low α population, and relatively less confinement in the high α population (see Fig. 2I & J for example tracks). Henceforth, tracks with $\alpha < 0.27$ are referred to as immobile and tracks with $\alpha \geq 0.27$ are referred to as mobile. The distribution of α values is significantly altered by 1-min DAMGO (Fig. 2C), 10-min DAMGO (Fig. 2D), and 10-min morphine (Fig. 2G) exposure compared to the no-drug condition (Fig. 2B). The fraction of immobile tracks in each condition is shown in Fig. 2H. In the no drug condition, the immobile fraction is 0.33 ± 0.03 . This decreased to 0.23 ± 0.02 in the 1-min DAMGO condition ($p = 0.016$) and increased after 10 min of DAMGO exposure to 0.45 ± 0.03 ($p = 0.009$). Morphine exposure for 1 min does not cause a statistically significant decrease in the immobile fraction (0.31 ± 0.05 ; $p = 0.842$ compared to no-drug, see Fig. 2F for distribution), but like 10 min DAMGO, 10 min of morphine exposure exhibits a higher immobile fraction at 0.42 ± 0.03 ($p = 0.047$). The difference between 1 min DAMGO and 1 min morphine might be due to the lower efficacy of morphine, differing effector coupling, or a differing time course of activation induced by the two agonists. Regardless, it is clear that acute exposure to DAMGO reduces the fraction

of immobile receptors, suggesting that mobility increases when the receptor is actively signaling. As expected, there is no significant change in the fraction of immobile trajectories caused by the neutral antagonist Naloxone (0.37 ± 0.03 , $p = 0.147$ compared to the no drug condition, see Fig. 2E for distribution), indicating that ligand binding alone was not sufficient to cause the altered mobility observed.





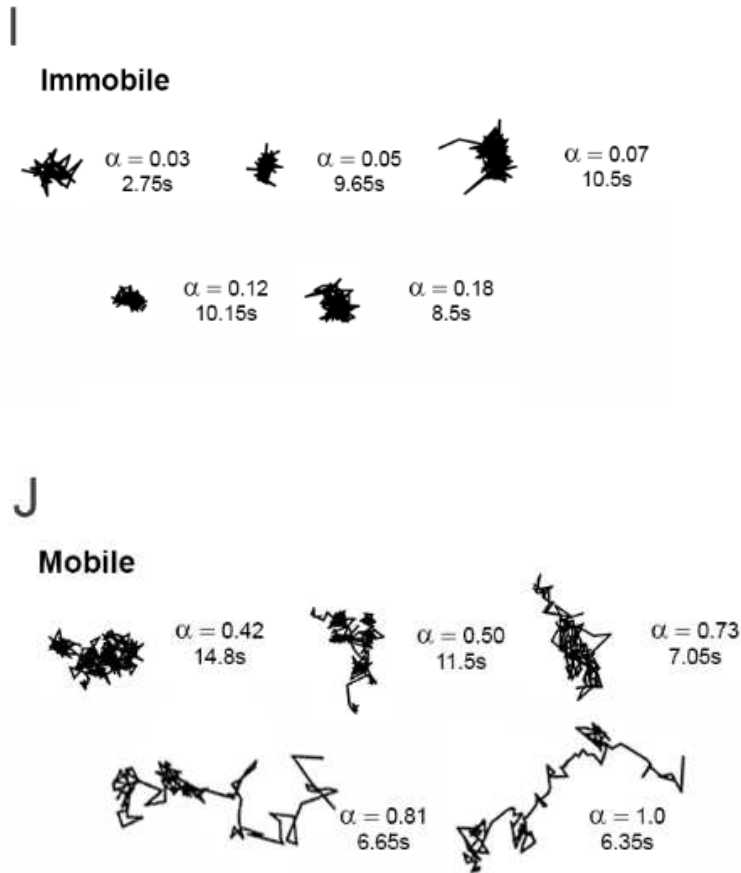


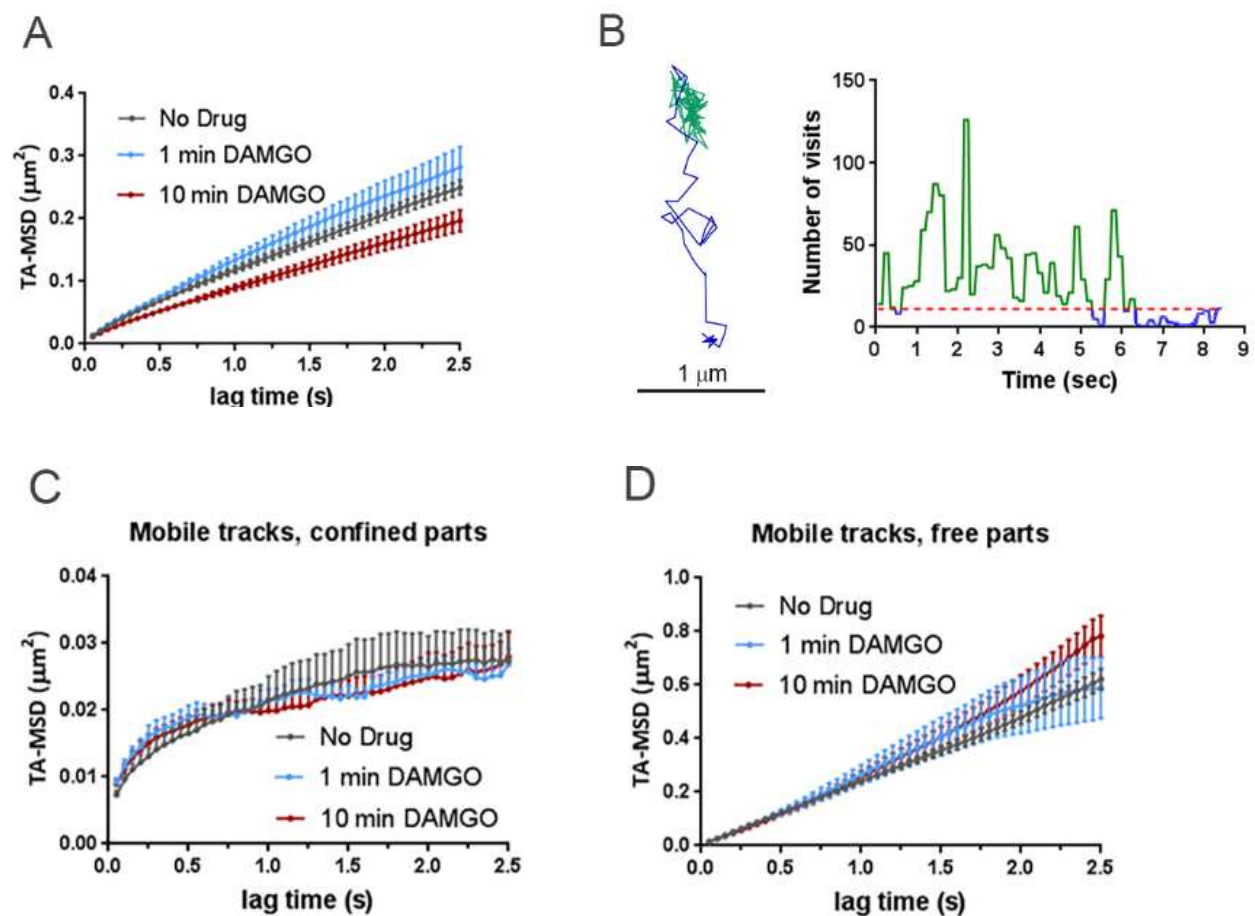
Figure 7. Dynamic changes in MOR mobility exist depending upon the time of drug application. **A)** Time averaged MSD averaged over all tracks for each experimental condition showing increases in the MSD with 1 min DAMGO, 1 min morphine, and 10 min morphine treatments and a decrease with 10 min DAMGO treatment (10 μ M agonist for all). Distribution of anomalous exponents α , obtained from the TA-MSD of individual trajectories for tracks in the **B)** no drug (n=17 cells, 8465 trajectories), **C)** 1 min DAMGO (n=12 cells, 930 trajectories), **D)** 10 min DAMGO (n=13 cells, 8465 trajectories), **F)** 1 min morphine (n=8 cells, 882 trajectories), **G)** 10 min morphine (n=10 cells, 2415 trajectories), **E)** and Naloxone (n=7 cells, 8227 trajectories) condition. All conditions exhibit bimodal distributions with peaks centered at $\alpha = 0.09$ and $\alpha = 0.71$ for immobile and mobile populations, respectively. **H)** Compared to the no drug condition, the population of $\alpha < 0.27$ decreases in the 1 min DAMGO condition, increases in the 10 min DAMGO and 10 min morphine conditions, and does not change after 1 min morphine or Naloxone application. Example trajectories from **I)** immobile ($\alpha < 0.27$) and **J)** mobile ($\alpha > 0.27$) populations of receptors in the no-drug condition are shown with their corresponding α values and lengths. * $p < .05$, ** $p < .01$, Kruskal-Wallis one-way ANOVA with multiple comparisons using Bonferroni correction, error bars represent SEM for cells.

Despite the advantages of Qdot labeling in terms of brightness and photostability (Michalet et al., 2005; Pinaud et al., 2010; Weigel et al., 2011), quantum dots have the potential to reduce surface protein mobility (Abraham et al., 2017). Further, antibody-based detection has the potential to cause receptor crosslinking. To address these concerns, we compared our results with Qdot-labeled MORs to measurements of the fluorescent agonist Dermorphin-488 (Arttamangkul et al., 2000) bound to Flag-MOR. MORs bound with Dermorphin-488 (60 pM, 10 min) showed α values similar to those obtained after 10 min of DAMGO exposure in cells with Qdot-labeled MORs (Fig. S2C). While the concentrations of DAMGO and Dermorphin-488 were orders of magnitude different, the concentrations were chosen based on labeling intensity such that imaging could be performed reliably. Given that Dermorphin-488 was applied at a very low concentration, but was left on for a prolonged time, it is unclear whether the mobility correlates to signaling receptor in this experiment. Regardless, it is notable that the diffusion states detected are in line with those for the Qdot studies suggesting minimal contribution of crosslinking in the studies with Qdots. Finally, if Qdots were crosslinked during tracking, the intensity of a measured particle would correspond to slower diffusion, as aggregates of Qdots would be expected to be both brighter and slower. This is not the case, however, as the MSD is not correlated with the intensity of each particle (Fig. S2D). Thus, we exclude Qdot artifacts and crosslinking as the root for the immobilization observed. Further, the key observations in this work relate to agonist-induced changes in mobility and any potential crosslinking artifact would be expected to occur equally in all test conditions since the receptors are labeled prior to experiment. Overall, the findings indicate that the MOR shows dynamic alterations in mobility depending upon whether it is observed 1 or 10 min after drug treatment.

Since there was a shift towards increased mobile receptors (reduced fraction of immobile tracks) with 1 min DAMGO exposure (Fig. 2H) when signaling is expected to be high (Borgland et al., 2003; Williams et al., 2013), we next focused on the mobile tracks specifically. The analysis of mobile tracks was focused on DAMGO since morphine did not cause a significant shift in the mobile fraction at 1 min. This lack of apparent mobility shift with morphine at 1 min could reflect differing time courses to max signaling or differing effector coupling underlying mobility shifts induced by the two agonists. When comparing the MSDs of mobile trajectories (Fig. 3A), the anomalous exponent of the average MSD in the no drug condition was 0.62 ± 0.01 and was similar (0.65 ± 0.02) after 1 min of DAMGO. However, 10 min of DAMGO exposure decreased the anomalous exponent of the average MSD to 0.54 ± 0.03 ($p = 0.02$). Further, the K_α of the averaged MSD for mobile trajectories was $0.11 \pm 0.02 \mu\text{m}^2/\text{s}^{0.62}$ in the no drug condition and $0.12 \pm 0.03 \mu\text{m}^2/\text{s}^{0.65}$ in the 1 min DAMGO condition, whereas it was $0.087 \pm 0.019 \mu\text{m}^2/\text{s}^{0.54}$ in the 10 min DAMGO condition ($p = 0.041$, no drug compared to 10 min DAMGO). This result suggests that, even within the mobile population of receptors, prolonged agonist exposure may lead to relatively reduced mobility.

To examine the root of this reduced mobility, we identified within the mobile trajectories ($\alpha > 0.27$) periods of time where the molecule is in one of the two modes of motion, namely, either confined or free. To identify the times at which MOR motion changes from confined to free and vice versa, we used a recently published method based on recurrence statistics (Sikora et al., 2017)(Sikora et al., 2018) This methodology allows the examination of the same receptor in two different mobility states. Briefly, for each two consecutive locations in a trajectory, a circle is drawn with its center halfway between them and the number of visits within this circle is counted. Periods that undergo confinement revisit the same region many times and thus the

recurrence statistic is very high (Sikora et al., 2017). However, during free periods, particle exploration is less compact and thus the recurrence statistic is low (also see materials and methods, Fig. 3B). After segmenting the mobile trajectories into free and confined states, the MSDs of free and confined states did not differ between experimental conditions (confined $p = 0.150$, free $p > 0.99$, Figs. 3C & D). To better understand this narrowing in the MSD values between experimental conditions after recurrence analysis segmentation, we measure the dwell times of trajectories within free and confined states. One minute of DAMGO treatment decreased the time mobile tracks spend confined from 0.515 ± 0.004 s to 0.454 ± 0.011 s ($p < 0.0001$, Fig. 3E, light blue bar) and 10 min DAMGO increased confined periods to 0.598 ± 0.006 s ($p < 0.0001$, Fig 3E, red bar).



E

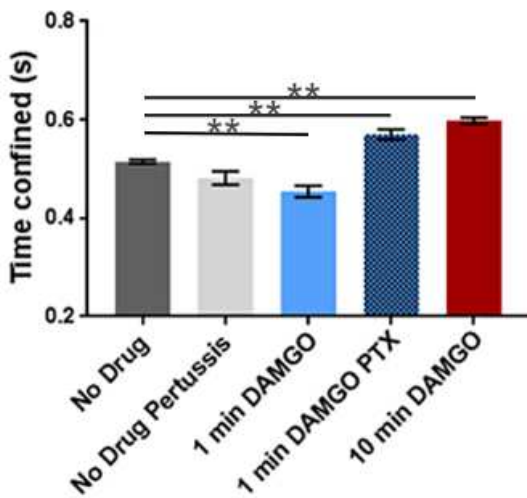


Figure 8. Differences between MSD of mobile tracks can be explained by dwell times between experimental conditions and G-protein binding. A) MSDs of mobile trajectories decreased after 10 min DAMGO treatment (10 μ M, $p = 0.031$). No drug (n=5855 trajectories), 1 min DAMGO (10 μ M, n= 697 trajectories), 10 min DAMGO (10 μ M, n=3958 trajectories). B) Example of a mobile track separated into free (blue) and confined (green) parts based on recurrence analysis (see materials and methods). A threshold value of 11 visits inside the circle was used to define confined portions (red dotted line). The right panel shows a time series of the number of visits inside the circle for the example track shown, and free and confined portions are colored as in the example track. When the trajectory is segmented into C) confined and D) free portions, the MSDs are no longer different between experimental conditions (confined $p = 0.150$, free $p > 0.99$). E) Confined dwell times decrease after acute DAMGO treatment and increase with longer DAMGO treatment. Application of 100 ng PTX increases confined dwell times. ** $p < 0.01$, Kruskal-Wallis one-way ANOVA with multiple comparisons using Bonferroni correction, error bars represent SEM for individual tracks.

The conformational shift in MORs introduced by agonist binding rapidly results in interactions with G-proteins to induce signaling. Thus, we next investigated how disrupting G-protein interactions affects the time mobile MORs spend in free and confined states to understand if confinement of mobile trajectories is associated with G-protein interaction or signaling. Cells were treated overnight with pertussis toxin (PTX, 100 ng) to inhibit G-protein/receptor interactions and dwell times in free and confined portions of mobile tracks were determined.

Treatment with PTX without subsequent application of drug did not change confined dwell times of mobile trajectories (0.482 ± 0.014 s, $p = 0.11$, $n = 9$ cells; Fig. 3E, light gray bar). 1 min DAMGO after PTX exposure increased confined time for mobile tracks (0.570 ± 0.011 s, $p < 0.0001$) compared to no drug, $n = 11$ cells, Fig. 3E, darker blue bar). Interestingly, the distribution of alpha values for DAMGO (1 min)-PTX treated cells shows no difference in the immobile fraction compared to the no drug condition (0.27 ± 0.03 , $p = 0.19$, data not shown). Changing the recurrence threshold did not affect the pattern of confinement observed in the various conditions (Fig. S3) indicating the robustness of our analysis. Therefore, G-protein binding/signaling appears to contribute specifically to the time mobile trajectories spend in the free state, and this is revealed using confinement analysis. This is consistent with the observation that G-proteins can exist in “hotspots” (Sungkaworn et al., 2017) and the receptor might dwell in such spots until G-protein binding and activation occurs.

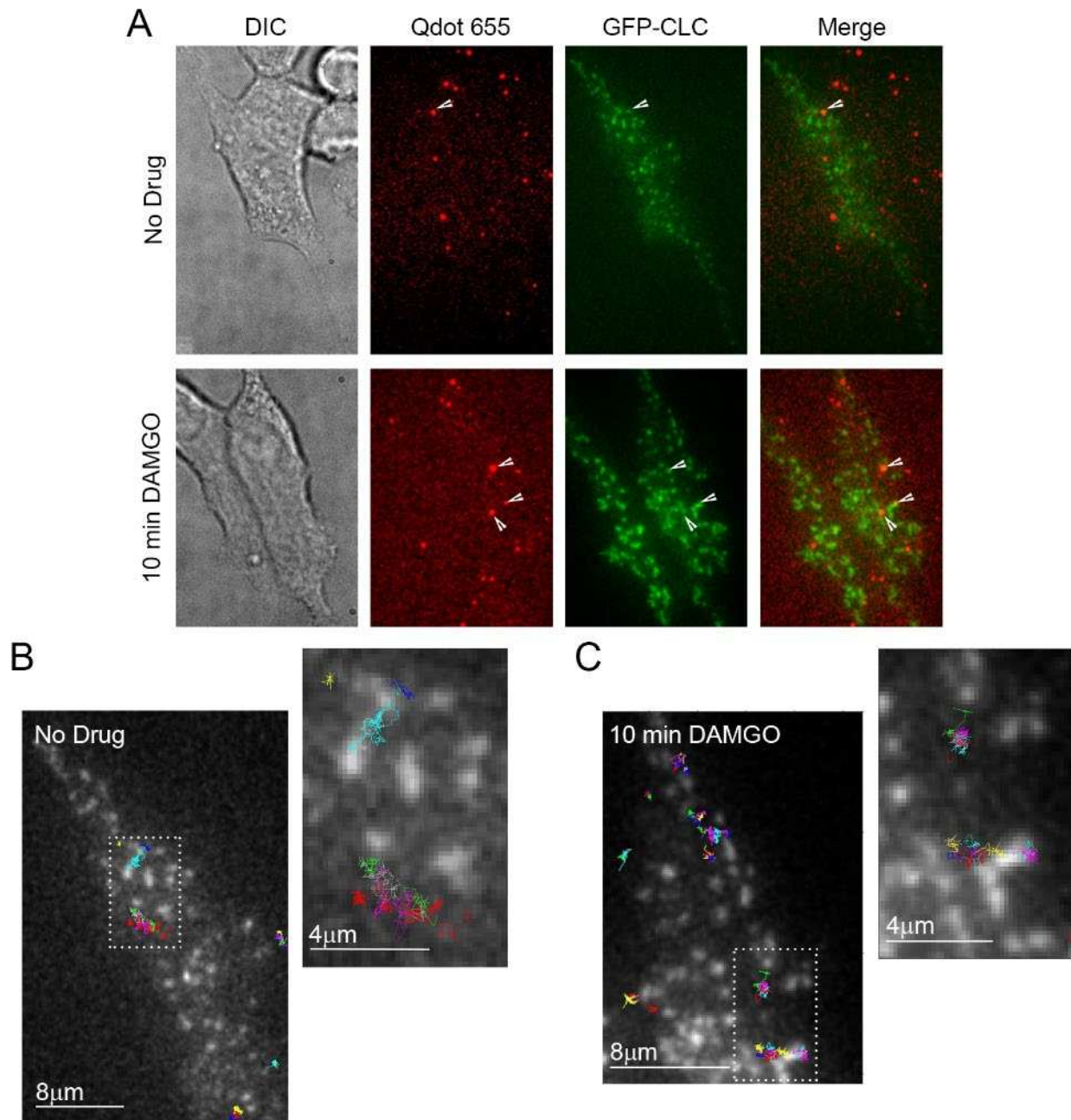


Figure 9. Representative GFP-CLC and Qdot655 co-tracking images. A) DIC and fluorescence images of cells labeled with Qdot 655-FLAG-MOR and GFP-CLC in the no drug and 10 min DAMGO (10 μ M) conditions. White arrows indicated co-localization of Qdot-labeled FLAG-MOR and GFP-CLC. B) Overlay of FLAG-MOR trajectories on GFP-CLC image from an untreated cell. White dotted boxes indicate the area represented in the zoomed image. C) FLAG-MOR trajectories overlaid on GFP-CLC from a cell treated for 10 min with 10 μ M DAMGO.

Previous work indicated that after 10 min of DAMGO exposure, half of Flag-MORs in AtT20 cells have been internalized and internalization is over half maximal (Borgland et al., 2003). Because of the observed shift towards lower α values after 10 min of DAMGO treatment in our study, we hypothesized that capture into CCPs accounted for this shift towards receptor immobility. Thus we examined colocalization of the MOR with GFP-labeled clathrin light chain (GFP-CLC) as previously described (Gaidarov et al., 1999; Kirchhausen, 2009; Weigel et al., 2011; Weigel et al., 2013). Representative images of GFP-CLC and MOR co-tracking can be seen in Fig. 4A along with representative tracks around GFP-CLC puncta in Figs. 4B&C. Ten minutes of DAMGO treatment increased colocalization with GFP-CLC (from $4.8 \pm 0.6\%$ to $12.1 \pm 1.2\%$, $p < 0.0001$, Fig. 5A), and the average distance to GFP-CLC was reduced by drug treatment (from $1.88 \pm 0.05 \mu\text{m}$ to $1.34 \pm 0.04 \mu\text{m}$, $p < 0.0001$, Fig. 5B & C). Furthermore, the distribution of distances to GFP-CLC exhibited a leftward shift in the individual track distances after 10 min DAMGO and a peak relative frequency at 0.13 and $0.75 \mu\text{m}$ for the no drug and 10 min DAMGO conditions, respectively. However, the immobile population of receptors was no more colocalized with GFP-CLC than the mobile population of receptors in the 10 min DAMGO condition (immobile $12.1 \pm 1.9\%$ vs mobile $12.1 \pm 1.5\%$, $p = 0.54$, Fig. 6A). Distance to GFP-CLC was also unchanged between mobile and immobile populations after 10 min of DAMGO treatment (immobile $1.34 \pm 0.07 \mu\text{m}$ vs. mobile $1.33 \pm 0.05 \mu\text{m}$, $p = 0.18$, Fig. 6C & D), and the distribution of distances to GFP-CLC was similar (red and green lines, Fig. 6C). Inspection of GFP-CLC colocalization within the confined and free portions of mobile receptors after 10 min of DAMGO treatment showed that neither of these populations fully accounted for GFP-CLC colocalization (confined $14.6 \pm 2.6\%$ vs. free $10.8 \pm 2.0\%$, $p = 0.99$, Fig. 6B). Distance to GFP-CLC was also unchanged between free and confined portions of mobile tracks (confined $1.29 \pm$

0.07 μm vs. free $1.38 \pm 0.07 \mu\text{m}$, $p = 0.32$, Fig. 6E & F), and the distribution of distances to GFP-CLC was similar with a slight leftward shift from 1.3 (green line) to 0.73 (red line) in the 10 min DAMGO free and confined portions, respectively (Fig. 6E). Thus, mobility itself is not a good proxy for association with CCPs.

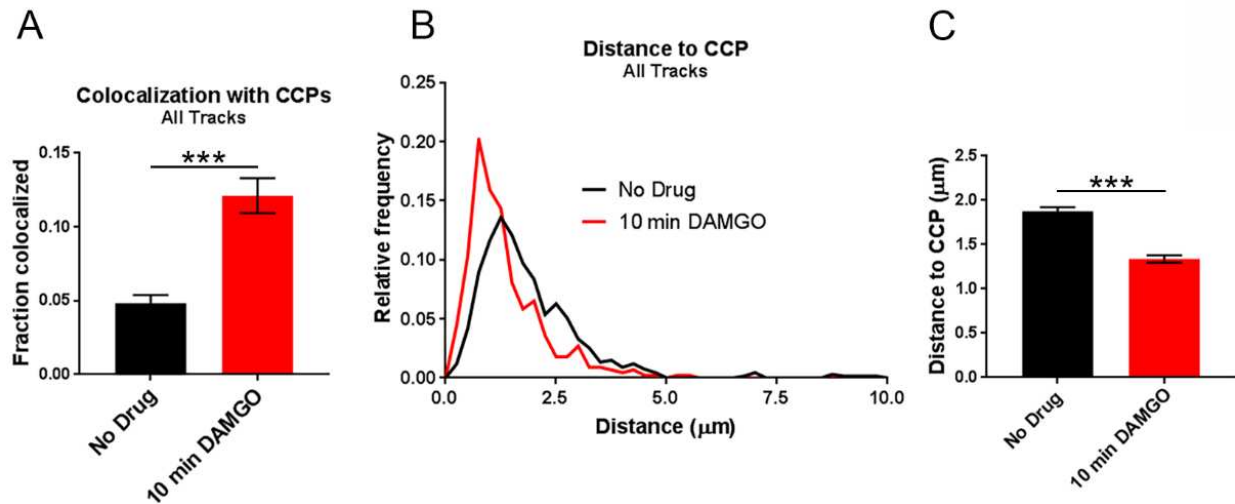


Figure 10. Colocalization with CCPs increases across all tracks after DAMGO (10 min) application. **A)** When comparing all tracks, colocalization with CCPs increases after 10 min of DAMGO treatment (10 μM). No drug $n = 9$ cells, 670 trajectories; 10 min DAMGO $n = 8$ cells, 446 trajectories. **B)** Distribution of distances to CCPs is shifted leftward after 10 min of DAMGO treatment **C)** Combined data from **(B)** showing an overall decrease in the distance to CCPs for MORs treated with DAMGO for 10 min. *** $p < 0.0001$, Kruskal-Wallis one-way ANOVA with multiple comparisons using Bonferroni correction, error bars represent SEM for individual tracks.

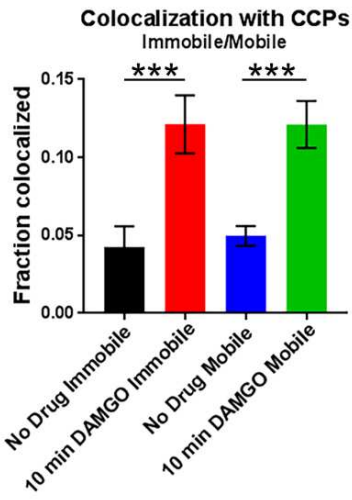
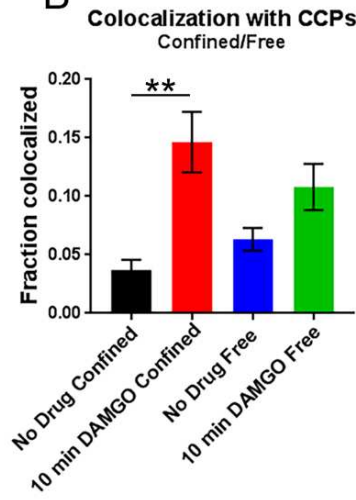
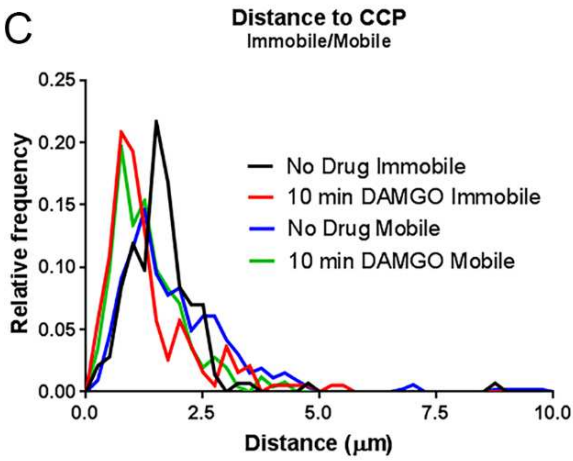
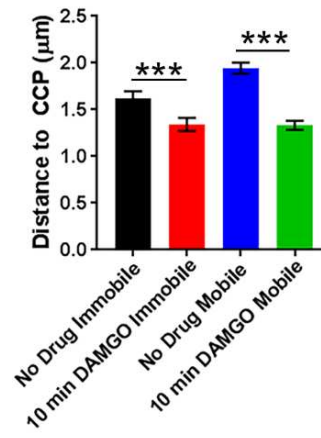
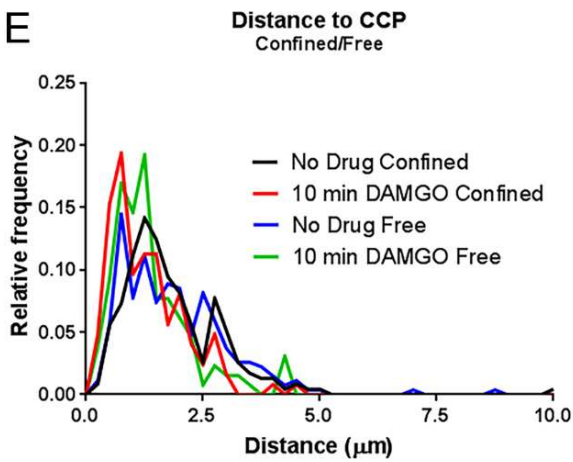
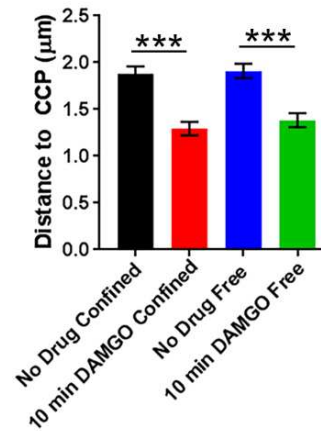
A**B****C****D****E****F**

Figure 11. Mobility state does not reflect colocalization with clathrin. **A)** Colocalization with CCPs does not differ between immobile and mobile populations within either the no drug nor the 10 min DAMGO experimental conditions. However, 10 min DAMGO (10 μ M) still increases the fraction of MORs colocalized with CCPs both in mobile and immobile populations compared to no drug. **B)** Colocalization with CCPs also does not differ between confined and free portions of mobile tracks within the 10 min DAMGO or no drug experimental conditions. **C)** Distance to CCPs is decreased between no drug and 10 min DAMGO experimental conditions, but is not different between immobile and mobile fractions within experimental conditions. **D)** Combined data from **(C)** shows a clear lack of difference for distance to CCPs between immobile and mobile fractions from no drug and DAMGO treated cells. **E)** Distance to CCPs is not changed between confined and free portions of mobile tracks within either no drug or 10 min DAMGO conditions. **F)** Combined data from **(E)**. $**p < 0.01$, $***p < 0.0001$, Kruskal-Wallis one-way ANOVA with multiple comparisons using Bonferroni correction, error bars represent SEM for individual tracks.

Discussion

The present single-molecule study was undertaken to characterize time-dependent changes in FLAG-MOR diffusion induced by acute and extended applications of the MOR agonists morphine and DAMGO and to understand if specific mobility states of the MOR could clearly reflect interactions with specific effectors. Under basal conditions, both mobile and immobile populations of FLAG-MORs were detected, evident in the bimodal distribution of the anomalous exponent α and consistent with recent work showing that MORs exist both in lipid-enriched nanodomains and more freely-distributed in the plasma membrane prior to agonist binding (Rogacki et al., 2018). The bimodal distribution of FLAG-MORs observed in the present study was skewed towards more mobile tracks when cells were exposed to a maximal concentration of DAMGO (10 μ M) for one minute. However, DAMGO treatment for ten minutes resulted in a dramatic increase in the proportion of immobile FLAG-MORs. Further, overall track mobility did not change in response to 1 min of morphine (10 μ M) treatment, but after 10 min of morphine treatment, tracks shifted towards immobility (but see Fig S3 for alterations in the 10 min morphine pattern with the k means selected threshold). Closer

inspection of mobile ($\alpha > 0.27$) tracks revealed that differences in MSD exist between experimental conditions even within the mobile subpopulation of receptors, and that this difference in MSD can be explained by an increase in confined dwell times of receptors treated with DAMGO for ten minutes. In contrast, MORs treated with DAMGO for one minute show a decrease in confined dwell times, and blockade of G-protein binding with pertussis toxin abrogates this decrease in confined period dwell times. Finally, CCP colocalization occurred similarly across all mobility states inspected so that a single mobility state could not fully account for colocalization of FLAG-MORs with CCPs.

Some studies have shown that Qdots can reduce molecule mobility and alter molecular interactions (Abraham et al., 2017; Howarth et al., 2005). In this study, great care was taken during the labeling approach to avoid receptor crosslinking and to ensure that the MOR was still undergoing G-protein coupling and recruitment to GFP-CLC when expected. Further, experiments with Dermorphin-488 and correlation of MSD and fluorescence intensity ensured that crosslinking likely plays a minimal role in these experiments. However, it is still possible that Qdots have slowed diffusion compared to an unlabeled MOR. Nevertheless, we were interested in the dynamic changes in response to drug application as opposed to basal receptor mobility and changes in mobility were observed in response to drug. Thus, our observations still stand even if Qdots have slowed mobility.

Previous studies of MOR mobility in response to agonist treatment have examined mobility at a minimum of ten minutes post-drug, although acute signaling processes occur much faster than this. In AtT20 cells, the receptor has already undergone G-protein coupling, desensitization, and internalization at this time point (Borgland et al., 2003). Thus, we were interested in understanding how MOR mobility is changed before internalization has begun and while the

process of signaling and desensitization are occurring. The marked difference in receptor mobility depending upon duration of agonist exposure reveals that mobility is likely dependent on receptor interactions with many different intracellular partners that play distinct roles depending upon the time of drug application. The difference in alpha value distribution between morphine (1 min) and DAMGO (1 min) is particularly interesting, as these agonists have distinct signaling characteristics. The fact that DAMGO, but not morphine, increased the mobile fraction of receptors at 1 min may be attributable to the relatively lower efficacy of morphine compared to DAMGO for recruiting G-proteins at the MOR (Kelly, 2013). However, it is also possible that morphine's lower ability to recruit other effectors such as specific kinases or β -arrestins could play a role in the lack of shift towards mobility at 1 min.

Upon inspection of mobile trajectories in free and confined states, it was initially surprising to note that acute DAMGO treatment resulted in a decrease in the time that mobile tracks spent confined. However, a recent study by Sungkaworn et al (Sungkaworn et al., 2017) revealed that G-protein coupled receptors and their respective G-proteins couple at specific hot spots at least partially defined by actin networks (Sungkaworn et al., 2017). It is possible that signaling receptors in AtT20 cells quickly hop between G-protein hot spots after activation, thus decreasing their confined dwell times. This possibility is supported by the fact that PTX increased confinement periods compared to baseline levels, potentially suggesting that ligand-bound receptors are recruited to hot spots but cannot leave unless they have encountered a G-protein. However, it should be noted that the change in dwell times between 1 min DAMGO and no drug conditions is small, therefore binding to other signaling partners likely also plays a role in how long a receptor remains confined or free.

Despite the difference in acute mobility shifts, both DAMGO and morphine increased the immobile fraction of receptors after 10 min of exposure. Morphine is known to be poor at inducing receptor internalization compared to DAMGO (Arden et al., 1995; Williams et al., 2001), yet track mobility still decreased after 10 min of exposure. At this time point, both DAMGO and morphine can cause receptor desensitization. Thus, the shift towards receptor immobility likely reflects interactions related to desensitization which can be agonist-specific and involve various mechanisms. Kinases such as protein kinase C are known to be involved in receptor desensitization and have been found to restrict the distribution of the MOR in cell membranes (Halls et al., 2016). It is possible that other kinases, association with lipid rafts (Zhao et al., 2006), or binding to structural proteins (Treppiedi et al., 2018) could contribute to immobility as well. Future studies using receptors that do not desensitize, such as non-phosphorylatable mutants (Birdsong et al., 2015; Yousuf et al., 2015), could best parse apart the contribution of desensitization and G-protein coupling to transient confinement in mobile MOR trajectories.

The present study shows increased colocalization of MORs with clathrin after 10 min of DAMGO exposure, consistent with the ability of DAMGO to strongly induce internalization. Morphine-induced colocalization was not examined because of its low ability to induce internalization and because we were unable to attribute any particular mobility state to receptor capture into CCPs. Our finding that colocalization with CCPs cannot fully account for any single mobility state suggests that this may be true at other effectors as well. Therefore, the immobile fraction of receptors observed after 10 min DAMGO treatment is likely due to the contribution of several effectors.

Because CCP colocalization was not associated with a particular mobility population that we identified, it is unlikely that single-particle tracking of the MOR alone would be a good proxy for distinct receptor signaling states. However, concurrent tracking of the MOR with its signaling effectors may be useful as a tool for studies of receptor/effector interaction. For example, concurrent single-particle tracking of the MOR, G-proteins, and β -arrestin or CCPs would allow for screening of ligand bias within the same cell with high temporal resolution and individual receptor sensitivity.

Materials and Methods

Cell Culture and Transfection

AtT20 cells stably expressing the FLAG-MOR (provided by Dr. MacDonald Christie, University of Sydney) were maintained at 37°C/5% CO₂ in Dulbecco's Modified Eagle Medium (DMEM) supplemented with 10% fetal bovine serum (ATCC), L-Glutamine (2 mM L-alanyl-L-glutamine), and 1% penicillin/streptomycin. Once cells reached confluence they were exposed to 0.25% trypsin-EDTA (Gibco) and re-plated at lower density. Cells were maintained for no more than 12 passages beyond their original plating.

N-terminally tagged GFP-clathrin light chain (GFP-CLC) was transfected into cells using 1:500 Lipofectamine (Invitrogen), 1:100 Opti-MEM (Gibco), and 1:1000 plasmid into 2 mL of culture media. Cells were incubated overnight, and all cells were imaged within 24 hours of transfection in order to avoid problems with overexpression. For experiments in which G-protein activity was inhibited, cells were treated with 100 ng pertussis toxin (Thermo Fisher) overnight. Cells were imaged within 24 hours of toxin treatment.

Live-Cell Labeling of the MOR

To prepare for imaging, AtT20 cells were diluted and plated on glass-bottom dishes (MatTek, Ashland, MA) containing the same supplemented DMEM solution as described above. Cells were imaged on the fourth day after plating. Labeling was performed immediately before imaging. Cells were rinsed multiple times with a saline solution containing: 35 mM KCl, 120 mM NaCl, 1 mM CaCl₂, 25 mM HEPES, 10 mM glucose, and pH was adjusted to 7.4 (NaOH). After thoroughly washing to remove DMEM, the plates were filled with saline containing 1% (w/v) bovine serum albumin (BSA, Sigma A7030) and incubated for 10 min at 37°C. The cells were incubated for 5 min at 37°C in the presence of a biotinylated anti-FLAG antibody (final concentration 1 µg/mL, BioM2 Anti-FLAG, Sigma F9291). After multiple rinses with saline (still containing 1% BSA) to remove unbound antibody, the cells were then incubated for 8 min at 37°C in the presence of streptavidin-coated quantum dots (1:10000, final concentration of 100 pM, Streptavidin Qdot 565, Life Technologies Q10133MP; or for two-color TIRF imaging Streptavidin Qdot 655, Life Technologies Q10121MP). The cells were rinsed multiple times with saline lacking BSA to remove unbound SA Qdot and BSA from the culture dish. In the 10 min DAMGO condition and Naloxone condition, 10 µM DAMGO or 1 µM Naloxone, respectively, was applied immediately after labeling. Drug was applied 10 min after the final wash on the microscope stage in the 1 min (10 µM) DAMGO condition. In experiments where morphine was used as the agonist rather than DAMGO, morphine (10 µM) was applied as described above for DAMGO. Many cells did not exhibit Qdot fluorescence upon imaging, so only those that had a moderate amount of labeling were chosen for imaging.

Confocal Microscopy

Single-channel imaging was carried on a spinning disk confocal microscope (Olympus IX83, Olympus UPlanSApo 100x/1.40 oil objective, Yokogawa CSU-X spinning disk, Andor

iXon Ultra 897 EMCCD camera) equipped with a temperature control unit (INU Stage Top Incubator, Tokai Hit, Shizuoka-ken, Japan). All culture dishes were kept in the chamber at 37°C for 10 min before images were acquired. This was done to ensure that all dishes were imaged at the same time after labeling. Qdot 565 was excited using a 488 nm laser and acquired with an emission filter (600/50). Videos were acquired at a rate of 20 frames/s.

TIRF Microscopy

GFP-CLC was found to bleach rapidly using the spinning disk confocal, so for concurrent imaging of GFP-CLC and the MOR, total internal reflection fluorescence (TIRF) microscopy was performed on a Nikon Eclipse Ti fluorescence microscope equipped with a Perfect-Focus system, AOTF-controlled 488 and 647 nm diode lasers, a 512x512 Andor iXon EMCCD DU-897 camera, and Plan Apo TIRF 100, NA 1.49 objective. Temperature was maintained at 37°C using Zeiss stage and objective heaters. Qdot 655 was used instead of Qdot 565 to avoid bleed-through into the 488 channel for imaging CLC-GFP. To avoid analyzing Qdots that occasionally were stuck to the culture dish glass, trajectories with MSDs characteristic of glass-stuck particles were removed before analysis. A sample of glass-stuck Qdots were imaged and found to have mostly MSDs below $0.0165 \mu\text{M}^2$ (Fig. S4A). Therefore, all trajectories with an MSD less than $0.0165 \mu\text{m}^2$ (measured up to a lag time of 2.5 s) were excluded from the data prior to analysis.

Image Processing and Analysis

Images were background-subtracted in ImageJ software. A Gaussian kernel filter was then applied to the images using a standard deviation of 0.8 pixels. After processing, Qdot-labeled MORs were detected and tracked using the u-track algorithm in MATLAB as previously described (Jaqaman et al., 2008). Detection of CLC-GFP puncta was also performed using the u-

track algorithm. MOR trajectories less than 60 frames in length were excluded from further analysis.

Trajectories were analyzed in terms of the time-averaged mean square displacement (TA-MSD) using algorithms written in MATLAB. For an individual trajectory the TA-MSD is obtained by averaging over the time series,

$$\overline{\delta^2(t_{lag})} = \frac{1}{T - t_{lag}} \int_0^{T-t_{lag}} |\mathbf{r}(t + t_{lag}) - \mathbf{r}(t)|^2 dt \quad (1)$$

where $\overline{\delta^2(t_{lag})}$ is the TA – MSD, $\mathbf{r}(t)$ is the two – dimensional position of the particle at time t , t_{lag} is the lag time (the time over which the displacement is computed), and T is the duration of the trajectory. For normal diffusion processes, the MSD scales linearly in lag time, namely in two dimensions $\overline{\delta^2(t_{lag})} = 4Dt_{lag}$ where D is the diffusion coefficient. However, measurements in live cells often exhibit anomalous diffusion, which manifests as a deviation from this simple law (Hofling and Franosch,2013; Krapf,2015; Metzler et al.,2014), and is characterized by a non-linear scaling of the MSD , $\overline{\delta^2(t_{lag})} = K_\alpha t_{lag}^\alpha$, where α is the anomalous exponent and K_α is the generalized diffusion coefficient which has units of $\text{cm}^2/\text{s}^\alpha$. Processes with $0 < \alpha < 1$ are considered subdiffusive, and those with $\alpha > 1$ are considered superdiffusive. Detection uncertainty increases the MSD by a constant value. Given a standard deviation σ of the detected position in both x and y direction due to uncertainty in the localization, the MSD is then

$$\overline{\delta^2(t_{lag})} = K_\alpha t_{lag}^\alpha + 4\sigma^2 \quad (2)$$

In order to obtain α and K_α from individual trajectories, we first obtained an average σ of 0.02 with the u-track algorithm and subtracted $4\sigma^2$ to obtain a static error-corrected MSD (see Fig.

S4B for a histogram of localization uncertainties, σ). Then we perform a linear regression in log-log plot to find α and K_α .

To separate mobile tracks into free and confined portions, recurrence analysis was performed as described previously (Sikora et al., 2017). Briefly, a circle is constructed equal to the diameter of two consecutive points in a trajectory, and the number of subsequent visits by the particle into this circle was calculated. Portions of tracks with subsequent visits ≥ 11 were classified as confined portions of mobile trajectories, and those that did not reach this threshold were classified as free portions. This threshold was determined by identifying the minimum number of visits at which most immobile ($\alpha < 0.27$) trajectories were classified as confined.

To calculate the colocalization and distance of the MOR to CCPs, spatial coordinates of GFP-CLC puncta were determined using the detection output in u-track. The coordinates of GFP-CLC puncta were then compared to the coordinates of MOR tracks files at each frame. MOR coordinates that were located within 3 pixels of the closest GFP-CLC pit center ($0.48 \mu\text{m}$) were considered to be colocalized.

Statistical Analysis

Data sets were compared using an unpaired Kruskal-Wallis one way ANOVA with post hoc tests performed with Bonferroni correction, and p values of less than 0.05 were considered significant. Prism was used to perform statistical tests as well as to obtain descriptive statistics. Compiled data are shown as the mean \pm SEM, or as histograms.

References

Abraham, L., Lu, H. Y., Falcao, R. C., Scurll, J., Jou, T., Irwin, B., . . . Coombs, D. (2017). Limitations of Qdot labelling compared to directly-conjugated probes for single particle tracking of B cell receptor mobility. *Sci Rep*, 7(1), 11379.

- Akin, E. J., Sole, L., Johnson, B., Beheiry, M. E., Masson, J. B., Krapf, D., & Tamkun, M. M. (2016). Single-Molecule Imaging of Nav1.6 on the Surface of Hippocampal Neurons Reveals Somatic Nanoclusters. *Biophys J*, *111*(6), 1235-1247.
- Arden, J. R., Segredo, V., Wang, Z., Lamah, J., & Sadee, W. (1995). Phosphorylation and agonist-specific intracellular trafficking of an epitope-tagged mu-opioid receptor expressed in HEK 293 cells. *J Neurochem*, *65*(4), 1636-1645.
- Arttamangkul, S., Alvarez-Maubecin, V., Thomas, G., Williams, J. T., & Grandy, D. K. (2000). Binding and internalization of fluorescent opioid peptide conjugates in living cells. *Mol Pharmacol*, *58*(6), 1570-1580.
- Baker, A., Sauliere, A., Dumas, F., Millot, C., Mazeret, S., Lopez, A., & Salome, L. (2007). Functional membrane diffusion of G-protein coupled receptors. *Eur Biophys J*, *36*(8), 849-860.
- Birdsong, W. T., Arttamangkul, S., Bunzow, J. R., & Williams, J. T. (2015). Agonist Binding and Desensitization of the mu-Opioid Receptor Is Modulated by Phosphorylation of the C-Terminal Tail Domain. *Mol Pharmacol*, *88*(4), 816-824.
- Borgland, S. L., Connor, M., Osborne, P. B., Furness, J. B., & Christie, M. J. (2003). Opioid agonists have different efficacy profiles for G protein activation, rapid desensitization, and endocytosis of mu-opioid receptors. *J Biol Chem*, *278*(21), 18776-18784.
- Calizo, R. C., & Scarlata, S. (2013). Discrepancy between fluorescence correlation spectroscopy and fluorescence recovery after photobleaching diffusion measurements of G-protein-coupled receptors. *Anal Biochem*, *440*(1), 40-48.
- Carayon, K., Mouledous, L., Combedazou, A., Mazeret, S., Haanappel, E., Salome, L., & Mollereau, C. (2014). Heterologous regulation of Mu-opioid (MOP) receptor mobility in the membrane of SH-SY5Y cells. *J Biol Chem*, *289*(41), 28697-28706.
- Celver, J., Xu, M., Jin, W., Lowe, J., & Chavkin, C. (2004). Distinct domains of the mu-opioid receptor control uncoupling and internalization. *Mol Pharmacol*, *65*(3), 528-537.
- Dang, V. C., & Christie, M. J. (2012). Mechanisms of rapid opioid receptor desensitization, resensitization and tolerance in brain neurons. *Br J Pharmacol*, *165*(6), 1704-1716.
- Daumas, F., Destainville, N., Millot, C., Lopez, A., Dean, D., & Salome, L. (2003). Confined diffusion without fences of a g-protein-coupled receptor as revealed by single particle tracking. *Biophys J*, *84*(1), 356-366.
- Gaidarov, I., Santini, F., Warren, R. A., & Keen, J. H. (1999). Spatial control of coated-pit dynamics in living cells. *Nat Cell Biol*, *1*(1), 1-7.
- Golebiewska, U., Johnston, J. M., Devi, L., Filizola, M., & Scarlata, S. (2011). Differential response to morphine of the oligomeric state of mu-opioid in the presence of delta-opioid receptors. *Biochemistry*, *50*(14), 2829-2837.
- Haberstock-Debic, H., Wein, M., Barrot, M., Colago, E. E., Rahman, Z., Neve, R. L., . . . Svingos, A. L. (2003). Morphine acutely regulates opioid receptor trafficking selectively in dendrites of nucleus accumbens neurons. *J Neurosci*, *23*(10), 4324-4332.
- Halls, M. L., Yeatman, H. R., Nowell, C. J., Thompson, G. L., Gondin, A. B., Civciristov, S., . . . Canals, M. (2016). Plasma membrane localization of the mu-opioid receptor controls spatiotemporal signaling. *Sci Signal*, *9*(414), ra16.
- Hofling, F., & Franosch, T. (2013). Anomalous transport in the crowded world of biological cells. *Rep Prog Phys*, *76*(4), 046602.

- Howarth, M., Takao, K., Hayashi, Y., & Ting, A. Y. (2005). Targeting quantum dots to surface proteins in living cells with biotin ligase. *Proceedings of the National Academy of Sciences of the United States of America*, *102*(21), 7583-7588.
- Jaqaman, K., Loerke, D., Mettlen, M., Kuwata, H., Grinstein, S., Schmid, S. L., & Danuser, G. (2008). Robust single-particle tracking in live-cell time-lapse sequences. *Nat Methods*, *5*(8), 695-702.
- Kelly, E. (2013). Efficacy and ligand bias at the mu-opioid receptor. *Br J Pharmacol*, *169*(7), 1430-1446.
- Kirchhausen, T. (2009). Imaging endocytic clathrin structures in living cells. *Trends Cell Biol*, *19*(11), 596-605.
- Knapman, A., & Connor, M. (2015). Fluorescence-based, high-throughput assays for mu-opioid receptor activation using a membrane potential-sensitive dye. *Methods Mol Biol*, *1230*, 177-185.
- Knapman, A., Santiago, M., Du, Y. P., Bennallack, P. R., Christie, M. J., & Connor, M. (2013). A continuous, fluorescence-based assay of mu-opioid receptor activation in AtT-20 cells. *J Biomol Screen*, *18*(3), 269-276.
- Krapf, D. (2015). Mechanisms underlying anomalous diffusion in the plasma membrane. *Curr Top Membr*, *75*, 167-207.
- Krapf, D. (2018). Compartmentalization of the plasma membrane. *Curr Opin Cell Biol*, *53*, 15-21.
- Manzo, C., & Garcia-Parajo, M. F. (2015). A review of progress in single particle tracking: from methods to biophysical insights. *Rep Prog Phys*, *78*(12), 124601.
- Melkes, B., Hejnova, L., & Novotny, J. (2016). Biased mu-opioid receptor agonists diversely regulate lateral mobility and functional coupling of the receptor to its cognate G proteins. *Naunyn Schmiedebergs Arch Pharmacol*, *389*(12), 1289-1300.
- Metz, M. J., Pennock, R. L., Krapf, D., & Hentges, S. T. (2019). Temporal dependence of shifts in mu opioid receptor mobility at the cell surface after agonist binding observed by single-particle tracking. *Sci Rep*, *9*(1), 7297.
- Metzler, R., Jeon, J. H., Cherstvy, A. G., & Barkai, E. (2014). Anomalous diffusion models and their properties: non-stationarity, non-ergodicity, and ageing at the centenary of single particle tracking. *Phys Chem Chem Phys*, *16*(44), 24128-24164.
- Michalet, X., Pinaud, F. F., Bentolila, L. A., Tsay, J. M., Doose, S., Li, J. J., . . . Weiss, S. (2005). Quantum dots for live cells, in vivo imaging, and diagnostics. *Science*, *307*(5709), 538-544.
- Pinaud, F., Clarke, S., Sittner, A., & Dahan, M. (2010). Probing cellular events, one quantum dot at a time. *Nat Methods*, *7*(4), 275-285.
- Rogacki, M. K., Golfetto, O., Tobin, S. J., Li, T., Biswas, S., Jorand, R., . . . Vukojevic, V. (2018). Dynamic lateral organization of opioid receptors (kappa, muwt and muN40D) in the plasma membrane at the nanoscale level. *Traffic*.
- Roumy, M., Lorenzo, C., Mazeret, S., Bouchet, S., Zajac, J. M., & Mollereau, C. (2007). Physical association between neuropeptide FF and micro-opioid receptors as a possible molecular basis for anti-opioid activity. *J Biol Chem*, *282*(11), 8332-8342.
- Sauliere-Nzeh Ndong, A., Millot, C., Corbani, M., Mazeret, S., Lopez, A., & Salome, L. (2010). Agonist-selective dynamic compartmentalization of human Mu opioid receptor as revealed by resolute FRAP analysis. *J Biol Chem*, *285*(19), 14514-14520.

- Sikora, G., Wylomanska, A., Gajda, J., Sole, L., Akin, E. J., Tamkun, M. M., & Krapf, D. (2017). Elucidating distinct ion channel populations on the surface of hippocampal neurons via single-particle tracking recurrence analysis. *Phys Rev E*, *96*(6-1), 062404.
- Sikora, G., Wylomanska, A., & Krapf, D. (2018). Recurrence statistics for anomalous diffusion regime change detection. *Computational Statistics & Data Analysis*, *128*, 380-394.
- Stoeber, M., Jullie, D., Lobingier, B. T., Laeremans, T., Steyaert, J., Schiller, P. W., . . . von Zastrow, M. (2018). A Genetically Encoded Biosensor Reveals Location Bias of Opioid Drug Action. *Neuron*, *98*(5), 963-976 e965.
- Sungkaworn, T., Jobin, M. L., Burnecki, K., Weron, A., Lohse, M. J., & Calebiro, D. (2017). Single-molecule imaging reveals receptor-G protein interactions at cell surface hot spots. *Nature*, *550*(7677), 543-547.
- Suzuki, K., Ritchie, K., Kajikawa, E., Fujiwara, T., & Kusumi, A. (2005). Rapid hop diffusion of a G-protein-coupled receptor in the plasma membrane as revealed by single-molecule techniques. *Biophys J*, *88*(5), 3659-3680.
- Thompson, G. L., Lane, J. R., Coudrat, T., Sexton, P. M., Christopoulos, A., & Canals, M. (2016). Systematic analysis of factors influencing observations of biased agonism at the mu-opioid receptor. *Biochem Pharmacol*, *113*, 70-87.
- Tobin, S. J., Wakefield, D. L., Terenius, L., Vukojevic, V., & Jovanovic-Taliman, T. (2018). Ethanol and Naltrexone Have Distinct Effects on the Lateral Nano-organization of Mu and Kappa Opioid Receptors in the Plasma Membrane. *ACS Chem Neurosci*.
- Treppiedi, D., Jobin, M. L., Peverelli, E., Giardino, E., Sungkaworn, T., Zabel, U., . . . Calebiro, D. (2018). Single-Molecule Microscopy Reveals Dynamic FLNA Interactions Governing SSTR2 Clustering and Internalization. *Endocrinology*, *159*(8), 2953-2965.
- Vukojevic, V., Ming, Y., D'Addario, C., Hansen, M., Langel, U., Schulz, R., . . . Terenius, L. (2008). Mu-opioid receptor activation in live cells. *FASEB J*, *22*(10), 3537-3548.
- Weigel, A. V., Simon, B., Tamkun, M. M., & Krapf, D. (2011). Ergodic and nonergodic processes coexist in the plasma membrane as observed by single-molecule tracking. *Proc Natl Acad Sci U S A*, *108*(16), 6438-6443.
- Weigel, A. V., Tamkun, M. M., & Krapf, D. (2013). Quantifying the dynamic interactions between a clathrin-coated pit and cargo molecules. *Proc Natl Acad Sci U S A*, *110*(48), E4591-4600.
- Weron, A., Burnecki, K., Akin, E. J., Sole, L., Balcerek, M., Tamkun, M. M., & Krapf, D. (2017). Ergodicity breaking on the neuronal surface emerges from random switching between diffusive states. *Sci Rep*, *7*(1), 5404.
- Williams, J. T., Christie, M. J., & Manzoni, O. (2001). Cellular and synaptic adaptations mediating opioid dependence. *Physiol Rev*, *81*(1), 299-343.
- Williams, J. T., Ingram, S. L., Henderson, G., Chavkin, C., von Zastrow, M., Schulz, S., . . . Christie, M. J. (2013). Regulation of mu-opioid receptors: desensitization, phosphorylation, internalization, and tolerance. *Pharmacol Rev*, *65*(1), 223-254.
- Yousuf, A., Miess, E., Sianati, S., Du, Y. P., Schulz, S., & Christie, M. J. (2015). Role of Phosphorylation Sites in Desensitization of micro-Opioid Receptor. *Mol Pharmacol*, *88*(4), 825-835.
- Yu, Y. J., Dhavan, R., Chevalier, M. W., Yudowski, G. A., & von Zastrow, M. (2010). Rapid delivery of internalized signaling receptors to the somatodendritic surface by sequence-specific local insertion. *J Neurosci*, *30*(35), 11703-11714.

Zhao, H., Loh, H. H., & Law, P. Y. (2006). Adenylyl cyclase superactivation induced by long-term treatment with opioid agonist is dependent on receptor localized within lipid rafts and is independent of receptor internalization. *Mol Pharmacol*, 69(4), 1421-1432.

Funding for these studies was provided by National Institutes of Health grants R01DA032562 (S.T.H.) and F31DA035586 (R.L.P.), as well as National Science Foundation grants DGE-1321845 (M.J.M) and 1401432 (D.K.).

CHAPTER 3—MODULATION OF ENDOGENOUS ENDORPHIN SYSTEMS USING LOW DOSE NALTREXONE

Preamble

A portion of the following material was published in the May/June 2021 edition of eNeuro under the title “Reported benefits of low-dose naltrexone appear to be independent of the endogenous opioid system involving proopiomelanocortin neurons and β -endorphin” (Metz, Daimon, & Hentges, 2021). A brief, unpublished background introduces the topic of low dose naltrexone (LDN). Following the background section, the published work is reproduced as it appeared in the original journal article.

Background

Work from the previous chapter showed that specific observation of desensitization is not possible using only single particle tracking methods and that more complex assays tracking multiple membrane proteins at once may be required. During our observations, however, it was clear that even under baseline conditions, MORs existed in multiple mobility states. While these may not directly correlate to specific signaling states, it suggests that the MOR population is not homogenous even at baseline, and that there is potential to nudge signaling in a particular direction, such as toward increased sensitivity to agonist application. Interestingly, one existing therapeutic option for chronic pain, termed LDN, may be an intervention that encourages the sensitization of MORs and may even modulate the endogenous opioid system by affecting MORs on POMC neurons that produce β -endorphin.

Potential for sensitization of the MOR by low dose naltrexone

As an antagonist, naltrexone prevents signaling of the MOR when bound. While the absence of signaling initially seems like it would not cause any downstream effects on the cell, it has been

shown that long term antagonism of MORs can actually change expression patterns and intracellular signaling (Díaz et al., 2002; Markowitz et al., 1992; Panigrahi et al., 2019; Tempel et al., 1984; Unterwald et al., 1998; Unterwald et al., 1995). Increased MOR expression can increase signal output upon activation by agonists, and sensitization has been shown in several types of GPCRs even in the absence of expression changes (Jordan & Devi, 1999; Chen et al., 2020; Lambert et al., 2010). Of course, any lasting changes induced by high dose naltrexone must be examined after naltrexone itself has been washed out, as otherwise MOR signaling would be completely blocked by the presence of antagonist. LDN treatment provides an alternative to this blockage issue, as LDN treatment may also confer intracellular effects by temporarily binding MORs to confer downstream signaling effects and then washing out easily due to its low dose and the pulsatile nature of administration. The following chapter examines this possibilities by examining MOR and endogenous opioid system activation in a mouse model of LDN administration.

Published Work

Reported Benefits of Low-Dose Naltrexone Appear to Be Independent of the Endogenous Opioid System Involving Proopiomelanocortin Neurons and β -Endorphin

Summary

Naltrexone is an opioid receptor antagonist approved for the treatment of alcohol and opioid use disorders at doses of 50-150 mg per day. Naltrexone has also been prescribed at much lower doses (3-6 mg per day) for the off-label treatment of inflammation and pain. Currently, a compelling mechanistic explanation for the reported efficacy of low dose naltrexone (LDN) is lacking and none of the proposed mechanisms can explain patient reports of improved mood and sense of well-being. Here, we examined the possibility that LDN might alter the activity of the

endogenous opioid system involving proopiomelanocortin (POMC) neurons in the arcuate nucleus of the hypothalamus in male and female mice. Known actions of POMC neurons could account for changes in pain perception and mood. However, using electrophysiologic, imaging and peptide measurement approaches, we found no evidence for such a mechanism. LDN did not change the sensitivity of opioid receptors regulating POMC neurons, the production of the β -endorphin precursor *Pomc* mRNA, nor the release of β -endorphin into plasma. Spontaneous post-synaptic currents onto POMC neurons were slightly decreased after LDN treatment and GCaMP fluorescent signal, a proxy for intracellular calcium levels, was slightly increased. However, LDN treatment did not appear to change POMC neuron firing rate, resting membrane potential, nor action potential threshold. Therefore, LDN appears to have only slight effects on POMC neurons that do not translate to changes in intrinsic excitability or baseline electrical activity and mechanisms beyond POMC neurons and altered opioid receptor sensitivity should continue to be explored.

Significance Statement

Naltrexone blocks opioid receptor activity and is used for the treatment of alcohol and opioid use disorders but is also prescribed at lower doses to treat inflammation and pain. A compelling mechanistic explanation for the reported efficacy of low dose naltrexone (LDN) is lacking, and understanding the central effects of LDN is important, both for basic science and to inform future applications of LDN for central disorders. We hypothesized that LDN might alter the activity of endogenous opioid systems in proopiomelanocortin (POMC) neurons of the hypothalamus. However, we found no evidence for such a mechanism and LDN appears to only slightly affect POMC neurons. We conclude that future studies should shift focus to other opioid systems outside of POMC neurons.

Introduction

Naltrexone is an antagonist of opioid receptors that has high binding affinity for the mu opioid receptor (MOR), although it also binds delta and kappa opioid receptors (Raynor et al., 1994). Naltrexone was approved for use at doses of 50-150 mg to lessen relapse to alcohol and opioid use, which is efficacious largely due to blocking the rewarding actions of these drugs heavily mediated through MORs (Gold et al., 1982; Matthes et al., 1996). In addition to use in treatment for substance use disorders, naltrexone has been prescribed at a much lower dose (3-6 mg) for off-label use in immune-related pain disorders and cancer (Toljan and Vrooman, 2018; Trofimovitch and Baumrucker, 2019). The reported efficacy for low-dose naltrexone (LDN) is paradoxical; MOR agonists, not antagonists, convey analgesic and rewarding properties that can be blocked by application of antagonists. Nonetheless, many anecdotal reports (Bolton et al., 2020; Chopra and Cooper, 2013; Ghai et al., 2014; Leonard et al., 2017; Ramanathan et al., 2012; Zappaterra et al., 2020), post-hoc studies (Ludwig et al., 2016; Raknes et al., 2018; Raknes and Småbrekke, 2017, 2019), and limited clinical trials (Brewer et al., 2018; Lie et al., 2018; Younger and Mackey, 2009; Younger et al., 2013) suggest that LDN may be useful for treating chronic pain and inflammation. Further, in many of these studies patients report effects such as improved feelings of well-being and vivid dreams (Bolton et al., 2020; Brewer et al., 2018; Lie et al., 2018; Younger and Mackey, 2009; Younger et al., 2013; Zappaterra et al., 2020), and recently LDN has been tested as an adjunct therapy for patients living with depression (Mischoulon et al., 2017) with some promising preliminary results. In the context of naltrexone's antagonist functions, these benefits are also surprising, as opioid receptor agonism typically induces feelings of euphoria and well-being.

To date, the beneficial effects of LDN have been primarily attributed to inhibition of peripheral inflammatory responses mediated through the Toll-like receptor 4, although a mechanism whereby ultra-LDN (<1 µg/d) acts on a MOR scaffolding protein, filamin A, has also been proposed (Burns and Wang, 2010; Wang and Burns, 2009). Patients receiving LDN often report subjective benefits in the absence of clear objective measures indicative of improvement (Patten et al., 2018). It may be that unrecognized or under-appreciated central actions of LDN underpin these anecdotal reports of “feeling better”. Studies from decades ago indicated that LDN could decrease tumor growth in mice, and the authors suggested a mechanism whereby LDN causes a resetting of the endogenous opioid system that allows for a period of rest and re-sensitization of receptors as well as a refilling of endogenous opioid stores to allow the system to function optimally (Zagon and McLaughlin, 1983). Here, we hypothesized that such a mechanism could underlie the positive effects of LDN on subjective affect.

The central β-endorphin system is a key endogenous opioid system within the brain, and knockout of β-endorphin causes deficits in reward-related behaviors (Hayward et al., 2002) and analgesia (Labuz et al., 2016; Parikh et al., 2011). β-endorphin is produced in the brain from the precursor peptide proopiomelanocortin (POMC), primarily in neurons in the arcuate nucleus of the hypothalamus (ARH; (Veening et al., 2012). Further, POMC neurons of the ARH are heavily regulated both pre- and post-synaptically by mu opioid receptors (Fox and Hentges, 2017; Pennock and Hentges, 2011). Because most of the neurons in the brain that produce β-endorphin are in the ARH, we hypothesized that LDN may exert effects directly on MORs affecting ARH POMC neuron activity and alter the production and release of β-endorphin to partially explain the centrally-mediated actions of LDN.

Methods

Animals

Mice were maintained with approval by the Animal Care and Use Committee of [Author University] and in accordance with the *Guide for the Care and Use of Laboratory Animals* (Council, 2011). Mice backcrossed to the C57BL/6 strain (Jackson Laboratories), were group-housed under a 12 h light/dark cycle (ZT0 = 06:00) and given *ad libitum* access to food and water. Male and female mice were used for all experiments, and all mice were between 8-12 weeks of age at the time of tissue collection. Transgenic mice expressing Discosoma red (*Pomc-DsRed*, gifted by Dr. Malcolm Low, University of Michigan) or enhanced green fluorescent protein (*Pomc-eGFP*, Jax stock #009593) under the control of the *Pomc* promoter were used to identify POMC cells during electrophysiological recordings. Mice expressing CRE recombinase driven by the *Pomc* promoter (*Pomc^{Cre/+}*; Jackson laboratories, stock #005965) mice were used for stereotaxic injection of the AAVGCaMP6f vector and subsequent GCaMP fluorescence imaging experiments.

LDN treatment

Naltrexone was dissolved in sterile saline to a concentration of 0.025 mg/ml to make LDN and was stored at -20°C for no more than 7 days. Mice were injected intraperitoneally (IP) with 0.1 mg/kg LDN between 7:00-8:00 and returned to their home cage. On day 3, 7 or 12, mice were euthanized 2 h after the final injection, when brain naltrexone concentrations will have fallen to, at most, 2-3% of peak (Misra et al., 1976).

Stereotaxic microinjection

For stereotaxic microinjections, *Pomc^{Cre/+}* animals were first deeply anesthetized with 5% isofluorane and then anesthesia was maintained with 2% isofluorane. Hair was removed and skin was cleaned for surgery before animals were placed in a stereotaxic headframe (David Kopf

Instruments) on top of a heating pad. A small hole was drilled into the skull, and a Neurosyringe (2 μ l; Hamilton) was lowered into place at 1 mm/sec into the arcuate nucleus of the hypothalamus (from bregma, A/P: -1.63 , M/L: ± 0.32 , D/V: -6.00). A double-floxed AAVGCaMP6f (AAV9.CAG.Flex.GCaMP6f.WRPE.SV40; Penn Vector Core, University of Pennsylvania School of Medicine, Philadelphia, PA) was injected at 100 nl/min for a total of 200 nl. The needle was left in place post-injection for 10 min and then raised at 1mm/min. This process was repeated to achieve bilateral injection. During recovery, animals were maintained on a heating pad for at least one hour and 5mg/kg carprofen (Rimadyl, Pfizer) was administered daily for 3 days following surgery. LDN injections commenced on day 4 post surgery and continued for 7 days before GCaMP imaging was performed.

Patch clamp electrophysiology

On the day of recording between 9:00-9:45 mice were deeply anesthetized with isoflurane and brains were immediately collected into ice-cold artificial cerebrospinal fluid (aCSF, 126 mM NaCl, 2.5 mM KCl, 1.2 mM MgCl₂•6H₂O, 2.4 mM CaCl₂•2H₂O, 1.2 mM NaH₂PO₄, 11.1 mM glucose, and 21.4 mM NaHCO₃) buffered with 95% O₂ and 5% CO₂ (carboxygen). Brains were transferred to a Leica VT1200S vibratome also containing ice-cold carboxygen-buffered aCSF and sliced 240 μ m thick in the region of the arcuate nucleus of the hypothalamus. Slices were then transferred to aCSF kept at 37°C in a water bath. Slices were allowed to rest for at least 1 h prior to recording.

For recording, slices were maintained in a chamber constantly perfused with carboxygen-infused aCSF kept at 37°C via an in-line temperature controller. For current clamp experiments and experiments isolating sIPSCs, MK 801 (15 μ M) was added to the bath solution to block NMDA receptors. POMC cells were identified by the presence of the eGFP or dsred reporter

visualized through a 40X water-immersion objective (Olympus). Glass patch-pipets were pulled with a Narishige PC-10 vertical pipette puller (Narishige International) to a resistance between 1.4-2.0 m Ω when filled with potassium methyl-sulfate/potassium chloride recording solution (57.5 mM KCl, 57.5 mM CH₃KO₄S, 20 mM NaCl, 1.5 mM MgCl₂, 5 mM HEPES potassium salt, 0.1 mM EGTA, 2 mM ATP, 0.5 mM GTP, and 10 mM phosphocreatine, pH 7.3) for voltage clamp experiments or potassium gluconate recording solution (110 mM K-gluconate, 10 mM KCl, 15 mM NaCl, 1.5 mM MgCl₂, 10 mM HEPES-potassium salt, 1 mM EGTA, 2 mM Mg-ATP, and 0.2 mM Na-GTP) for current clamp experiments, made fresh weekly and stored at -20°C. An AxoPatch 200B amplifier (Molecular Devices) was used to maintain membrane potential at -60 mV. Test pulses of 10 pA were used to ensure that cells were maintained with a series resistance no greater than 20 m Ω , and that the series resistance did not deviate by more than 5 m Ω from the original measured value upon break in. Recordings were collected via AxoGraph software at 10 kHz and filtered at 5 kHz. [Met5]-enkephalin (ME, Sigma M6638) was prepared as a 10 mM solution in sterile water and kept at 4°C for no more than one month. Before adding to slices, ME was diluted in aCSF, buffered with carboxygen, and passively perfused over the slice during recording. A similar paradigm was followed for preparing drugs for experiments isolating sIPSCs and sEPSCs, where 10 μ M of the competitive AMPA antagonist DNQX (Sigma) was perfused onto the slice to isolate sIPSCs, or 10 μ M of the GABA_A antagonist Bicuculline methiodide (Tocris) was perfused to isolate sEPSCs.

To analyze spontaneous activity, a model sPSC was created from an averaged sample of recordings via Axograph and used as a template for detection. Potassium currents were measured by sampling an average current prior to ME application and subtracting this value from the peak current measured 2-4 min after drug application.

For action potential threshold experiments, a $>1 \text{ G}\Omega$ seal was obtained in voltage clamp mode and the holding voltage brought to -60 mV . Upon break-in, the AxoPatch 200B amplifier was quickly switched to current clamp mode ($I=0$) and the membrane potential recorded. DNQX ($10 \mu\text{M}$) and Bicuculline ($10 \mu\text{M}$) were washed onto the slice prior to and during the experiment to block AMPA- and GABAA-mediated currents. After at least 3 min of exposure to these blockers, the cell was current clamped to a membrane potential of -60mV and a current ramp of $0\text{-}110 \text{ pA}$ was applied three separate times.

GCaMP imaging as an indicator of intracellular calcium levels

For GCaMP fluorescence monitoring, slices were maintained as described above. GCaMP6f was visualized using a 470nm LED (ThorLabs) and a 40X water immersion objective (Olympus). Slices were allowed to sit for 10 min in the recording chamber prior to allow the GCaMP6f fluorescence to stabilize in the condition. GCaMP fluorescence was then recorded using CellSens Dimension software (Olympus) at 10 Hz with a 50 ms exposure using an electron-multiplying charge-coupled device (Evolve 512 Delta, Photometrics) for 10 min of baseline activity. After 10 min, $10 \mu\text{M}$ ME was washed onto the slice as recording continued. To analyze baseline GCaMP6f fluorescence, all traces were normalized in Axograph to the reduced level of signal occurring in response to the ME application which significantly decreases calcium influx. These normalized traces were transferred to Prism (version 8) software for area under the curve analysis.

Perfusion and fluorescent in situ hybridization (FISH)

Mice were first deeply anesthetized with sodium pentobarbital. Transcardial perfusion was then commenced first with 10% sucrose followed by 4% paraformaldehyde, both diluted in potassium

phosphate buffer. Brains were extracted into 4% paraformaldehyde solution and stored overnight at 4°C.

On day 1 of *FISH*, the arcuate nucleus of the hypothalamus was collected on ice in 50 µm slices using a Leica VT100S vibratome. Slices were incubated at room temperature in 6% H₂O₂ for 15 minutes to quench endogenous peroxidase activity and then incubated for 15 minutes in proteinase K (10 µg/ml) diluted in PBS containing 0.1% Tween 20 (PBT). Proteinase K was deactivated with incubation in 2mg/ml glycine in PBT for 10 minutes. Following two 5 min washes in PBT, tissue was postfixed for 20 min in solution containing 4% paraformaldehyde and 0.2% gluteraldehyde. Tissue was washed once more in PBT, then dehydrated in ascending concentrations of EtOH diluted in DEPC-treated water (50, 70, 95, and 100%) and then briefly rehydrated in PBT. Slices were transferred to vials and prehybridized in 66% deionized formamide, 13% dextran sulfate, 260 mM NaCl, 1.3× Denhardt's solution, 13 mM Tris-HCL [pH 8.0], and 1.3 mM EDTA [pH 8.0] for 1 hour at 60°C. Fluorescein isothiocyanate (FITC)-labeled *Pomc* probe (corresponding to base 532-1000 of Genbank sequence NM_008895.3) was denatured at 85°C for 5 min and then added at 200 pg/µl, along with 0.5mg/ml tRNA and 10 mM DTT, to the hybridization buffer bathing the slices and allowed to hybridize at 70°C for 18-20 h.

On day 2 following hybridization, slices were first washed at 60°C three times in solution containing 50% formamide and 5X SSC followed by three washes at 60°C in 50% formamide and 2X SSC. Slices were then digested for 30 min at 37°C with RNase A (20 µg/ml in 0.5 M NaCl, 10 mM Tris-HCL [pH 8.0], 1 mM EDTA) and washed three times for 15 min at room temperature in TNT (0.1 M Tris-HCL [pH 7.5], 0.15 M NaCl, 0.05% Tween-20). Slices were blocked for 1 hour in TNB (TNT plus 0.5% Blocking Reagent provided in the TSA kit; Perkin

Elmer, Oak Brook IL) and then incubated overnight at 4°C in sheep anti-FITC (1:1,000; Roche Applied Sciences) antibody conjugated to horseradish peroxidase.

On day 3, probe was detected using a TSA PLUS DNP (HRP) system (Perkin Elmer). Slices were then washed for 15 min three times in TNT and then incubated for 30 min in a 1:50 dilution of DNP Amplification Reagent. Slices were then washed in TNT and exposed to 1:400 rabbit anti-DNP-KLH conjugated to Alexa Fluor 488 (1 hour; Invitrogen, Eugene, OR) in TNT. Tissue was mounted in Aqua Poly/Mount (Polysciences, Inc., Warrington).

FISH imaging and analysis

Images were collected using an LSM 800 Airyscan confocal microscope (Zeiss) using Zen Blue software (Zeiss). Stacks of images (6-8 slices per stack) were collected for each slice at an interval of 3 μm through the entire rostral-caudal extent of the arcuate nucleus. All images were collected with the same laser power and digital gain. All analyses were performed using Fiji (ImageJ) software. To control for probe penetration, top and bottom stack images were eliminated prior to stack merging via max intensity projection followed by intensity-based thresholding. This created a mask for analysis, which then allowed fluorescence intensity of each cell within the stack to be measured. Fluorescence intensity values were subtracted by a representative sampling of the background intensity to control for variability of staining between slices. An average intensity was calculated for each brain from the fluorescent intensities of all analyzed cells.

Radioimmunoassay

At time of tissue collection, serum samples were collected from trunk blood and stored at -80°C until measurements were made. β -endorphin levels in plasma were determined using a commercial radioimmunoassay kit according to the manufacturer's instructions (RK-022-33,

Phoenix Pharmaceuticals, Inc., Burlingame, CA). In brief, samples were incubated overnight at 4°C with rabbit anti-beta-endorphin, followed by another overnight incubation with ¹²⁵I-beta-endorphin. Samples were then incubated with goat-anti-rabbit IgG serum and normal rabbit serum, centrifuged, and the supernatant discarded prior to detection of bound ¹²⁵I-beta-endorphin in the remaining pellet with a gamma-counter (Perkin-Elmer, Waltham, MA). A standard curve was generated from which the concentration of beta-endorphin present in each sample was extrapolated.

Statistics

Results for male and female mice were examined separately for each experiment and were not statistically different. Therefore, all datasets pooled to include both male and female mice. Normality tests were performed on all data sets using the Royston (Royston 1995) method of the Shapiro-Wilk normality test. Normal datasets were analyzed using unpaired t-tests, and non-normal datasets were analyzed using Mann-Whitney t-tests where indicated. ME-induced dose response curves were compared by non-linear regression and sum-of-squares F test to compare EC50. All data are presented as mean ± SD. Dose x time responses to LDN were analyzed by two-way ANOVA with Tukey's multiple comparison test performed in the case of a statistically significant interaction.

Results

Treatment with LDN does not alter ME-induced outward currents

To determine whether LDN might produce its beneficial effects by increasing the sensitivity of opioid receptors on POMC neurons, we examined responses to the opioid receptor agonist [Met5]-enkephalin (ME) in slices from mice treated with LDN or vehicle. Mice were injected daily with either 0.1 mg/kg naltrexone in 0.1 ml saline or 0.1 ml saline intraperitoneally for one

week. This treatment plan was selected as animal studies suggest that this dosage and time period is enough to elicit peripheral effects of LDN (Hammer et al., 2016; Ludwig et al., 2017; Van Bockstaele et al., 2006). On day seven, two hours after the final LDN injection, brains were extracted and whole cell patch-clamp recordings were made from POMC neurons in slices containing the arcuate nucleus of the hypothalamus. ME application induced an outward current, which on POMC neurons has been shown to be mediated largely by MORs coupled to inwardly rectifying potassium channels (GIRKs, Fig 1A) (Fox and Hentges, 2017; Pennock and Hentges, 2011). If LDN conferred an increased sensitivity to opioids, ME application would be expected to increase the amplitude of the outward current. However, treatment with LDN did not alter the dose response of the ME-induced peak outward current (Fig 1B, EC50 saline = 1.315, EC50 LDN = 1.071, $F(1, 67) = 0.033$, $p = 0.855$). Therefore, LDN does not appear to confer enhanced sensitivity or coupling of opioid receptors on POMC neurons to GIRKs.

Treatment with LDN does not alter ME-induced inhibition of sPSCs

Spontaneous postsynaptic currents (sPSCs), mediated by inputs to POMC neurons, are inhibited by the activation of opioid receptors on presynaptic terminals and show a greater sensitivity to opioid agonist application than outward currents (Pennock and Hentges, 2011). Therefore, we also determined how sPSCs were affected by ME application in LDN- and saline-treated mice. Because opioid agonists do not appear to preferentially suppress inhibitory or excitatory inputs (Pennock and Hentges, 2011), both excitatory (EPSCs) and inhibitory (IPSCs) currents were examined at once. As shown in Figures 1 C&D, no significant change was observed between LDN and saline treated groups in the inhibition of sPSCs onto POMC neurons in response to ME application (EC50 saline = 0.30, EC50 LDN = 0.10; $F(1, 59) = 1.219$, $p = 0.274$). Therefore,

LDN treatment does not appear to alter the sensitivity of opioid receptor inhibition of transmitter release in neurons upstream of POMC neurons.

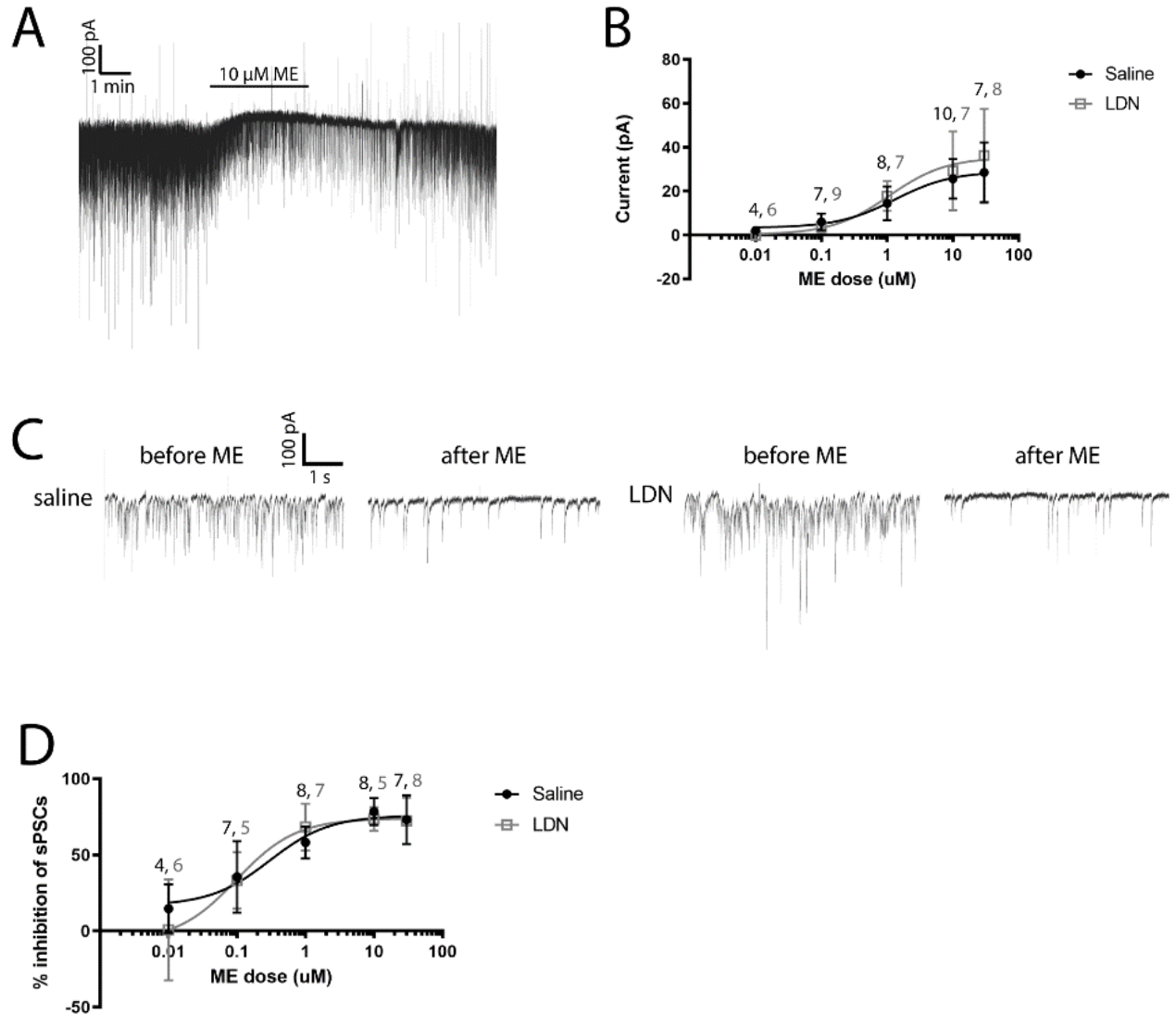


Figure 12. Treatment with LDN did not alter dose responses of opioid receptors on POMC neurons or on neurons presynaptic to POMC. A) Example outward currents elicited by ME application (10 μ M). B) Dose response curves for outward current generated by application of ME. No significant difference was found between dose response curves. C) Example sPSCs recorded before and after ME application for saline and LDN injected groups. D) Dose response curves generated from the inhibition of spontaneous events after ME application compared to before ME application in saline and LDN groups. No significant difference was found between dose response curves. Numbers in (black = saline, gray = LDN) represent the number of cells recorded from for each condition. Slice numbers are the same as cell numbers. Total mice for all dose responses: saline = 21, LDN = 19.

Expression of POMC mRNA and release of β -endorphin peptide

Finding no evidence for overt changes in pre- or postsynaptic sensitivity of MORs, we explored the possibility that LDN may alter the production or release of endogenous opioids to mediate the reported efficacy of the treatment. Previous studies have shown that high dose naltrexone treatment can alter production of POMC peptides relevant to analgesia (Markowitz et al., 1992; Panigrahi et al., 2019). To begin to explore whether LDN may alter the release of the opioid β -endorphin from POMC neurons, we first examined the expression of *Pomc* mRNA as this is the transcriptional precursor to the prohormone from which β -endorphin is cleaved. *Pomc* mRNA was detected using fluorescent *in situ* hybridization (FISH) in tissue from LDN and vehicle treated animals. Fluorescence intensity of the *Pomc* FISH signal was determined and reported relative to background fluorescence with all tissue processed and imaged under identical conditions (Fig 2A-C). We found no difference in signal intensity in cells from the two treatments (vehicle versus LDN; $t(9) = 1.023, p = 0.3329$).

While *Pomc* FISH provides an indication of relative mRNA production and potential peptide changes centrally, it is possible that release into plasma is selectively altered by LDN treatment. Therefore, we also examined whether LDN treatment altered the presence of β -endorphin in the plasma of treated animals (Fig 2D). However, no difference was observed in plasma concentration of β -endorphin between LDN and saline treated animals (saline = 79.17 ± 37.88 , LDN = 83.24 ± 36.52 pg/ml, $t(5) = 0.143, p = 0.892$). Therefore, LDN treatment does not appear to alter POMC mRNA production in the arcuate nucleus of the hypothalamus nor release of β -endorphin into blood plasma.

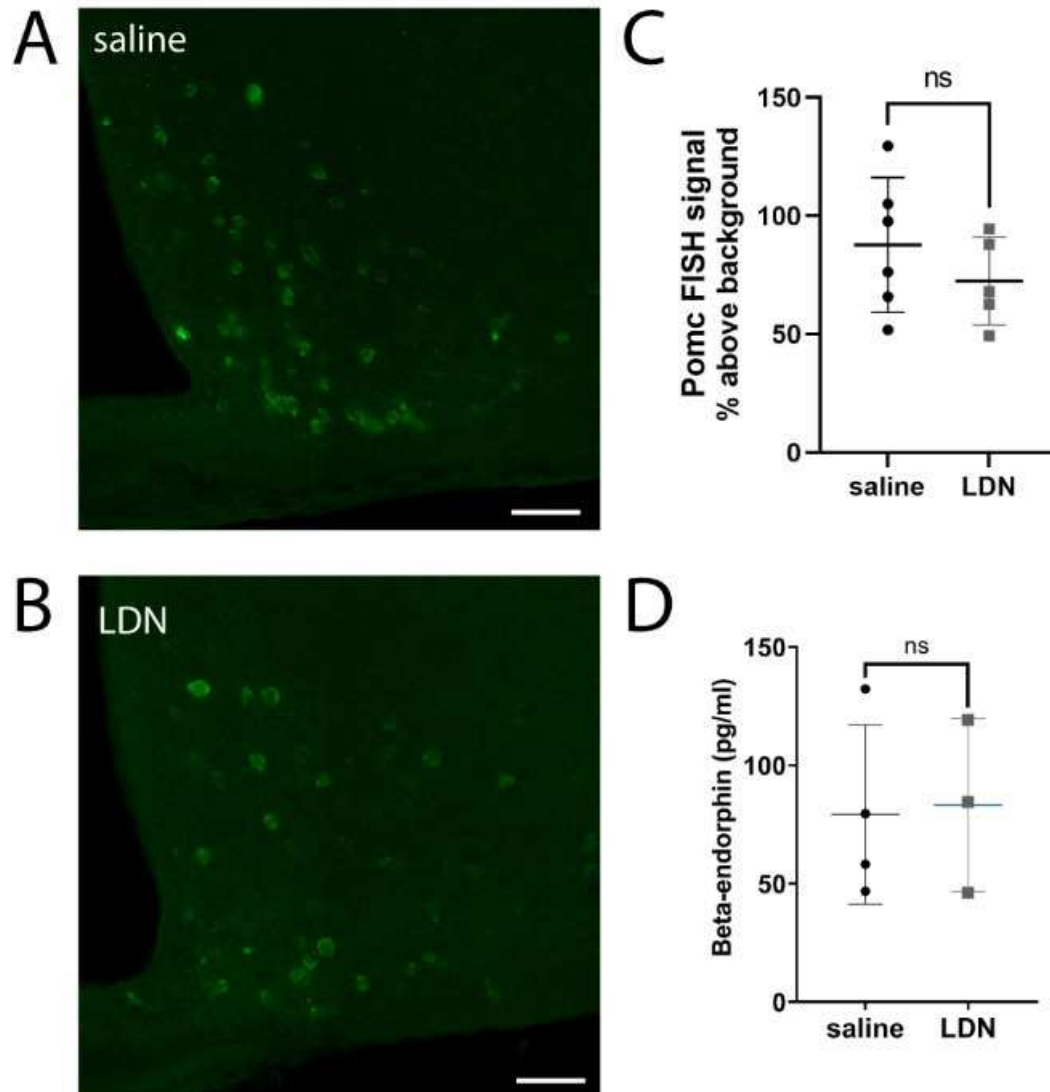


Figure 13. Treatment with LDN did not alter mRNA production of POMC in the arcuate nucleus or release of β -endorphin into plasma. A) Representative FISH images from the medial arcuate nucleus in animal treated with saline and B) LDN. Scale bars are 50 μ m. C) No significant difference was observed in POMC FISH intensity between animals treated with saline or LDN. Data points are average intensities of all cells in one brain (saline cell count per brain = 1008 ± 314.7 , LDN cell count per brain = 578.8 ± 211.5). D) No change in β -endorphin concentrations in blood plasma was observed after LDN treatment. Each data point represents the average of individual cell fluorescence from one mouse.

Baseline characteristics of POMC neurons in animals treated with LDN or saline

Despite the lack of noted effects thus far in the studies, we could not rule the possibility that LDN might change the activity of POMC neurons and perhaps peptide release centrally. In fact, during baseline recording for opioid dose response experiments, it was observed that while

opioid responses did not differ, some intrinsic properties of POMC neurons were different in tissue from LDN treated mice. Intrinsic properties and statistics of POMC neurons from animals treated with LDN or saline are shown in Table 1. POMC neurons from animals treated with LDN

	Resting Membrane Potential (mV)	Membrane Capacitance (pF)	Input Resistance (M Ω)	sPSC frequency (Hz)	sPSC amplitude (pA)	AP Threshold (mV)	AP frequency (Hz)
Saline Mean \pm SD n = 10	-39.44 \pm 6.33	23.65 \pm 7.72 n = 32	820.8 \pm 737.1 n = 32	8.789 \pm 4.30 n = 33	59.86 \pm 31.73 n = 33	-38.98 \pm 5.78 n = 11	7.13 \pm 4.08 n = 9
LDN Mean \pm SD n = 11	-41.39 \pm 11.30	19.38 \pm 6.12 n = 34	743.7 \pm 699.1 n = 34	6.185 \pm 4.16 n = 32	42.82 \pm 23.64 n = 31	-41.89 \pm 6.25 n = 12	5.24 \pm 5.76 n = 11
<i>p</i>	0.6355	0.0151	0.6642	0.0160	0.0183	0.2606	0.4190
<i>t</i> (df)	0.4818 (19)	2.498 (64)	0.4362 (64)	2.475 (63)	2.424 (62)	1.156 (21)	0.827 (18)

had a slightly smaller capacitance than POMC neurons from animals treated with saline and exhibited spontaneous postsynaptic currents (sPSCs) with lower amplitudes and frequency than POMC neurons in the saline group. Recordings from a subset of LDN and saline treated mice confirmed that the frequency of inhibitory postsynaptic currents (saline = 7.35 \pm 4.97, LDN = 5.08 \pm 4.20) was higher than the frequency of excitatory postsynaptic currents (saline = 1.83 \pm 1.48, LDN = 1.37 \pm 1.47) in both groups, confirming previous studies showing that the majority of sPSCs in POMC neurons are mediated by presynaptically-released GABA (Hentges et al., 2009; Pinto et al., 2004). Therefore, it may be that LDN decreases inhibitory tone onto POMC neurons.

Table 1. Basal properties of POMC neurons in slices from mice treated for 7 days with LDN or saline. Membrane capacitance, sPSC frequency, and sPSC amplitude were all lower in the LDN group as compared to saline ($p > 0.05$). Values are expressed as mean \pm SD. n represents cell numbers. Total slices for each group: (col 2-5) same as cell numbers, (col 1, 6, 7) saline =

10, LDN = 9. Total mice for each group: (col 2-5) saline = 21, LDN = 19; (col 1, 6, 7) saline = 5, LDN = 4.

GCaMP-derived calcium responses in POMC neurons are altered by ME

To determine if the LDN-induced decrease in sPSCs in POMC neurons leads to enhanced POMC neuron activity, we first examined signal indicative of calcium level and flux in POMC neurons from mice treated with LDN or saline as a proxy for POMC neuron activity. GCaMP fluorescence reporter imaging was chosen as a starting point, as this assay has been reported to be a very sensitive indicator of altered POMC neuron activity (Fox and Hentges, 2017) and generally correlates with depolarization and firing rate changes (Hartung and Gold, 2020; Jayaraman and Laurent, 2007). For calcium-dependent GCaMP imaging, AAV containing a floxed sequence for GCaMP6f was delivered into the arcuate nucleus of *Pomc*^{Cre/+} mice and 7 days of LDN administration was completed. GCaMP-derived calcium signal was recorded and normalized to the loss of calcium signal induced by 10 μ M ME application after baseline signal recording was completed. This normalization was chosen due to the reliable ME response in cells and because electrophysiological experiments showed no difference in opioid responsiveness between cells in slices from LDN or saline treated mice. All neurons that appeared healthy and responded to 10 μ M ME were included, and baseline calcium fluorescence was analyzed as area under the curve after normalization to ME. POMC neurons from animals treated with LDN showed greater calcium signal at baseline compared to POMC neurons from animals treated with saline (Fig 3; Mann–Whitney $U = 1=86$, $n_{\text{sal}} = 22$ $n_{\text{LDN}} = 15$, $p = 0.0138$). Therefore, LDN treatment may generally enhance excitability as suggested by the increase in GCaMP-derived calcium signal.

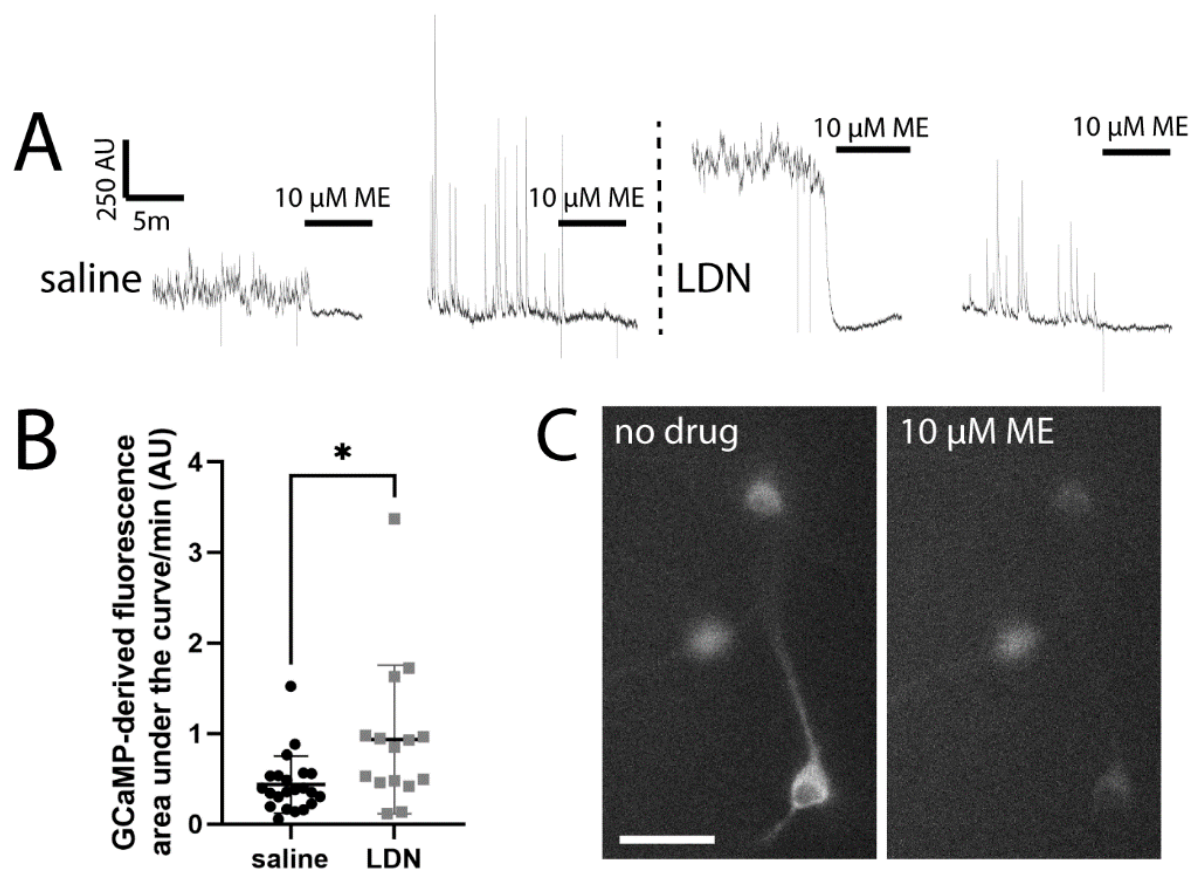


Figure 14. Treatment with LDN slightly increased baseline GCaMP calcium indicator derived fluorescence **A)** Baseline GCaMP-derived fluorescence and fluorescence after 10uM ME treatment from cells of animals treated with saline or LDN. **B)** Baseline fluorescence normalized to 10uM ME application differed significantly between saline and LDN groups. $*p < .05$. Each data point represents one cell. Total slices for each group: saline = 10, LDN = 8. Total mice for each group: saline = 5, LDN = 5. **C)** Example image of GCaMP expressing POMC neurons before and after treatment with 10uM ME. Scale bar is 50 μm.

Intrinsic excitability of POMC neurons

To test whether an increase in GCaMP-based calcium activity was indeed accompanied by an increase in POMC neuron intrinsic excitability, action potential thresholds were determined for POMC neurons from animals treated with LDN and saline (see Table 1). Neither resting membrane potential frequency of action potentials was different between groups (Fig 4). Action

potential threshold was measured in the presence of presynaptic blockers for GABA_A receptors (Bicuculline methiodide, 10 μM), AMPA receptors (DNQX, 10 μM), and NMDA receptors (MK-801, 15 μM). Action potentials were elicited with a 0-110 pA current ramp. The amount of current required to elicit an action potential from a holding potential of -60 mV did not differ between groups (saline = 33.63 ± 21.69 pA, LDN = 30.09 ± 23.86 pA, $t(17) = 0.3215$, $p = 0.7518$; Fig 4 C & D). Therefore, LDN treatment does not appear to alter baseline firing nor intrinsic excitability of POMC neurons.

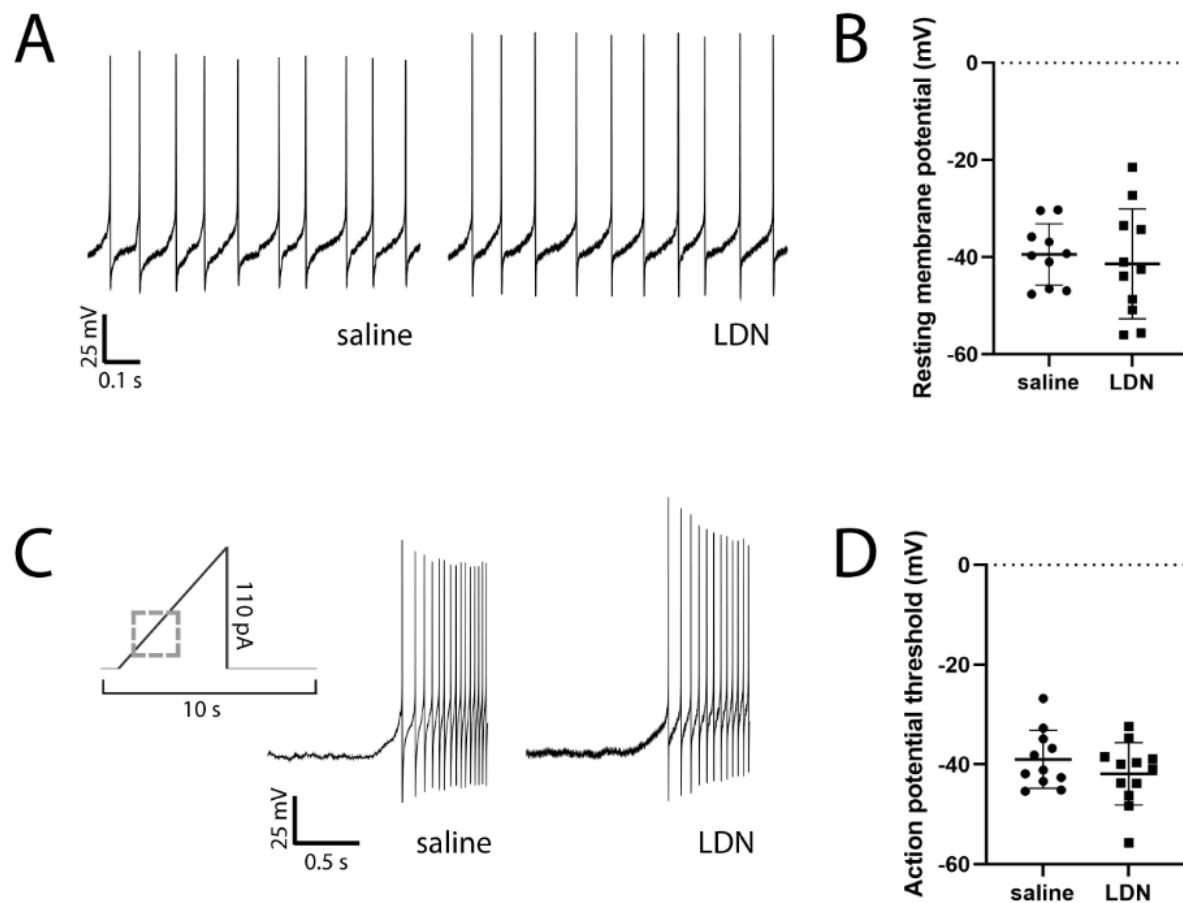


Figure 15. Treatment with LDN did not alter intrinsic excitability of POMC neurons. A) Example current clamp recordings from POMC neurons of saline and LDN treated mice. **B)** Resting membrane potential did not differ between POMC neurons from animals treated with saline and LDN. **C)** Representation of ramp used to determine action potential threshold. The threshold ramp was 5 s and ramped from 0 to 110 pA with a 1 s delay pre-ramp. Dashed gray

box represents location of saline and LDN representative traces during action potential ramp. Example traces from saline and LDN treated cells are shown from the beginning of the ramp protocol, with action potentials beginning 0.3 s after initiation of the ramp. **D**) Action potential threshold did not differ between POMC neurons from animals treated with saline and LDN. Each data point represents one cell. Total slices used for each group (from a total of saline = 5 and LDN = 4 mice per group): saline = 10, LDN = 9.

Dose x time response of POMC neuron intrinsic excitability and β -endorphin release

While the above experiments indicate that seven days of 0.1 mg/kg LDN does not appear to change β -endorphin release into plasma or POMC neuron intrinsic excitability, it is possible that LDN effects on the β -endorphin system could be short-lasting or take longer than 7 days to manifest. Therefore, we examined these parameters after 3, 7, and 12 days of LDN exposure at 0.1 mg/kg and 3 mg/kg LDN compared to saline controls (Table 2). No main effects of dose ($F(2, 73) = 0.39, p = 0.68$), nor time ($F(2, 73) = 1.31, p = 0.28$) were apparent for resting membrane potential (Fig 5A). Similarly, action potential threshold did not appear to be altered by dose ($F(2, 74) = 2.82, p = 0.60$) or time ($F(2, 74) = 2.02, p = 0.14$; Fig 5B), and action potential frequency also showed no main effects of dose ($F(2, 73) = 0.45, p = 0.64$) or time ($F(2, 73) = 0.97, p = 0.38$; Fig 5C). β -endorphin concentrations in plasma were also measured after the dose x time experiment and there were no main effects (dose: $F(2, 32) = 0.62, p = 0.54$; time: $F(2, 32) = 2.23, p = 0.12$), but an interaction was observed between groups ($F(4, 32) = 2.95, p = 0.04$) with the concentration of β -endorphin being slightly lower in the 0.1 mg/kg group compared to the saline group at 3 days ($p = 0.02$; Fig 5D). No other groups were significantly different in their plasma β -endorphin concentrations within any of the treatment time blocks.

Table 2. Baseline properties of POMC neurons from animals treated with varied doses and times of LDN Resting membrane potential, action potential threshold, and action potential frequency mean \pm SD are presented for cells from slices taken from mice treated with saline, 0.1 or 3mg/kg LDN for 3, 7, or 12d. No main effects were detected for any parameter. n= number of cells recorded from and comes from 2 or more slices from at least three mice.

	RMP (mV)	AP threshold (mV)	AP frequency (Hz)
Saline 3 day Mean ± SD	-45.18 ± 8.16 n = 12	-45.42 ± 5.58 n = 13	7.18 ± 8.15 n = 12
mg/kg 3 day Mean ± SD	-45.82 ± 14.70 n = 9	-44.26 ± 4.80 n = 8	3.61 ± 4.93 n = 9
3 mg/kg 3 day Mean ± SD	-33.77 ± 10.52 n = 10	-44.81 ± 3.02 n = 9	13.26 ± 14.73 n = 10
Saline 7 day Mean ± SD	-43.60 ± 6.28 n = 8	-44.74 ± 4.14 n = 8	11.73 ± 11.80 n = 8
mg/kg 7 day Mean ± SD	-45.56 ± 16.49 n = 11	-45.29 ± 4.69 n = 11	6.65 ± 8.11 n = 11
3 mg/kg 7 day Mean ± SD	-49.37 ± 11.36 n = 8	-49.39 ± 3.54 n = 8	2.54 ± 3.39 n = 8
Saline 12 day Mean ± SD	-40.11 ± 12.99 n = 10	-46.71 ± 7.09 n = 11	7.08 ± 10.41 n = 10
mg/kg 12 day Mean ± SD	-44.11 ± 12.36 n = 6	-47.49 ± 6.66 n = 7	5.19 ± 6.90 n = 6
3 mg/kg 12 day Mean ± SD	-53.86 ± 12.44 n = 8	-50.00 ± 2.44 n = 8	4.53 ± 7.78 n = 8

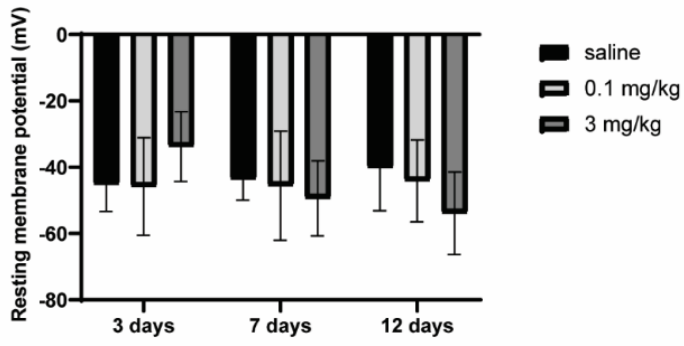
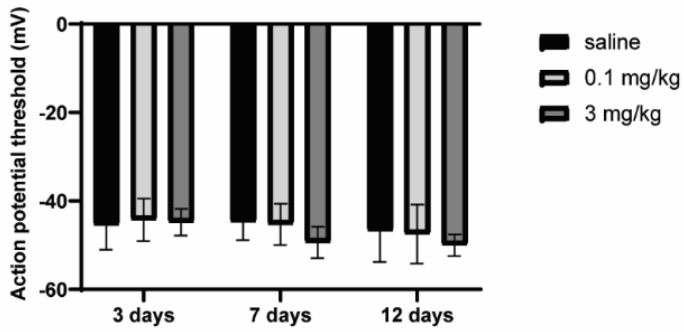
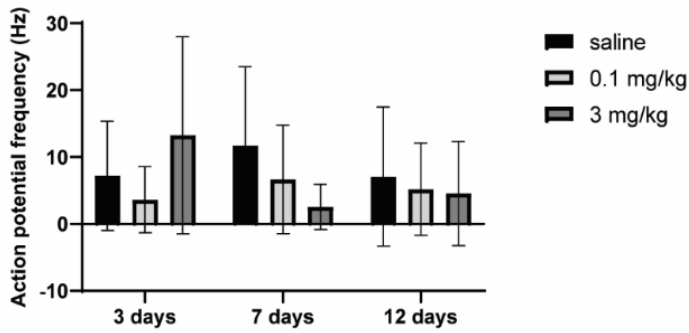
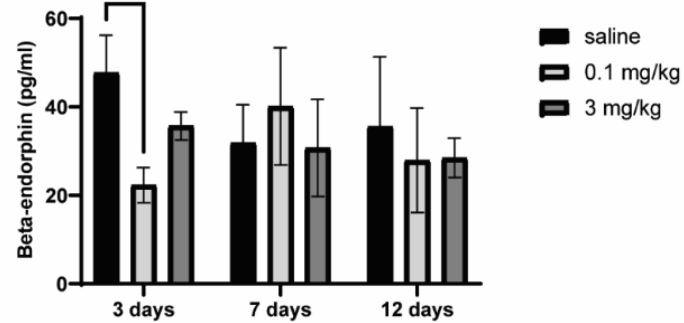
A**B****C****D**

Figure 16. Increased dose of LDN or varied the time of LDN exposure did not cause sustained changes in POMC neuron intrinsic excitability or β -endorphin plasma concentrations. A) Resting membrane potential did not change after 3-, 7-, or 12-day LDN treatment at either 0.1 mg/kg or 3 mg/kg. B) Varying the time or dose of LDN treatment also did not change POMC neuron action potential threshold or C) action potential frequency. D) LDN treatment did not systematically alter β -endorphin concentrations in plasma, although a transient decrease in β -endorphin concentration was observed with 0.1mg/kg at three days of treatment. Number of mice used for each group in the β -endorphin group are as follows: 3 day saline = 3, 0.1 mg/kg LDN = 3, 3 mg/kg LDN = 4; 7 day saline = 7, 7 day 0.1 mg/kg = 8, 7 day 3 mg/kg = 4; 12 day saline = 5, 12 day 0.1 mg/kg LDN = 4, 12 day 3 mg/kg = 4. * $p < .05$

Discussion

Overall, LDN appears to have minimal effects on the activity of POMC neurons. The amplitude and frequency of PSCs onto POMC neurons was slightly decreased, and GCaMP-derived calcium signal from POMC neurons was increased. However, the resting membrane potential, firing frequency, and intrinsic excitability of POMC neurons were all unaltered by LDN, even when dosage and time of treatment was altered. Consistent with this, LDN treatment did not consistently change the production of *Pomc* mRNA or the release of β -endorphin into blood plasma. Thus, we found no evidence to support the hypothesis that LDN may exert its reported mood enhancing and pain reducing actions by stimulating the endogenous β -endorphin system.

It has repeatedly been shown that high doses of naltrexone increase mu-opioid receptor expression throughout the brain (Díaz et al., 2002; Tempel et al., 1984; Unterwald et al., 1998; Unterwald et al., 1995). Further, studies examining behavioral effects show enhanced respiratory depression and analgesia after extended high dose naltrexone followed by acute agonist administration (Díaz et al., 2002), therefore it appears these upregulated opioid receptors are functional. However, our studies indicate that LDN does not increase coupling to effectors in POMC neurons, and likely does not induce increased expression, unless there are extra non-

signaling receptors. Thus, LDN does not appear to have the same effect as higher, more chronic doses of naltrexone *in vivo* on opioid receptors in POMC neurons.

The lack of consequences found in the current study do not rule out that LDN could be affecting opioid receptor function in other brain regions. Opioid receptor expression is widespread throughout the central nervous system (Corder et al., 2018; Le Merrer et al., 2009), and some regions may be more sensitive to antagonist-induced changes than POMC neurons. While long-term analgesic effects of LDN are speculated to occur peripherally, it is known that top-down activation is important for pain relief. The central analgesic system contains the periaqueductal gray (PAG), which sends inhibitory projections to the rostral ventromedial medulla (RVM), and both of these brain regions are known to express opioid receptors, which could be affected by LDN (Gutstein et al., 1998). Further, effects on mood and dreaming reported by many patients taking LDN likely have a central mechanism, and several brain regions involved in affecting mood, including parts of the limbic system, express opioid receptors (George et al., 1994; Zubieta et al., 2003). Thus, LDN could affect opioid receptor systems in these regions to account for alterations to mood previously reported by patients.

Investigation of central β -endorphin expression and release in response to LDN also revealed little change. Changes in endogenous β -endorphin tone after LDN were hypothesized to occur because β -endorphin is known to improve affect and thus could account for improvements in mood reported by patients taking LDN. Further, previous studies administering high dose naltrexone show increases in β -endorphin and POMC peptide expression in plasma and brain (Gordon et al., 2017; Jaffe et al., 1994; Markowitz et al., 1992; Nikolarakis et al., 1987; Panigrahi et al., 2019). Therefore, we examined the effect of LDN on *Pomc* transcript and β -endorphin in plasma. It is worth commenting on the different y-axis scale bars referring to β -

endorphin concentrations in Figure 2 vs 5. The samples shown in Figure 5 were analyzed using reagents with different production lot numbers as those used in Figure 2 and this likely explains the difference observed in absolute concentration. Within each experiment, it is clear no difference in plasma β -endorphin levels is observed whether animals receive saline or one of two doses of LDN except that only 0.1 mg/kg LDN treatment for three days, may have slightly decreased β -endorphin concentration in plasma. This was in the opposite direction of our hypothesized increase in β -endorphin but could be indicative of an earlier release event followed by a dip in plasma peptide concentration. However, if anything, this change is transient and seems to resolve by seven days, therefore it is unlikely to explain the reported efficacy of LDN that may last for months or years (Ludwig et al., 2016).

It is also plausible that LDN could have effects on other opioid peptide systems in the brain. POMC neurons of the arcuate nucleus of the hypothalamus are the most prominent source of β -endorphin in the brain (Zakarian and Smyth, 1982). However, other opioid peptides, such as enkephalins and dynorphins, are also known to affect anxiety, aversion, and stress, all of which could be related to mood changes reported by patients using LDN (Femenía et al., 2011; Melo et al., 2014; Ménard et al., 2013; Nam et al., 2019; Wittmann et al., 2009). The production of precursors for enkephalin and endorphin are much more widespread in the brain than the production of the precursor polypeptide POMC (Corder et al., 2018; Le Merrer et al., 2009), and thus the ease in detecting changes in these systems would likely depend upon how generalized the alterations in the production of those specific peptides are, if present at all. Peripherally, LDN does appear to induce increases in the level of met-enkephalin in patients with multiple sclerosis (Ludwig et al., 2017), therefore changes in central enkephalin systems may also be possible. Further, many previous studies use LDN treatments for populations in which opioid systems may

already be dysfunctional, and LDN may be acting to reset this system back to normal. Because our studies were in healthy animals, we cannot rule out the possibility that LDN could confer effects in conditions of pathological opioid system function.

Overall, our lack of LDN-induced changes within POMC neurons does not rule out changes in animals with dysfunctional opioid tone, changes with longer term LDN treatment, or changes within the rest of the brain. Understanding the central effects of LDN is important, not only from the perspective of basic science, but also to inform future applications of LDN, as LDN is already being explored as a potential treatment for depression (Mischoulon et al., 2017). From our studies, it appears that future inquiries would be best served by focusing on opioid systems other than the central β -endorphin system or by examining the effects of LDN in conditions where dysfunctions in β -endorphin tone likely exist.

References

- Bolton, M. J., Chapman, B. P., & Van Marwijk, H. (2020). Low-dose naltrexone as a treatment for chronic fatigue syndrome. *BMJ Case Rep*, *13*(1).
- Brewer, K. L., Mainhart, A., & Meggs, W. J. (2018). Double-blinded placebo-controlled cross-over pilot trial of naltrexone to treat Gulf War Illness. *Fatigue*, *6*(3), 132-140.
- Burns, L. H., & Wang, H. Y. (2010). PTI-609: a novel analgesic that binds filamin A to control opioid signaling. *Recent Pat CNS Drug Discov*, *5*(3), 210-220.
- Chopra, P., & Cooper, M. S. (2013). Treatment of Complex Regional Pain Syndrome (CRPS) using low dose naltrexone (LDN). *J Neuroimmune Pharmacol*, *8*(3), 470-476.
- Corder, G., Castro, D. C., Bruchas, M. R., & Scherrer, G. (2018). Endogenous and Exogenous Opioids in Pain. *Annu Rev Neurosci*, *41*, 453-473.
- Council, N. R. (2011). *Guide for the Care and Use of Laboratory Animals: Eighth Edition*. Washington, DC: The National Academies Press.
- Díaz, A., Pazos, A., Flórez, J., Ayesta, F. J., Santana, V., & Hurlé, M. A. (2002). Regulation of mu-opioid receptors, G-protein-coupled receptor kinases and beta-arrestin 2 in the rat brain after chronic opioid receptor antagonism. *Neuroscience*, *112*(2), 345-353.
- Femenía, T., Pérez-Rial, S., Urigüen, L., & Manzanares, J. (2011). Prodynorphin gene deletion increased anxiety-like behaviours, impaired the anxiolytic effect of bromazepam and altered GABAA receptor subunits gene expression in the amygdala. *J Psychopharmacol*, *25*(1), 87-96.

- Fox, P. D., & Hentges, S. T. (2017). Differential Desensitization Observed at Multiple Effectors of Somatic μ -Opioid Receptors Underlies Sustained Agonist-Mediated Inhibition of Proopiomelanocortin Neuron Activity. *J Neurosci*, *37*(36), 8667-8677.
- George, S. R., Zastawny, R. L., Briones-Urbina, R., Cheng, R., Nguyen, T., Heiber, M., . . . O'Dowd, B. F. (1994). Distinct distributions of mu, delta and kappa opioid receptor mRNA in rat brain. *Biochem Biophys Res Commun*, *205*(2), 1438-1444.
- Ghai, B., Bansal, D., Hota, D., & Shah, C. S. (2014). Off-Label, Low-Dose Naltrexone for Refractory Chronic Low Back Pain. *Pain Med*, *15*(5), 883-884.
- Gold, M. S., Dackis, C. A., Pottash, A. L., Sternbach, H. H., Annitto, W. J., Martin, D., & Dackis, M. P. (1982). Naltrexone, opiate addiction, and endorphins. *Med Res Rev*, *2*(3), 211-246.
- Gordon, R. J., Panigrahi, S. K., Meece, K., Atalayer, D., Smiley, R., & Wardlaw, S. L. (2017). Effects of Opioid Antagonism on Cerebrospinal Fluid Melanocortin Peptides and Cortisol Levels in Humans. *J Endocr Soc*, *1*(10), 1235-1246.
- Gutstein, H. B., Mansour, A., Watson, S. J., Akil, H., & Fields, H. L. (1998). Mu and kappa opioid receptors in periaqueductal gray and rostral ventromedial medulla. *Neuroreport*, *9*(8), 1777-1781.
- Hammer, L. A., Waldner, H., Zagon, I. S., & McLaughlin, P. J. (2016). Opioid growth factor and low-dose naltrexone impair central nervous system infiltration by CD4 + T lymphocytes in established experimental autoimmune encephalomyelitis, a model of multiple sclerosis. *Exp Biol Med*, *241*(1), 71-78.
- Hartung, J. E., & Gold, M. S. (2020). GCaMP as an indirect measure of electrical activity in rat trigeminal ganglion neurons. *Cell Calcium*, *89*, 102225.
- Hayward, M. D., Pintar, J. E., & Low, M. J. (2002). Selective reward deficit in mice lacking β -endorphin and enkephalin. *J Neurosci*, *22*(18), 8251-8258.
- Hentges, S. T., Otero-Corchon, V., Pennock, R. L., King, C. M., & Low, M. J. (2009). Proopiomelanocortin expression in both GABA and glutamate neurons. *J Neurosci*, *29*(43), 13684-13690.
- Jaffe, S. B., Sobieszczyk, S., & Wardlaw, S. L. (1994). Effect of opioid antagonism on beta-endorphin processing and proopiomelanocortin-peptide release in the hypothalamus. *Brain Res*, *648*(1), 24-31.
- Jayaraman, V., & Laurent, G. (2007). Evaluating a genetically encoded optical sensor of neural activity using electrophysiology in intact adult fruit flies. *Front Neural Circuits*, *1*, 3.
- Labuz, D., Celik, M., Zimmer, A., & Machelska, H. (2016). Distinct roles of exogenous opioid agonists and endogenous opioid peptides in the peripheral control of neuropathy-triggered heat pain. *Sci Rep*, *6*, 32799.
- Le Merrer, J., Becker, J. A., Befort, K., & Kieffer, B. L. (2009). Reward processing by the opioid system in the brain. *Physiol Rev*, *89*(4), 1379-1412.
- Leonard, J. B., Nair, V., Diaz, C. J., Penoyar, J. B., & Goode, P. A. (2017). Potential drug interaction with opioid agonist in the setting of chronic low-dose opioid antagonist use. *Am J Emerg Med*, *35*(8), 1209.e1203-1209.e1204.
- Lie, M., van der Giessen, J., Fuhler, G. M., de Lima, A., Peppelenbosch, M. P., van der Ent, C., & van der Woude, C. J. (2018). Low dose Naltrexone for induction of remission in inflammatory bowel disease patients. *J Transl Med*, *16*(1), 55.
- Ludwig, M. D., Turel, A. P., Zagon, I. S., & McLaughlin, P. J. (2016). Long-term treatment with low dose naltrexone maintains stable health in patients with multiple sclerosis. *Mult Scler J Exp Transl Clin*, *2*, 2055217316672242.

- Ludwig, M. D., Zagon, I. S., & McLaughlin, P. J. (2017). Featured Article: Serum [Met(5)]-enkephalin levels are reduced in multiple sclerosis and restored by low-dose naltrexone. *Exp Biol Med (Maywood)*, 242(15), 1524-1533.
- Markowitz, C. E., Berkowitz, K. M., Jaffe, S. B., & Wardlaw, S. L. (1992). Effect of opioid receptor antagonism on proopiomelanocortin peptide levels and gene expression in the hypothalamus. *Mol Cell Neurosci*, 3(3), 184-190.
- Matthes, H. W., Maldonado, R., Simonin, F., Valverde, O., Slowe, S., Kitchen, I., . . . Kieffer, B. L. (1996). Loss of morphine-induced analgesia, reward effect and withdrawal symptoms in mice lacking the mu-opioid-receptor gene. *Nature*, 383(6603), 819-823.
- Melo, I., Drews, E., Zimmer, A., & Bilkei-Gorzo, A. (2014). Enkephalin knockout male mice are resistant to chronic mild stress. *Genes Brain Behav*, 13(6), 550-558.
- Ménard, C., Tse, Y. C., Cavanagh, C., Chabot, J. G., Herzog, H., Schwarzer, C., . . . Quirion, R. (2013). Knockdown of prodynorphin gene prevents cognitive decline, reduces anxiety, and rescues loss of group 1 metabotropic glutamate receptor function in aging. *J Neurosci*, 33(31), 12792-12804.
- Metz, M. J., Daimon, C. M., & Hentges, S. T. (2021). Reported Benefits of Low-Dose Naltrexone Appear to Be Independent of the Endogenous Opioid System Involving Proopiomelanocortin Neurons and β -Endorphin. *eNeuro*, 8(3).
- Mischoulon, D., Hylek, L., Yeung, A. S., Clain, A. J., Baer, L., Cusin, C., . . . Fava, M. (2017). Randomized, proof-of-concept trial of low dose naltrexone for patients with breakthrough symptoms of major depressive disorder on antidepressants. *J Affect Disord*, 208, 6-14.
- Misra, A. L., Bloch, R., Vardy, J., Mulé, S. J., & Verebely, K. (1976). Disposition of (15,16-3H)naltrexone in the central nervous system of the rat. *Drug Metab Dispos*, 4(3), 276-280.
- Nam, H., Chandra, R., Francis, T. C., Dias, C., Cheer, J. F., & Lobo, M. K. (2019). Reduced nucleus accumbens enkephalins underlie vulnerability to social defeat stress. *Neuropsychopharmacology*, 44(11), 1876-1885.
- Nikolarakis, K. E., Almeida, O. F., & Herz, A. (1987). Feedback inhibition of opioid peptide release in the hypothalamus of the rat. *Neuroscience*, 23(1), 143-148.
- Panigrahi, S. K., Meece, K., & Wardlaw, S. L. (2019). Effects of Naltrexone on Energy Balance and Hypothalamic Melanocortin Peptides in Male Mice Fed a High-Fat Diet. *J Endocr Soc*, 3(3), 590-601.
- Parikh, D., Hamid, A., Friedman, T. C., Nguyen, K., Tseng, A., Marquez, P., & Lutfy, K. (2011). Stress-induced analgesia and endogenous opioid peptides: the importance of stress duration. *Eur J Pharmacol*, 650(2-3), 563-567.
- Patten, D. K., Schultz, B. G., & Berlau, D. J. (2018). The Safety and Efficacy of Low-Dose Naltrexone in the Management of Chronic Pain and Inflammation in Multiple Sclerosis, Fibromyalgia, Crohn's Disease, and Other Chronic Pain Disorders. *Pharmacotherapy*, 38(3), 382-389.
- Pennock, R. L., & Hentges, S. T. (2011). Differential expression and sensitivity of presynaptic and postsynaptic opioid receptors regulating hypothalamic proopiomelanocortin neurons. *J Neurosci*, 31(1), 281-288.
- Pinto, S., Roseberry, A. G., Liu, H., Diano, S., Shanabrough, M., Cai, X., . . . Horvath, T. L. (2004). Rapid rewiring of arcuate nucleus feeding circuits by leptin. *Science*, 304(5667), 110-115.
- Raknes, G., Simonsen, P., & Småbrekke, L. (2018). The Effect of Low-Dose Naltrexone on Medication in Inflammatory Bowel Disease: A Quasi Experimental Before-and-After Prescription Database Study. *J Crohns Colitis*, 12(6), 677-686.

- Raknes, G., & Småbrekke, L. (2017). Low dose naltrexone in multiple sclerosis: Effects on medication use. A quasi-experimental study. *PLoS One*, *12*(11), e0187423.
- Raknes, G., & Småbrekke, L. (2019). Changes in the consumption of antiepileptics and psychotropic medicines after starting low dose naltrexone: A nation-wide register-based controlled before-after study. *Sci Rep*, *9*(1), 15085.
- Ramanathan, S., Panksepp, J., & Johnson, B. (2012). Is fibromyalgia an endocrine/endorphin deficit disorder? Is low dose naltrexone a new treatment option? *Psychosomatics*, *53*(6), 591-594.
- Raynor, K., Kong, H., Chen, Y., Yasuda, K., Yu, L., Bell, G. I., & Reisine, T. (1994). Pharmacological characterization of the cloned kappa-, delta-, and mu-opioid receptors. *Mol Pharmacol*, *45*(2), 330-334.
- Tempel, A., Gardner, E. L., & Zukin, R. S. (1984). Visualization of opiate receptor upregulation by light microscopy autoradiography. *Proc Natl Acad Sci U S A*, *81*(12), 3893-3897.
- Toljan, K., & Vrooman, B. (2018). Low-Dose Naltrexone (LDN)-Review of Therapeutic Utilization. *Med Sci*, *6*(4).
- Trofimovitch, D., & Baumrucker, S. J. (2019). Pharmacology Update: Low-Dose Naltrexone as a Possible Nonopioid Modality for Some Chronic, Nonmalignant Pain Syndromes. *Am J Hosp Palliat Care*, *36*(10), 907-912.
- Unterwald, E. M., Anton, B., To, T., Lam, H., & Evans, C. J. (1998). Quantitative immunolocalization of mu opioid receptors: regulation by naltrexone. *Neuroscience*, *85*(3), 897-905.
- Unterwald, E. M., Rubenfeld, J. M., Imai, Y., Wang, J. B., Uhl, G. R., & Kreek, M. J. (1995). Chronic opioid antagonist administration upregulates mu opioid receptor binding without altering mu opioid receptor mRNA levels. *Brain Res Mol Brain Res*, *33*(2), 351-355.
- Van Bockstaele, E. J., Rudoy, C., Mannelli, P., Oropeza, V., & Qian, Y. (2006). Elevated mu-opioid receptor expression in the nucleus of the solitary tract accompanies attenuated withdrawal signs after chronic low dose naltrexone in opiate-dependent rats. *J Neurosci Res*, *83*(3), 508-514.
- Veening, J. G., Gerrits, P. O., & Barendregt, H. P. (2012). Volume transmission of beta-endorphin via the cerebrospinal fluid; a review. *Fluids Barriers CNS*, *9*(1), 16.
- Wang, H. Y., & Burns, L. H. (2009). Naloxone's pentapeptide binding site on filamin A blocks Mu opioid receptor-Gs coupling and CREB activation of acute morphine. *PLoS One*, *4*(1), e4282.
- Wittmann, W., Schunk, E., Rosskoth, I., Gaburro, S., Singewald, N., Herzog, H., & Schwarzer, C. (2009). Prodynorphin-derived peptides are critical modulators of anxiety and regulate neurochemistry and corticosterone. *Neuropsychopharmacology*, *34*(3), 775-785.
- Younger, J., & Mackey, S. (2009). Fibromyalgia symptoms are reduced by low-dose naltrexone: a pilot study. *Pain Med*, *10*(4), 663-672.
- Younger, J., Noor, N., McCue, R., & Mackey, S. (2013). Low-dose naltrexone for the treatment of fibromyalgia: findings of a small, randomized, double-blind, placebo-controlled, counterbalanced, crossover trial assessing daily pain levels. *Arthritis Rheum*, *65*(2), 529-538.
- Zagon, I. S., & McLaughlin, P. J. (1983). Naltrexone modulates tumor response in mice with neuroblastoma. *Science*, *221*(4611), 671-673.
- Zakarian, S., & Smyth, D. G. (1982). β -Endorphin is processed differently in specific regions of rat pituitary and brain. *Nature*, *296*(5854), 250-252.

- Zappaterra, M., Shouse, E., & Levine, R. L. (2020). Low-Dose Naltrexone reduces symptoms in Stiff-Person Syndrome. *Med Hypotheses*, *137*, 109546.
- Zubieta, J. K., Ketter, T. A., Bueller, J. A., Xu, Y., Kilbourn, M. R., Young, E. A., & Koeppe, R. A. (2003). Regulation of human affective responses by anterior cingulate and limbic mu-opioid neurotransmission. *Arch Gen Psychiatry*, *60*(11), 1145-1153.

CHAPTER 4—EXPLORING THE ORGANIZATION OF THE ENDOGENOUS β - ENDORPHIN SYSTEM

Preamble

A portion of the following material is under revision with the American Journal of Physiology: Regulatory, Integrative, and Comparative Physiology under the title “Individual arcuate nucleus proopiomelanocortin neurons project to select target sites”. A brief background which was not submitted in the latest revision introduces the topic of POMC neuron organization. Following the background section, the submitted work is reproduced as it appeared in the latest submission on October 29, 2021.

Background

In the previous chapter, ARH POMC neurons were treated as a whole population when examining the possibility that LDN sensitizes MORs and the endogenous opioid system. This is because when an exogenous opioid modulator such as naltrexone is administered, the entire brain is bathed in drug and all POMC neurons are likely exposed to antagonist (Djurendic-Brenesel et al., 2012). However, within an endogenous context, ARH POMC neurons may or may not act together to signal at the same time or to the same regions. Even when LDN appeared to alter baseline GCaMP fluorescent activity, not all POMC neurons from LDN treated animals showed this increase in fluorescence compared to no treatment at the time points examined. Though all ARH POMC neurons are traditionally grouped together as they all produce the same peptides including β -endorphin and α -MSH, it is becoming increasingly clear that ARH POMC neurons are heterogenous in how they respond to various interventions. This begs the question of how ARH POMC neurons may be organizing themselves as a heterogenous population of neurons that is involved in many different behavioral processes related to analgesia, reward, food intake,

and more (Harno et al., 2018; Quarta et al., 2021). In this chapter, we examine the organization of ARH POMC neurons with respect to their projections toward downstream targets.

Submitted Work

Individual arcuate nucleus proopiomelanocortin neurons project to select target sites

Summary

Proopiomelanocortin (POMC) neurons in the arcuate nucleus of the hypothalamus (ARH) are a diverse group of neurons that project widely to different brain regions. It is unknown how this small population of neurons organizes its efferent projections. In this study, we hypothesized that individual ARH POMC neurons exclusively innervate select target regions. To investigate this hypothesis, we first verified that only a fraction of ARH POMC neurons innervate the lateral hypothalamus (LH), the paraventricular nucleus of the hypothalamus (PVN), the periaqueductal gray (PAG), or the ventral tegmental area (VTA) using the retrograde tracer cholera toxin B (CTB). Next, two versions of CTB conjugated to distinct fluorophores were injected bilaterally into two of the regions such that PVN and VTA, PAG and VTA, or LH and PVN received tracers simultaneously. These pairs of target sites were chosen based on function and location. Few individual ARH POMC neurons projected to two brain regions at once, suggesting that there are ARH POMC neuron subpopulations organized by their efferent projections. We also investigated whether increasing the activity of POMC neurons could increase the number of ARH POMC neurons labeled with CTB, implying an increase in new synaptic connections to downstream regions. However, chemogenetic enhancement of POMC neuron activity did not increase retrograde tracing of CTB back to ARH POMC neurons from either the LH, PVN, or VTA. Overall, subpopulations of ARH POMC neurons with distinct efferent projections may serve as a way for the POMC population to organize its many functions.

Introduction

Proopiomelanocortin (POMC) neurons in the arcuate nucleus of the hypothalamus (ARH) have been heavily studied for the role that their peptide product α -MSH plays in metabolism and the inhibition of food intake (Cone, 2005; Harno et al., 2018; McMinn et al., 2000; Millington, 2007). However, these neurons produce and release other peptide transmitters such as ACTH and β -endorphin from the pre-pro hormone POMC (Harno et al., 2018). Additionally, these cells also release non-peptide transmitters including GABA, glutamate and endocannabinoids (Dicken et al., 2012; Hentges et al., 2005; Pennock et al., 2012). This diversity in neurotransmitters may explain how these neurons play a role not only in energy balance regulation, but also in the stress response (Greenman et al., 2013; Liu et al., 2007; Qu et al., 2020), analgesia (Loh et al., 1976), reward-related behaviors (Amalric et al., 1987; Dum et al., 1983), and aversion-related behaviors (Klawonn et al., 2018; Quarta et al., 2021). For example, α -MSH released from POMC neurons is involved in energy balance regulation whereas β -endorphin from these neurons is involved in analgesia and reward. While such generalizations can be made, they are clearly oversimplifications since, like β -endorphin, α -MSH also has some role in reward and aversion (Klawonn et al., 2018; Quarta et al., 2021) and β -endorphin can affect food intake (Appleyard et al., 2003; Bodnar, 2019). Thus, it appears that the identity of the transmitter released is, in itself, insufficient to account for specific actions attributed to POMC neurons. Rather, the temporal and anatomic specificity in which transmitters are released may be key to the specific and differential actions attributable to POMC neurons.

While heterogeneity among POMC neurons is evident, it is also surprising given the small number of cells that express POMC peptides and their spatial restriction within the hypothalamus to the ARH (Quarta et al., 2021). The ability of a small, diverse population of cells to participate

in such a variety of behaviors can perhaps be attributed to the widespread nature of the projections from these neurons throughout the vast extent of the brain (Chronwall, 1985; King & Hentges, 2011; Wang et al., 2015; Zheng et al., 2005). POMC neuron projections have been identified in far-spread brain regions associated with specific behaviors that POMC neurons are involved in. For example, the presence of β -endorphin and POMC fibers in the periaqueductal grey (PAG) and ventral tegmental area (VTA) is consistent with POMC neurons being involved in antinociception and reward, respectively, and POMC fibers in the paraventricular nucleus (PVN) and lateral hypothalamic nucleus (LH) is consistent with α -MSH-mediated roles in energy balance regulation (Elias et al., 1999; King & Hentges, 2011; Wang et al., 2015). Despite the low number of POMC neurons, only a very small portion of them appears to project to each target region based on retrograde tracing studies (King & Hentges, 2011; Sawchenko et al., 1982; Yoon et al., 2013; Zheng et al., 2005). This limited projection profile, together with heterogeneity of transmitters, regulation, and functions, led us to hypothesize that individual POMC neurons selectively innervate target sites with distinct functions. To test this hypothesis, we employed double retrograde-labeling approaches to examine if efferent projections from individual POMC neurons simultaneously target multiple brain regions. Further, we used chemogenetic stimulation combined with retrograde tracing to determine if pharmacologic stimulation of POMC neurons affects the number of ARH POMC neurons taking up retrograde tracer from target sites.

Methods

Animals:

Mice were maintained with approval by the Animal Care and Use Committee of Colorado State University in accordance with the Guide for the Care and Use of Laboratory Animals (National

Research Council, 2011). Mice had ad libitum access to food and water except where noted during fast/refeed experiments. A 12 h light/dark cycle (ZT0 = 06:00) was used and temperature and humidity were maintained within a steady range. Male and female mice were used for all experiments and were between 8-14 weeks of age at the time of stereotaxic microinjection. Transgenic mice used to identify POMC cells expressed Discosoma red (PomcdsRED; gifted by Dr. Malcolm Low, University of Michigan) or enhanced green fluorescent protein (PomcEGFP, Jax stock #009593) under the control of the Pomc promoter were congenic on the C57BL/6J strain (Cowley et al., 2001; Hentges et al., 2009). Cre recombinase was expressed in POMC neurons using PomcCre/+ (Jackson laboratories, stock #005965) or Pomc-cre:ERT2 (gifted by Dr. Joel Elmquist, University of Texas Southwestern) transgenic mice for constitutive or tamoxifen-inducible Cre expression, respectively (Berglund et al., 2013). Mice expressing a Cre-inducible version of a Gq DREADD (hm3Dq) sequence tagged with human influenza hemagglutinin (B6N; 129-Gt(ROSA)26Sortm2(CAG-CHRM3-mCitrine)1Ute/J, Jax stock #026220) were used for studies where POMC neuron activity was stimulated (Zhu et al., 2016). Mice constitutively expressing Cre from the POMC promoter (PomcCre/+ mice) were only used in validation experiments with GCaMP6f (see below).

Delivery of tracer:

For stereotaxic microinjections, mice were deeply anesthetized with 5% isoflurane and then anesthesia was maintained with 2% isoflurane. After shaving and scrubbing the incision site, animals were placed on a heating pad in a stereotaxic headframe (David Kopf Instruments) and a midline incision made. A small hole was drilled into the skull, and a Neurosyringe (2 µl; Hamilton) preloaded with red fluorescent FluoSpheres™ (Invitrogen) or cholera toxin -B (CTB) conjugated either to Alexa Fluor™ 488, 555, or 647 was lowered into place at 1 mm/sec

into either the PVN (all coordinates from bregma; female A/P: -0.65 , M/L: ± 0.35 , D/V: -4.9 ; male A/P: -0.75 , M/L: ± 0.3 , D/V: -5.0), VTA (female A/P: -2.9 , M/L: ± 0.65 , D/V: -4.75 ; male A/P: -2.93 , M/L: ± 0.65 , D/V: -4.8), LH (female A/P: -1.4 , M/L: ± 0.98 , D/V: -5.4 ; male A/P: -1.4 , M/L: ± 0.98 , D/V: -5.4) or PAG (female A/P: -4.9 , M/L: ± 0.75 , D/V: -3.0 ; male A/P: -4.9 , M/L: ± 0.75 , D/V: -3.0) The needle was left in place for 5 min post-injection and then raised at 1mm/min. This process was repeated to achieve bilateral injection. After bilateral injection into the first region, the Neurosyringe was thoroughly cleaned, lambda and bregma coordinates were recalibrated, a second tracer was loaded into the syringe, and a second bilateral injection was performed in the next brain region. During recovery, animals were maintained on a heating pad for at least one hour and 5mg/kg carprofen (Rimadyl, Pfizer) was administered daily for 3 days following surgery.

Tissue collection:

Mice were housed for 8-10 days following surgery to allow tracer to traffic to neuron cell bodies (King & Hentges, 2011). Then, mice were deeply anesthetized and perfused with 10% sucrose followed by 4% paraformaldehyde (PFA) diluted in potassium phosphate buffered saline. Brains were collected and allowed to sit overnight in 4% PFA before slicing. Brain slices (50 μm) were collected using a VT100S Leica vibratome. Slices were mounted in Polymount (Polysciences) and slides were allowed to dry overnight before imaging.

Imaging and analysis:

Images were collected using a LSM 800 Airyscan (Zeiss) confocal microscope using Zen Blue software (Zeiss) and collected at 3 μm intervals through the depth of the entire visible slice. The entire rostral-caudal extent of POMC neurons in the arcuate nucleus was imaged. Once images

were collected, cells were counted by hand using Zen lite software (Zeiss). On average, 2128 ± 187 total POMCEGFP or POMCdsRED cells were counted per brain. All counts were verified by at least two researchers, and inter-rater reliability was measured for each fluorophore, and was found to be greater than 66% in all cases (POMCEGFP $86.44 \pm 5.33\%$, POMCdsRED $86.89 \pm 12.51\%$, CTB-488 $93.20 \pm 4.57\%$, CTB-555 $75.20 \pm 8.48\%$, CTB-647 $83.91 \pm 10.22\%$).

Immunohistochemistry:

To visualize hemagglutinin (HA) tagged Gq DREADD receptors, fixed brain slices were washed three times in potassium phosphate buffer solution for 10 minutes and then blocked for 1 h in blocking solution containing 2% goat serum. Slices were incubated overnight in primary antibody against the human influenza HA tag (Cell Signaling, 37245) at a 1:1000 dilution. The next day, after three washes, slices were incubated in for 1 h at room temperature in a 1:250 dilution of goat anti-mouse Alexa Fluor 488 antibody (Invitrogen). Slices went through a final series of washes and were then mounted on glass slides for imaging as described above. No labeling was detected with omission of either primary or secondary antibody.

GCaMP-based calcium imaging:

To express both Gq DREADDs and GCaMP6f in POMC neurons for calcium imaging experiments, 200 nl of a solution containing a 1:1 mix of an adeno-associated virus (AAV) encoding a double-floxed inverse orientation of GCaMP6f (AAV9.CAG.Flex.GCaMP6f.WRPE.SV40; Penn Vector Core, University of Pennsylvania School of Medicine, Philadelphia, PA) and an AAV encoding a Cre recombinase-dependent version of the excitatory designer receptor hM3Dq (pAAV-hSyn-DIO-hMD3(Gq)-mCherry; Addgene) was delivered bilaterally into the arcuate nucleus (from bregma, A/P: -1.63 , M/L:

± 0.32 , D/V: -6.00) of PomcCre/+ mice. For all injections, virus was infused over the course of 1 min and the needle was left in place for 150 s following the end of solution delivery.

Calcium imaging experiments were conducted 2–6 weeks following surgery. Following induction of a deep anesthetic plane with isoflurane, mice were decapitated and their brains were removed and placed into ice-cold artificial CSF (aCSF) consisting of the following (in mM): 126 NaCl, 2.5 KCl, 1.2 MgCl₂·6H₂O, 2.4 CaCl₂·2H₂O, 1.2 NaH₂PO₄, 11.1 glucose, and 21.4 NaHCO₃, and bubbled with 95% O₂ and 5% CO₂. Sagittal slices containing the ARC were cut at a thickness of 240 μ m using a Leica VT1200S vibratome. Brain slices were allowed to recover for at least 1 h at 37°C in aCSF containing the NMDA receptor blocker MK-801 (15 μ M). Slices were then transferred to a recording chamber and perfused with oxygenated, 37°C aCSF at a flow rate of \sim 2 ml/min. Once in the recording chamber, GCaMP6f was excited with 470 nm light generated by an LED (Thorlabs) through a 40 \times water-immersion objective (LUMPlanFL, Olympus). The co-expression of hm3Dq was confirmed by exciting the mCherry reporter with 565 nm light generated by an LED (Thorlabs). Images were captured using CellSens Dimension software (Olympus) and were acquired at \sim 10 Hz with a 50 ms exposure time using an electron-multiplying charge-coupled device (Evolve 512 Delta, Photometrics). A value of 1 was assigned to the median fluorescence intensity over a 5 min baseline period that immediately preceded CNO application (F₀) to normalize the raw fluorescence intensity of individual POMC neurons. Normalized data were then imported to AxoGraph X software where the average fluorescent intensity over the final 5 min of a 10 min drug application was used to calculate the average change in fluorescence, relative to the normalized baseline fluorescence ($\Delta F/F_0$). The washout period was defined as the average fluorescent intensity over a 5-minute period, 15 minutes after the end of CNO application.

Fast/Refeed:

The evening prior to the test, POMC cre-ERT2-expressing or -lacking mice that carried a floxed Gq DREADD sequence were singly housed in fresh cages with no food (water was freely available). The next morning, after fasting 18-20 h, a single injection of CNO was administered (1 mg/kg i.p.) and a premeasured amount of food returned to the animal 30 minutes after injection. Food was measured again 2 hours later. Food and water remained freely available following the test, and animals remained in singly housed conditions until sacrifice.

In vivo POMC neuron activation:

For experiments requiring Gq DREADD expression, PomcdsRED mice were bred with mice expressing Pomc-cre:ERT2 and hm3Dqflox/flox. Mice were given 75mg/kg tamoxifen intraperitoneally (IP) once per day for 5 days in the afternoon. After treatment with tamoxifen, mice were singly housed for one week prior to surgery. Treatment with clozapine-n-oxide (CNO) began 1.5 h prior to surgery, as previous studies show this is an adequate amount of time to increase POMC neuron activity via Gq DREADDs (Zhan et al., 2013). Following surgery, mice were given 1 mg/kg CNO twice daily 30 min prior to lights off (17:30) and 5.5 h following the first injection (23:00) for 10 days until tissue collection. Control mice lacked the Pomc-cre:ERT2 transgene but received both tamoxifen and CNO.

Statistics:

Results for male and female mice were examined separately for each experiment and were not found to be statistically different. Therefore, all datasets were pooled to include both male and female mice, except for food intake data. Datasets were analyzed with Prism software using one-

way ANOVAs with Tukey's multiple comparison tests or with t tests where appropriate. Data are reported as Mean +/- SEM.

Results

Retrograde labeling of ARC POMC neurons projecting to individual target sites

To quantify the relative number of ARH POMC neurons projecting to select target sites, bilateral microinjections of the retrograde tracer cholera toxin B (CTB) were made into downstream target sites of mice expressing a fluorophore to identify POMC cells 10 days prior to tissue collection. Fluorescent images revealed that only a small percentage of POMC neurons labeled with CTB when it was placed into the ventral tegmental area (VTA, $4.94 \pm 1.07\%$; Fig 1A), the paraventricular nucleus of the hypothalamus (PVN, $5.26 \pm 0.95\%$; Fig 1B), the periaqueductal gray (PAG, $7.50 \pm 2.48\%$; Fig 1C), or the lateral hypothalamus (LH, $6.91 \pm 2.25\%$; Fig 1D) consistent with prior reports (Baker & Herkenham, 1995; Fodor et al., 1994; King & Hentges, 2011; Zheng et al., 2005).

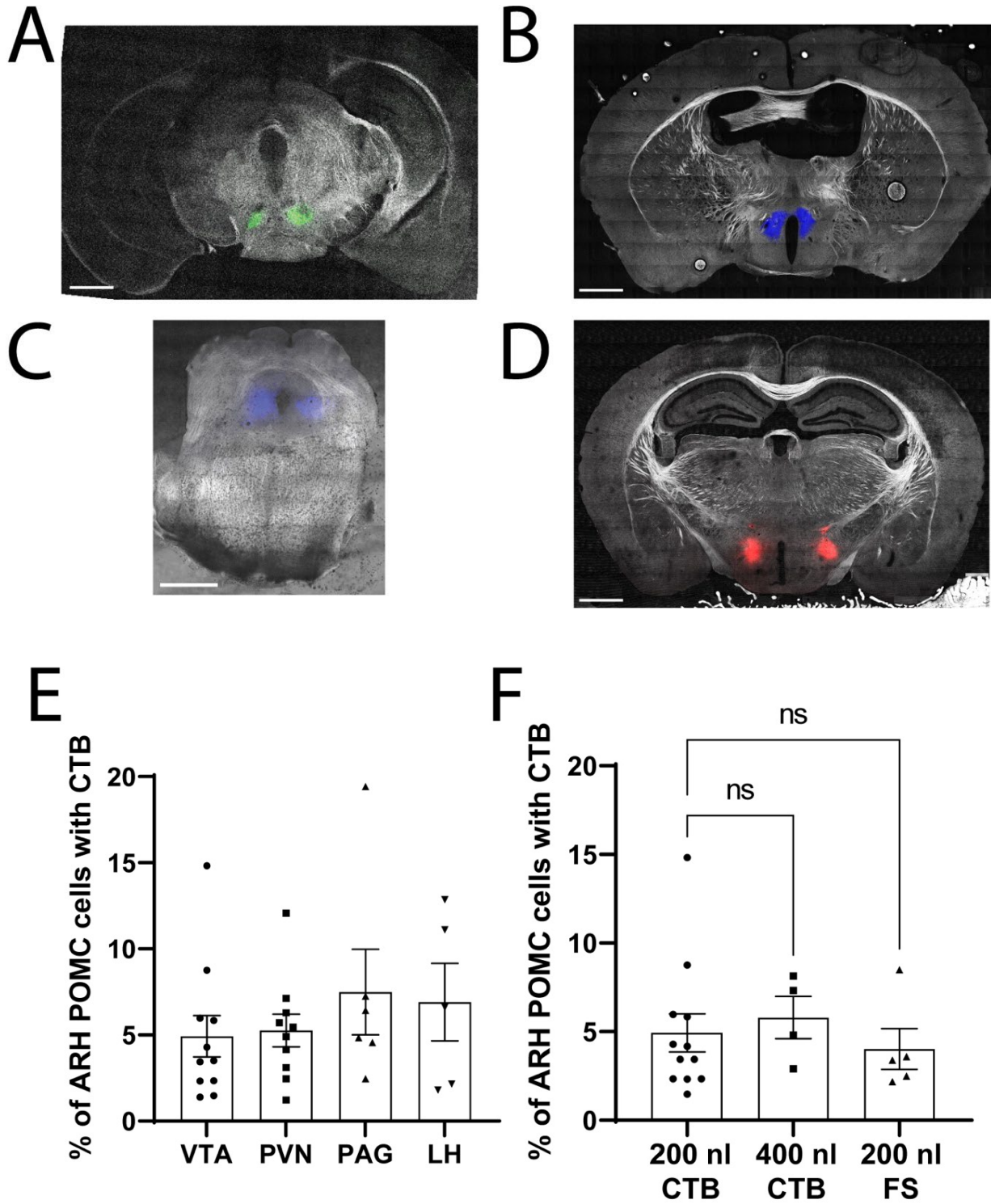


Figure 17. Retrograde tracing from target regions yields a small percentage of CTB-labeled ARH POMC neurons. Representative images of CTB injections into the VTA (A) at approximately -2.92 mm from bregma, PVN (B) at approximately -0.46 mm from bregma,

ventrolateral PAG (C) at approximately -4.72 mm from bregma, and LH (D) at approximately -1.22 mm from bregma. All estimates from bregma are based on Paxinos and Franklin stereotaxic coordinates (Paxinos & Franklin, 2001). All scale bars are 1mm. E) Bar graph showing the percentage of labeled POMC cell bodies containing CTB from individual target regions. F) Bar graph showing the percentage of labeled POMC cell bodies containing CTB for control experiments in the VTA. 200 nl CTB data are the same data in E. FS = FluoSpheres™. Each point represents colocalization from a single animal and data are shown as mean \pm SEM.

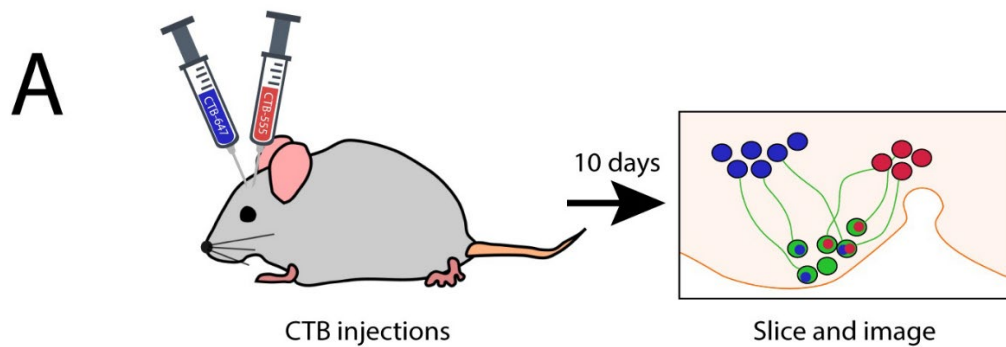
To ensure that the low level of retrograde labeling did not reflect insufficient coverage of the target region by the injected tracer, the volume of retrograde tracer injected into one target site (the VTA) was doubled. Doubling of the injection volume to 400 nl did not result in more ARH POMC neurons labeled with CTB (Fig 1F 1st and 2nd bars; 200nl CTB = $4.94 \pm 1.07\%$; 400 nl CTB = $5.80 \pm 1.20\%$, $p = 0.98$) indicating that the POMC neuron terminals in the region were fully covered by lower volume of the tracer. Thus, further studies were performed with 200 nl of tracer.

To determine whether another tracer would reveal similarly low labeling of ARH POMC neurons, bilateral injections of 200 nl of fluorescent microspheres were made into the VTA 10 days prior to tissue collection. The percentage of POMC neurons with the microspheres was not different from the percentage labeled with 200 nl of CTB (Fig 1F 1st and 3rd bars; CTB $4.94 \pm 1.07\%$; FS $4.03 \pm 1.15\%$; $F(2, 13) = 0.34$, $p = 0.74$). Thus, it is unlikely that the low number of retrogradely-labeled POMC neurons is an artifact of the tracer type.

POMC neuron projections to multiple targets

To determine whether individual ARH POMC neurons project to multiple target regions simultaneously we used two versions of CTB each conjugated to a different fluorophore (either Alexa-488 or Alexa-647). One conjugate was injected bilaterally into one target region and another conjugate was injected bilaterally into another target region in POMCdsRED transgenic

mice 10 days prior to tissue collection (Fig 2A-C). When one CTB conjugate was injected into the PVN and a different CTB conjugate was injected into the VTA, very few POMC neurons contained both CTB conjugates (Fig 2D, first bar; $0.33 \pm 0.09\%$). Additionally, of the CTB-containing POMC neurons, only 4.54% had both conjugates. Thus, it is most common for an individual POMC neuron to project to either the PVN or the VTA, not both. Similarly, tracer from the VTA and PAG were rarely found together in individual POMC neurons (Fig 2D, middle bar; $1.15 \pm 0.41\%$). Of all CTB-labeled POMC neurons, only 7.97% contained both CTB conjugates.



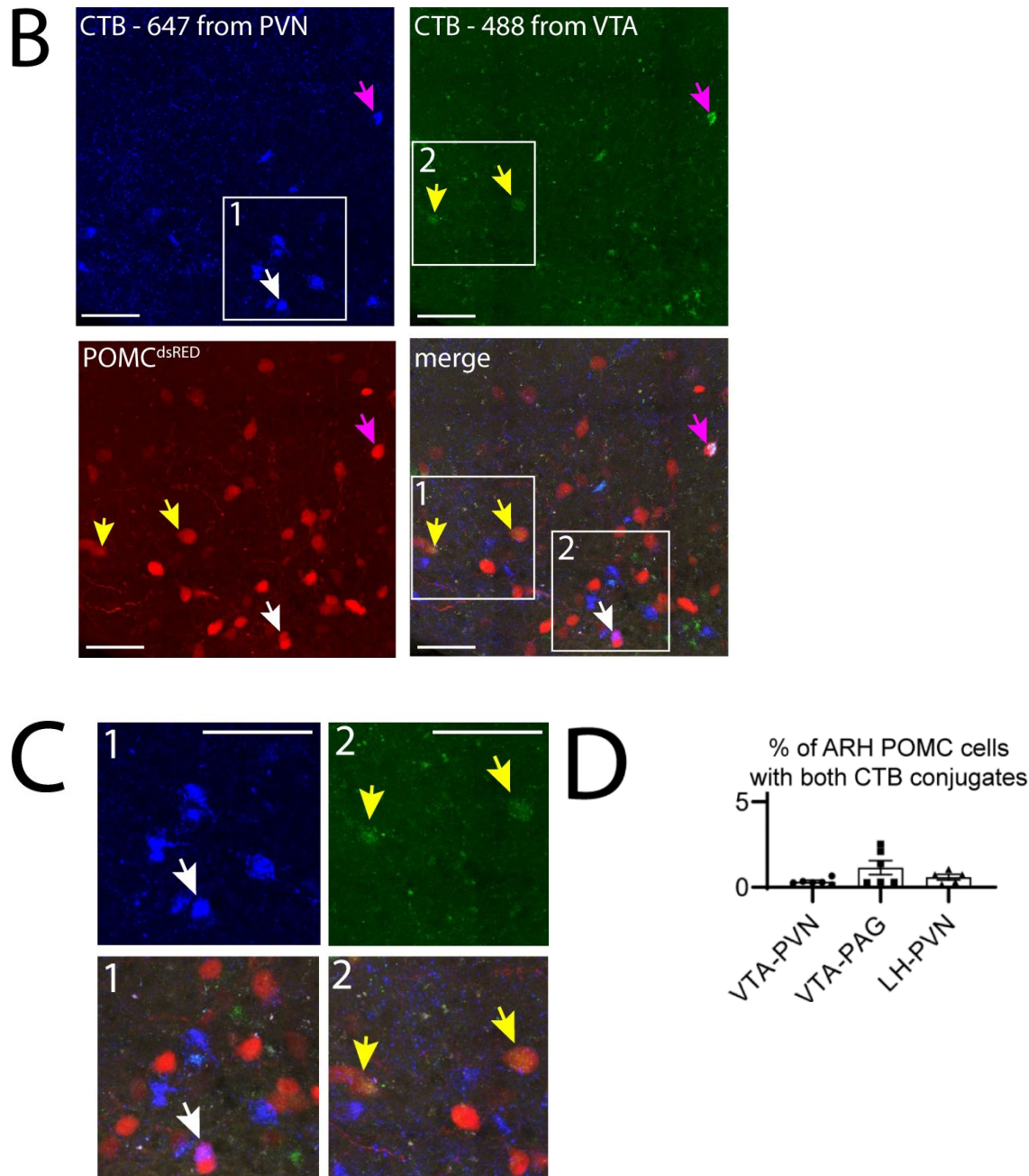


Figure 18. Dual retrograde labeling of CTB conjugates in ARH POMC from target regions is negligible. A) Schematic of experimental procedure depicting CTB injection of two different CTB conjugates into two different brain regions in POMC^{dsRED} mice followed by 10 days of incubation. After the incubation period, brains were sliced and imaged in the area of the arcuate nucleus of the hypothalamus, where POMC neurons expressed a fluorescent tag. B) Images of CTB and POMC^{dsRED} cells in the ARH from a brain injected with CTB-647 into the PVN and CTB-488 into the VTA. Scale bar is 50 μ m. Slice is approximately -1.94 mm from bregma based on Paxinos and Franklin stereotaxic coordinates (Paxinos & Franklin, 2001). C) Boxes 1 and 2 in figure A showing CTB-647 and CTB-488 (top) with respective

merged images with POMCdsRED cells (bottom). Scale bar is 50 μm . D) Bar graph showing the percentage of labeled POMC cell bodies containing two conjugates of CTB, one conjugate from each target region indicated. Each point represents colocalization from a single animal and data are shown as mean \pm SEM.

To determine if two intrahypothalamic sites with some shared functions were more likely to receive projections from single POMC neurons, we performed dual retrograde labeling from the PVN and the lateral hypothalamus (LH). Here again, were very few POMC neurons that took up tracer from both regions (Fig 2D, 3rd bar; $0.59 \pm 0.16\%$) with only 4.02% of the total number of CTB-labeled POMC neurons expressing both conjugates. Overall, it seems that a low number of individual POMC neurons project to any downstream target region and that it is uncommon for a POMC neuron to project to multiple target sites at once, at least under basal conditions to the sites examined here.

POMC neuron activation and tracer uptake

Being largely peptidergic, it is possible that POMC neurons maintain a low level of innervation and synaptic activity basally which could account for the low level of retrograde labeling in POMC neurons observed thus far. Thus, we set out to determine if increased POMC neuron activity would increase the amount of retrograde labeling observed in POMC neurons. We first confirmed functional activation of Gq DREADD (hM3Dq)-expressing POMC neurons upon exposure to the agonist CNO. Brain slices made from POMC cre⁺ mice expressing both Gq DREADDs and GCaMP6f showed an increase in GCaMP-derived fluorescent signal upon application of 10 μM CNO (multiple comparisons baseline vs peak: $p = 0.0003$) with a slight decline in fluorescence with sustained agonist exposure that remained significantly higher than baseline (multiple comparisons baseline vs 10 min: $p = 0.02$; $F(1.275, 20.39) = 24.03$, $p < 0.0001$; Fig 3A & B). As an indicator of in vivo chemogenetic activation of POMC neurons,

mice expressing or lacking Gq-coupled DREADDs in POMC neurons (POMC cre-ERT2+ or POMC cre-ERT2-, respectively) were given CNO (1 mg/kg i.p.) after an overnight fast 30 minutes before food was presented for 2 h. Consistent with the expectation for activating an anorexigenic neuron population, POMC cre-ERT2+ animals expressing the DREADD ate less than POMC cre-ERT2- animals during the 2-hour refeed (Fig 3C, D). Therefore, it appears CNO is able to activate POMC neurons in vivo.

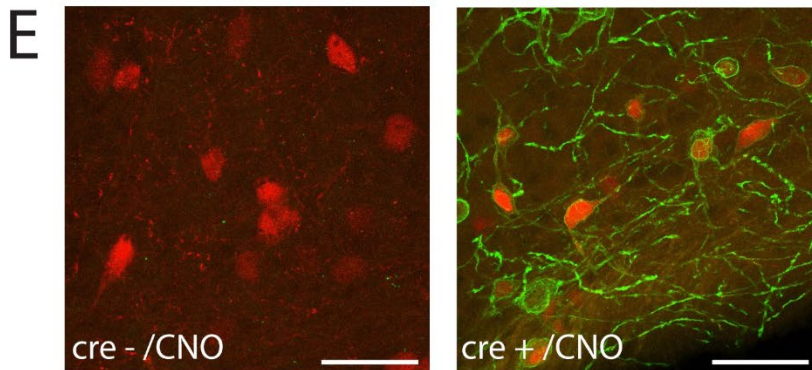
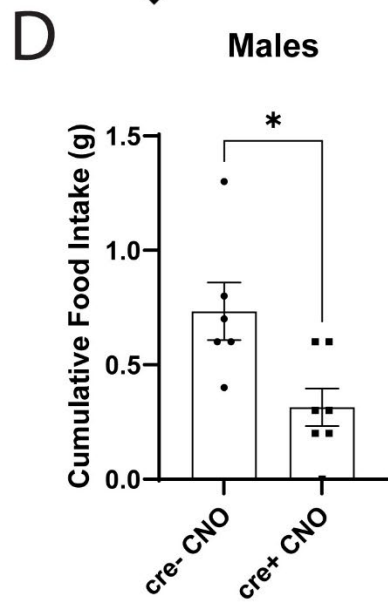
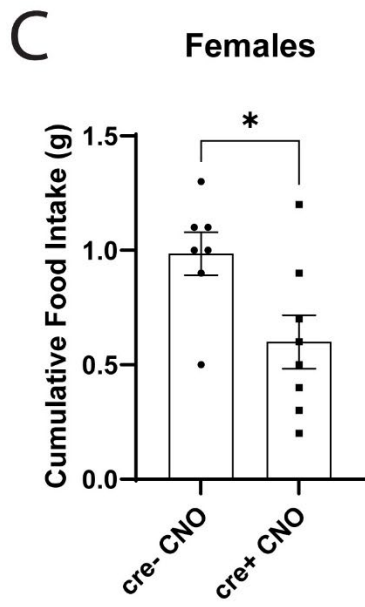
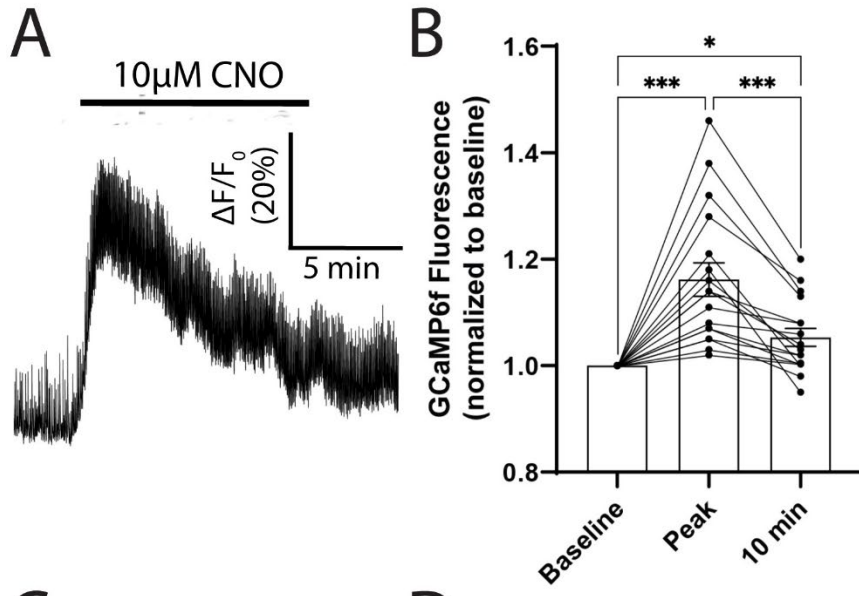


Figure 19. Gq DREADDs activate POMC neurons in vitro and in vivo. A) Representative trace of GCaMP6f fluorescent activity in an ARH POMC neuron virally expressing AAV-hM3Dq (Gq DREADDs) in a POMC cre⁺ mouse after 10 μ M CNO application. B) GCaMP6f fluorescence increased soon after CNO application and decreased within 10 min of continuous CNO application but remained significantly above baseline fluorescence. Each point represents a single POMC cell. Number of animals = 2. Analyzed with one-way ANOVA with Tukey's multiple comparisons. Cumulative food intake during a 2 h refeed after an overnight fast was decreased in POMC cre-ER^{T2+} mice compared to POMC cre-ER^{T2-} mice for C) female and D) male mice. Analyzed with unpaired t test. *p > 0.05, **p > 0.001. E) Immunohistochemical detection of HA-tagged Gq DREADDs (green) in ARH POMC cre-ER^{T2+}; POMC^{dsRED} neurons (red). No detectable Gq DREADD expression was observed in tissue from POMC cre-ER^{T2-} mice (left), but Gq DREADDs were detected in tissue from POMC cre⁺ mice (right). Scale bar is 50 μ m. Slice is approximately -1.58 mm from bregma based on Paxinos and Franklin stereotaxic coordinates (Paxinos & Franklin, 2001).

Chemogenetic activation of POMC neurons was performed using mice cre-ERT2-expressing or -lacking mice that carried a floxed Gq DREADD sequence. All mice received tamoxifen injections twice daily for 5 days starting at 8 weeks of age to induce the expression of Cre or as a control in the absence of the cre-ERT2 transgene. DREADD expression in POMC neurons was confirmed by immunohistochemical detection of the HA-tagged Gq DREADD in POMC^{dsRED} neurons (Fig 3E). Mice with (or without) DREADD receptors expressed in POMC neurons were treated twice daily with CNO just prior to and during the dark period. The first CNO injection occurred 90 minutes before CTB was injected bilaterally into the VTA, LH or PAG and CNO injections went on for 10 days following CTB injection as indicated in Figure 4A. Treatment with CNO to activate the Gq DREADD in POMC neurons did not increase the percentage of POMC neurons regardless of whether the tracer was placed into the VTA (Fig 4B; cre-ERT2⁻: 6.17 \pm 0.89%, cre-ERT2⁺: 5.51 \pm 0.91%; t(13) = 0.51, p = 0.62), LH (Fig 4C; cre-ERT2⁻: 5.76 \pm 1.70%, cre-ERT2⁺: 3.26 \pm 1.11%; t(9) = 1.17, p = 0.27), or PAG (Fig 4D; cre-ERT2⁻: 7.42 \pm 1.43, cre-ERT2⁺: 11.08 \pm 3.07; t(11) = 1.02, p = 0.33). Thus, using this DREADD approach, no evidence of an activity-dependent increase in tracer uptake was found.

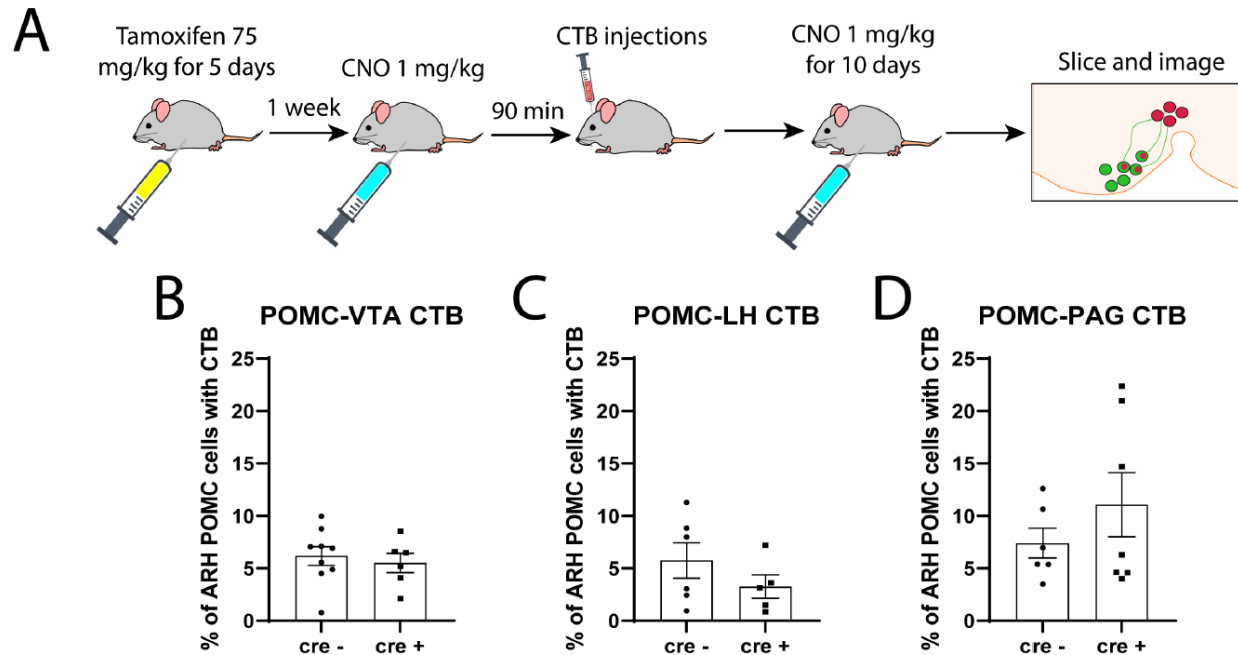


Figure 20. Activation of ARH POMC neurons with Gq DREADDs does not increase colocalization with CTB injected into target regions. A) Schematic of experimental procedure depicting five days of tamoxifen injections to express tamoxifen-inducible cre in POMC neurons to cause the expression of Gq DREADDs in POMC neurons. At least one week later, mice received CNO 90 min prior to CTB stereotaxic injection into two brain regions with two different conjugates of CTB. After surgery, mice received CNO twice per day for 10 days. Tissue was then collected and imaged in the region of the arcuate nucleus. Percent colocalization of CTB in cell bodies of ARH POMC neurons from brains injected in either the VTA (B), LH (C) or PAG (D) was not different between POMC cre-ER^{T2+} and - mice treated with CNO. Each point represents colocalization from a single animal and data are shown as mean +/- SEM.

Discussion

The results here indicate that ARH POMC neurons form small subpopulations based on their efferent projections to downstream regions. Retrograde tracing from the VTA, PVN, PAG, and LH revealed that a small percentage of ARH POMC neurons projects to any one of these regions. Further, retrograde CTB tracing back to individual ARH POMC neurons from brains injected in both the PVN-VTA, PAG-VTA, or LH-PVN shows a negligible percentage of individual POMC neurons projecting to two of these regions simultaneously. Increasing the

activity of POMC neurons did not alter the fraction of ARH POMC neurons that took up the tracer suggesting the inputs to target regions may be fairly stable and not activity dependent. However, we did not investigate all of the possible brain regions that POMC neurons are known to connect to; there may be other regions that receive input from more POMC neurons and regions that individual POMC neurons do project to simultaneously. Putting the present work together with prior tracing studies and studies indicating selective activation of subpopulations of POMC neurons under different conditions, it seems that POMC neurons likely exert specificity of action through activation of neuronal subsets that release neurotransmitter into select target regions under specific conditions. Future studies should examine if specific neurotransmitters are released from POMC subpopulations or if POMC subpopulations are subject to modulation under different physiologic conditions.

It is remarkable that ARH POMC neurons and their transmitters are so strongly involved in diverse physiologic functions (Harno et al., 2018; Mercer et al., 2013) considering the heterogeneity of the population (Quarta et al., 2021) and the small number of POMC neurons in the arcuate (~3000-9,000 in mouse (Baker & Herkenham, 1995; Baker & Shoemaker, 1992; Cowley et al., 2001; Lemus et al., 2015)). The results here suggest that the axons from POMC neurons do not commonly diverge to send collaterals into multiple regions as indicated by the relative lack of dual tracer labeled POMC neurons observed. Thus, it appears that downstream actions may be mediated by just a small subset of ARH POMC neurons that project to a target. This is quite feasible considering the peptidergic nature of POMC neurons and the ability of peptides to diffuse far from the release site to affect extrasynaptic receptors (Veening et al., 2012). This may explain why, regardless of whether CTB and fluorescent microspheres (King & Hentges, 2011; Zheng et al., 2005; SON, PVN, LH, VTA, PAG, BnST, and DVC), wheat-germ

agglutinin (Fodor et al., 1994; PVN), fluorogold (Baker & Herkenham, 1995; PVN), or true blue (Sawchenko et al., 1982; PVN) are used, there has been good consensus that only a small fraction (~3-15%) of POMC neurons in the ARH are labeled. Further, the uptake of retrograde tracer is often dependent on synaptic uptake and vesicle recycling which may make the label more appropriate for tracing fibers from neurons that utilize fast amino acid transmitters as their primary means of cell-to-cell communication. Given that POMC neurons can release the amino acid transmitters GABA and glutamate (Dicken et al., 2012), we may have stimulated vesicular release and reuptake of tracers in the present, but this did not result in additional POMC neurons labeled nor an obvious increase in the label per cell.

Despite the lack of ability to alter uptake and retrograde tracing to POMC neurons from select target regions upon POMC neuron activation, the small subpopulations observed in our studies are likely functional and may respond to unique stimuli. Studies examining ARH POMC neuron activation through detection of the immediate-early gene expression, *c-fos*, show that refeeding after a fast (Olszewski et al., 2001; Wu et al., 2014), dietary fat ingestion (Matsumura et al., 2012), acute stress (Liu et al., 2007), and hemorrhage (Göktalay et al., 2006), activate only a subgroup (~20-60%) of ARH POMC neurons. The fact that each type of stimulus only appears to activate a subset of ARH POMC neurons hints at their differing roles depending upon behavioral state. Further, activation of ARH POMC neuron subpopulations in select target regions shows that even smaller percentages of the overall ARH POMC neuron population can confer observable behavioral effects. ARH POMC terminals expressing channel rhodopsin have been activated in the VTA to modulate anhedonia (Qu et al., 2020), in the medial amygdala to inhibit feeding (Kwon & Jo, 2020), and in the medial preoptic nucleus to inhibit female lordosis (Johnson et al., 2020). Also, chemogenetic activation of ARH POMC neurons projecting to the

ventral striatum has been shown to increase aversion (Klawonn et al., 2018). Based on the results of this study and the results of previous studies, these activated subpopulations likely only make up a very small percentage of ARH POMC neurons, and yet there is an observable influence on behavior in response to stimulation. Thus, the POMC subpopulations we observed with retrograde tracing have the potential to independently act and modulate behavior via their actions in downstream regions.

Perspectives and Significance

The differences found in this study for projection patterns of POMC neuron subpopulations suggests an even more complex regulation of POMC neuron functions than previously thought. It is possible that very small groups of ARH POMC neurons are responsible for communicating relevant information to widespread target regions. Though each POMC subpopulation shares a common set of peptides, it is largely unknown if the *in vivo* activation of each subpopulation, as defined by efferent projection localization, represents the action of a unified group or if individual subpopulations act separately at different times. Activation of the ARH POMC population as a whole in experimental studies may, therefore, create a pattern of activity within the brain that is very different from what occurs *in vivo*. If POMC neuron subpopulations act in opposition to one another through the activation of different brain regions, this could result in an overall lack of observable effect when, in reality, small subpopulations actually may be changing activity throughout the brain. In the future, it will be important to understand the *in vivo* patterning of POMC neuron activation in relation to where POMC neurons are projecting, as this could inform experimental design for investigating the many functional effects conferred by POMC neurons.

References

- Amalric, M., Cline, E. J., Martinez, J. L., Jr., Bloom, F. E., & Koob, G. F. (1987). Rewarding properties of beta-endorphin as measured by conditioned place preference. *Psychopharmacology (Berl)*, 91(1), 14-19. doi:10.1007/bf00690919
- Appleyard, S. M., Hayward, M., Young, J. I., Butler, A. A., Cone, R. D., Rubinstein, M., & Low, M. J. (2003). A role for the endogenous opioid beta-endorphin in energy homeostasis. *Endocrinology*, 144(5), 1753-1760. doi:10.1210/en.2002-221096
- Baker, R. A., & Herkenham, M. (1995). Arcuate nucleus neurons that project to the hypothalamic paraventricular nucleus: neuropeptidergic identity and consequences of adrenalectomy on mRNA levels in the rat. *J Comp Neurol*, 358(4), 518-530. doi:10.1002/cne.903580405
- Baker, R. A., & Shoemaker, W. J. (1992). beta-Endorphin-immunoreactive neurons in the hypothalamus and medulla of the rat brain: Effect of prenatal ethanol. *Mol Cell Neurosci*, 3(2), 106-117. doi:10.1016/1044-7431(92)90014-s
- Berglund, E. D., Liu, C., Sohn, J. W., Liu, T., Kim, M. H., Lee, C. E., . . . Elmquist, J. K. (2013). Serotonin 2C receptors in pro-opiomelanocortin neurons regulate energy and glucose homeostasis. *J Clin Invest*, 123(12), 5061-5070. doi:10.1172/jci70338
- Bodnar, R. J. (2019). Endogenous opioid modulation of food intake and body weight: Implications for opioid influences upon motivation and addiction. *Peptides*, 116, 42-62. doi:10.1016/j.peptides.2019.04.008
- Chronwall, B. M. (1985). Anatomy and physiology of the neuroendocrine arcuate nucleus. *Peptides*, 6, 1-11.
- Cone, R. D. (2005). Anatomy and regulation of the central melanocortin system. *Nat Neurosci*, 8(5), 571-578. doi:10.1038/nn1455
- Cowley, M. A., Smart, J. L., Rubinstein, M., Cerdán, M. G., Diano, S., Horvath, T. L., . . . Low, M. J. (2001). Leptin activates anorexigenic POMC neurons through a neural network in the arcuate nucleus. *Nature*, 411(6836), 480-484. doi:10.1038/35078085
- Dicken, M. S., Tooker, R. E., & Hentges, S. T. (2012). Regulation of GABA and glutamate release from proopiomelanocortin neuron terminals in intact hypothalamic networks. *J Neurosci*, 32(12), 4042-4048. doi:10.1523/jneurosci.6032-11.2012
- Djurendic-Brenesel, M., Pilija, V., Mimica-Dukic, N., Budakov, B., & Cvjeticanin, S. (2012). Distribution of opiate alkaloids in brain tissue of experimental animals. *Interdiscip Toxicol*, 5(4), 173-178. doi:10.2478/v10102-012-0029-y
- Dum, J., Gramsch, C., & Herz, A. (1983). Activation of hypothalamic beta-endorphin pools by reward induced by highly palatable food. *Pharmacol Biochem Behav*, 18(3), 443-447. doi:10.1016/0091-3057(83)90467-7
- Elias, C. F., Aschkenasi, C., Lee, C., Kelly, J., Ahima, R. S., Bjorbæk, C., . . . Elmquist, J. K. (1999). Leptin differentially regulates NPY and POMC neurons projecting to the lateral hypothalamic area. *Neuron*, 23(4), 775-786.
- Fodor, M., Csaba, Z., Kordon, C., & Epelbaum, J. (1994). Growth hormone-releasing hormone, somatostatin, galanin and beta-endorphin afferents to the hypothalamic periventricular nucleus. *J Chem Neuroanat*, 8(1), 61-73. doi:10.1016/0891-0618(94)90036-1
- Göktalay, G., Cavun, S., Levendusky, M. C., Resch, G. E., Veno, P. A., & Millington, W. R. (2006). Hemorrhage activates proopiomelanocortin neurons in the rat hypothalamus. *Brain Res*, 1070(1), 45-55. doi:10.1016/j.brainres.2005.11.076
- Greenman, Y., Kuperman, Y., Drori, Y., Asa, S. L., Navon, I., Forkosh, O., . . . Chen, A. (2013). Postnatal ablation of POMC neurons induces an obese phenotype characterized by

- decreased food intake and enhanced anxiety-like behavior. *Mol Endocrinol*, 27(7), 1091-1102. doi:10.1210/me.2012-1344
- Harno, E., Gali Ramamoorthy, T., Coll, A. P., & White, A. (2018). POMC: The Physiological Power of Hormone Processing. *Physiol Rev*, 98(4), 2381-2430. doi:10.1152/physrev.00024.2017
- Hentges, S. T., Low, M. J., & Williams, J. T. (2005). Differential regulation of synaptic inputs by constitutively released endocannabinoids and exogenous cannabinoids. *J Neurosci*, 25(42), 9746-9751. doi:10.1523/jneurosci.2769-05.2005
- Hentges, S. T., Otero-Corchon, V., Pennock, R. L., King, C. M., & Low, M. J. (2009). Proopiomelanocortin expression in both GABA and glutamate neurons. *J Neurosci*, 29(43), 13684-13690. doi:10.1523/jneurosci.3770-09.2009
- Johnson, C., Hong, W., & Micevych, P. (2020). Optogenetic Activation of β -Endorphin Terminals in the Medial Preoptic Nucleus Regulates Female Sexual Receptivity. *eNeuro*, 7(1). doi:10.1523/eneuro.0315-19.2019
- King, C. M., & Hentges, S. T. (2011). Relative Number and Distribution of Murine Hypothalamic Proopiomelanocortin Neurons Innervating Distinct Target Sites. *PLOS ONE*, 6(10), e25864. doi:10.1371/journal.pone.0025864
- Klawonn, A. M., Fritz, M., Nilsson, A., Bonaventura, J., Shionoya, K., Mirrasekhian, E., . . . Engblom, D. (2018). Motivational valence is determined by striatal melanocortin 4 receptors. *J Clin Invest*, 128(7), 3160-3170. doi:10.1172/jci97854
- Kwon, E., & Jo, Y.-H. (2020). Activation of the ARCPOMC→MeA Projection Reduces Food Intake. *Frontiers in Neural Circuits*, 14(73). doi:10.3389/fncir.2020.595783
- Lemus, M. B., Bayliss, J. A., Lockie, S. H., Santos, V. V., Reichenbach, A., Stark, R., & Andrews, Z. B. (2015). A stereological analysis of NPY, POMC, Orexin, GFAP astrocyte, and Iba1 microglia cell number and volume in diet-induced obese male mice. *Endocrinology*, 156(5), 1701-1713. doi:10.1210/en.2014-1961
- Liu, J., Garza, J. C., Truong, H. V., Henschel, J., Zhang, W., & Lu, X. Y. (2007). The melanocortinergic pathway is rapidly recruited by emotional stress and contributes to stress-induced anorexia and anxiety-like behavior. *Endocrinology*, 148(11), 5531-5540. doi:10.1210/en.2007-0745
- Loh, H. H., Tseng, L. F., Wei, E., & Li, C. H. (1976). beta-endorphin is a potent analgesic agent. *Proc Natl Acad Sci U S A*, 73(8), 2895-2898. doi:10.1073/pnas.73.8.2895
- Matsumura, S., Eguchi, A., Okafuji, Y., Tatsu, S., Mizushige, T., Tsuzuki, S., . . . Fushiki, T. (2012). Dietary fat ingestion activates β -endorphin neurons in the hypothalamus. *FEBS Lett*, 586(8), 1231-1235. doi:10.1016/j.febslet.2012.03.028
- McMinn, J. E., Wilkinson, C. W., Havel, P. J., Woods, S. C., & Schwartz, M. W. (2000). Effect of intracerebroventricular alpha-MSH on food intake, adiposity, c-Fos induction, and neuropeptide expression. *Am J Physiol Regul Integr Comp Physiol*, 279(2), R695-703. doi:10.1152/ajpregu.2000.279.2.R695
- Mercer, A. J., Hentges, S. T., Meshul, C. K., & Low, M. J. (2013). Unraveling the central proopiomelanocortin neural circuits. *Front Neurosci*, 7, 19. doi:10.3389/fnins.2013.00019
- Millington, G. W. (2007). The role of proopiomelanocortin (POMC) neurones in feeding behaviour. *Nutr Metab (Lond)*, 4, 18. doi:10.1186/1743-7075-4-18
- National Research Council, N. (2011). *Guide for the Care and Use of Laboratory Animals: Eighth Edition.* (978-0-309-15400-0). Washington, DC: The National Academies Press

- Retrieved from <https://www.nap.edu/catalog/12910/guide-for-the-care-and-use-of-laboratory-animals-eighth>
- Olszewski, P. K., Wirth, M. M., Shaw, T. J., Grace, M. K., Billington, C. J., Giraudo, S. Q., & Levine, A. S. (2001). Role of alpha-MSH in the regulation of consummatory behavior: immunohistochemical evidence. *Am J Physiol Regul Integr Comp Physiol*, 281(2), R673-680. doi:10.1152/ajpregu.2001.281.2.R673
- Paxinos, G., & Franklin, K. B. J. (2001). *The Mouse Brain in Stereotaxic Coordinates* (2nd ed.): Academic Press.
- Pennock, R. L., Dicken, M. S., & Hentges, S. T. (2012). Multiple inhibitory G-protein-coupled receptors resist acute desensitization in the presynaptic but not postsynaptic compartments of neurons. *J Neurosci*, 32(30), 10192-10200. doi:10.1523/jneurosci.1227-12.2012
- Qu, N., He, Y., Wang, C., Xu, P., Yang, Y., Cai, X., . . . Xu, Y. (2020). A POMC-originated circuit regulates stress-induced hypophagia, depression, and anhedonia. *Mol Psychiatry*, 25(5), 1006-1021. doi:10.1038/s41380-019-0506-1
- Quarta, C., Claret, M., Zeltser, L. M., Williams, K. W., Yeo, G. S. H., Tschöp, M. H., . . . Cota, D. (2021). POMC neuronal heterogeneity in energy balance and beyond: an integrated view. *Nat Metab*. doi:10.1038/s42255-021-00345-3
- Sawchenko, P. E., Swanson, L. W., & Joseph, S. A. (1982). The distribution and cells of origin of ACTH(1-39)-stained varicosities in the paraventricular and supraoptic nuclei. *Brain Res*, 232(2), 365-374. doi:10.1016/0006-8993(82)90280-3
- Veening, J. G., Gerrits, P. O., & Barendregt, H. P. (2012). Volume transmission of beta-endorphin via the cerebrospinal fluid; a review. *Fluids Barriers CNS*, 9(1), 16. doi:10.1186/2045-8118-9-16
- Wang, D., He, X., Zhao, Z., Feng, Q., Lin, R., Sun, Y., . . . Zhan, C. (2015). Whole-brain mapping of the direct inputs and axonal projections of POMC and AgRP neurons. *Front Neuroanat*, 9, 40. doi:10.3389/fnana.2015.00040
- Wu, Q., Lemus, M. B., Stark, R., Bayliss, J. A., Reichenbach, A., Lockie, S. H., & Andrews, Z. B. (2014). The temporal pattern of cfos activation in hypothalamic, cortical, and brainstem nuclei in response to fasting and refeeding in male mice. *Endocrinology*, 155(3), 840-853. doi:10.1210/en.2013-1831
- Yoon, Y. S., Lee, J. S., & Lee, H. S. (2013). Retrograde study of CART- or NPY-neuronal projection from the hypothalamic arcuate nucleus to the dorsal raphe and/or the locus coeruleus in the rat. *Brain Res*, 1519, 40-52. doi:10.1016/j.brainres.2013.04.039
- Zhan, C., Zhou, J., Feng, Q., Zhang, J.-e., Lin, S., Bao, J., . . . Luo, M. (2013). Acute and long-term suppression of feeding behavior by POMC neurons in the brainstem and hypothalamus, respectively. *Journal of Neuroscience*, 33(8), 3624-3632.
- Zheng, H., Patterson, L. M., Phifer, C. B., & Berthoud, H. R. (2005). Brain stem melanocortinergic modulation of meal size and identification of hypothalamic POMC projections. *Am J Physiol Regul Integr Comp Physiol*, 289(1), R247-258. doi:10.1152/ajpregu.00869.2004
- Zhu, H., Aryal, D. K., Olsen, R. H., Urban, D. J., Swearingen, A., Forbes, S., . . . Hochgeschwender, U. (2016). Cre-dependent DREADD (Designer Receptors Exclusively Activated by Designer Drugs) mice. *Genesis*, 54(8), 439-446. doi:10.1002/dvg.22949

CHAPTER 5—CONCLUSION

The studies presented in this dissertation have dissected components of the opioid system to better understand opioid signaling from receptor to circuit. In Chapter 2, we discovered that while MORs exhibit an extensive range of mobilities, specific functional states do not necessarily correspond to a single mobility state (Metz et al., 2019). The range of mobility states (and assumed range in functional states) observed in baseline conditions in Chapter 2 prompted an attempt in Chapter 3 to shift more receptors toward sensitization using a well-characterized drug paradigm used in the clinic today, LDN. LDN had little to no effect on MOR sensitization or on activation of the endogenous opioid system within POMC neurons of the hypothalamus (Metz et al., 2021). Therefore, we turned our attention in Chapter 4 to understanding how POMC neurons are organized in hopes of better understanding the circuitry of neurons that play an important role in the endogenous opioid system. We found that POMC neurons are mostly divided into subpopulations based upon where they project, with very few single neurons projecting to two locations at once. This opens up the promising possibility of further exploring how these subpopulations function, together or separately, to juggle the many functions of POMC neurons and the endogenous opioid system.

Exogenous versus endogenous opioid signaling

The experiments described in the preceding chapters touch on different aspects of the endogenous and exogenous opioid system. We tried to take into account how endogenous opioid systems are responding to exogenously applied drugs as well as how the endogenous system itself is wired to handle opioid signaling in the absence of drug application. When exogenous opioids are applied, MORs are activated throughout the entire brain and body, with perhaps some subtle variation in opioid binding to MORs between different regions (Djurendic-Brenesel et al.,

2012). This is why when exogenous opioids are administered, processes handled by areas within the brain stem, such as respiratory depression, can be observed in concert with processes handled in other regions, such as analgesia (Bagley & Ingram, 2020; Stott & Pleuvry, 1991; Varga et al., 2020). In contrast to this brain-wide flooding with exogenous opioid, based on our retrograde tracing studies in Chapter 4, the endogenous opioid system shows potential for region-specific release of POMC-derived peptides into regions with different functions. Whether differential activation of POMC neuron subpopulations allows for region-specific peptide release, however, is unknown. While it appears that only fractions of POMC neurons are activated in response to a stimuli at any one time (Göktalay et al., 2006; Liu et al., 2007; Matsumura et al., 2012; Olszewski et al., 2001; Wu et al., 2014), none of these studies measured where and exactly when when peptide was being released. Therefore, ARH POMC subpopulations projecting to different regions could be activated at the same time or separately. With further development of peptide-sensing strategies, this could be an avenue of future study.

However, there may be cases in which volume transmission of β -endorphin resembles the application of exogenous opioid through bulk transmission of the peptide through cerebrospinal fluid. The proximity of endorphin-containing fibers to ventricles allows for the possibility of dumping peptide into the cerebrospinal fluid, which would result in a wider distribution of signaling (Rodríguez et al., 2010; Veening et al., 2012). Volume transmission occurs on the order of several minutes, whereas direct release of peptide only takes a few seconds (Izquierdo & Netto, 1985; Wan et al., 1996). In an evolutionary context, seconds count when providing analgesia to run from a predator, for instance. Therefore, perhaps direct release of β -endorphin into specific regions provides a faster mode of transmission that is later reinforced by CSF-derived peptide. No matter what the mechanism, the endogenous opioid system clearly has more

apparent potential for fine-tuning where and when opioids signal compared to exogenous opioid application.

The importance of this fine-tuning is apparent when considering the negative effects on brain chemistry and signaling in the context of chronic exogenous opioids. Not only are reward systems drastically altered by chronic opioid applications, but analgesia and the endogenous opioid system itself is dysregulated by exogenous opioid application. Studies of morphine administration in rodents have shown that β -endorphin synthesis in the pituitary is inhibited as early as 3 days post-administration (Gianoulakis et al., 1981). Hypothalamic POMC transcription and brain β -endorphin concentrations are also decreased within 7 days of morphine administration (Le Merrer et al., 2009; Vuong et al., 2010). These findings point to a general decrease in functioning of the endogenous opioid system after just a few days of agonist administration. At the molecular level, changes may occur even faster. Chapter 2 corroborates earlier findings that changes can be observed in MOR activity after just a few minutes of agonist administration (Metz et al., 2019). As mentioned in Chapter 3, antagonist administration appears to have the opposite effect on the endogenous opioid system, at least at high doses, as long-term administration of high dose naltrexone increases MOR expression as well as Pomc mRNA and POMC peptide expression (Díaz et al., 2002; Markowitz et al., 1992; Panigrahi et al., 2019; Tempel et al., 1984; Unterwald et al., 1998; Unterwald et al., 1995). The increase in MOR expression likely accounts for enhanced responsiveness to subsequent exogenous agonist application (Díaz et al., 2002). We did not find, however, that low dose naltrexone conveys the same effects in POMC neurons, though changes in the opioid system within other brain regions or throughout the body cannot be ruled out (Metz et al., 2021).

The many effects of opioid signaling

It is well-known that opioid signaling confers many effects, including analgesia, reward and reinforcement, respiratory depression, and more. In many studies, it is often the goal to avoid understand how certain undesirable behavioral side effects may be separated from more desirable target behaviors. For instance, in Chapter 4 the inclusion of the PAG and VTA in dual retrograde tracing studies was for the purpose of attempting to understand how a region highly involved in analgesia was connected to a region highly involved in reward and reinforcement at the level of POMC afferents. It appears very few individual ARH POMC neurons project to both of these regions at once. This brings up the interesting future possibility of searching for specific markers on PAG-projecting POMC neurons in hopes of activating these neurons specifically to amplify analgesic effects of the endogenous opioid system at the exclusion of rewarding effects. Finding a non-rewarding analgesic would be impactful, considering that opioid analgesics currently used in the clinic have a high abuse liability; 8-12% of people who use prescription opioids for chronic pain develop an addictive disorder (Vowles et al., 2015).

Yet, it is important to remember that the concurrent activation of analgesia and reward also serves an important purpose, and completely eradicating reward in favor of analgesia could result in a loss of the unique pain-relieving effects of opioids. As described in Chapter 1, pain relief through the opioid system comprises an important emotional component, especially through opioid receptors of the ACC (Porreca & Navratilova, 2017). Connections between midbrain dopaminergic reward systems and the ACC ensure that the relief of aversive emotional states handled by MORs of the ACC is closely linked to systems of reward and reinforcement (Navratilova & Porreca, 2014). It may be that this unique connection to reward is what makes opioid analgesics more powerful than other analgesics such as NSAIDs in the short term. The power of opioids may also lie in the preference that patients have for them and in the expectation

of powerful analgesia. The expectation of pain relief can be a powerful determiner in how much analgesia one experiences, and many patients report a preference for opioids because of the perception that they are stronger analgesics (Matthias et al., 2018). This preference could play a role in how much pain relief patients perceive.

The future of opioid analgesics

Perceptions about opioids are beginning to change in the clinic. In 2018, the Food and Drug Administration (FDA) updated requirements to include black box warnings on all opioid products, alerting practitioners to risk evaluation and mitigation strategies for avoiding tolerance, dependence, and overdose associated with opioid prescribing (FDA, 2021). Further, the utility of opioids for chronic use is now consistently being brought into question, and in several small clinical trials have been found opioids to be no more effective than NSAIDs for chronic pain (Busse et al., 2018; Holdgate & Pollock, 2005; Huang et al., 2019; Krebs et al., 2018; Pathan et al., 2018; Schüchen et al., 2018; Sobieraj et al., 2020). However, NSAIDs do carry a serious risk for severe adverse events, especially gastrointestinal bleeding, ulceration, and perforation (Nalamachu, 2013). In response to the limited options clinicians have for treating pain, especially chronic pain, the National Institutes of Health has recently launched initiatives to accelerate the discovery and development of non-addictive, non-opioid analgesics (Iyengar et al., 2020). As of the end of 2019, 115 non-opioid analgesics were in various phases of clinical investigation.

Historically, non-opioid analgesics have consisted of surgical interventions and targeting ion channels important for the conduction of pain signals to the brain. Surgery is a successful intervention for some patients, for example when the cause of pain is clear in cases of nerve compression. However, in many cases of chronic pain there is not a readily identifiable cause, or the cause is not surgically targetable. In these cases, medical interventions have attempted to co-

opt drugs that target ion channels, often indicated for treating epilepsy, to inhibit inappropriate pain signaling. These non-selective ion channel blockers most frequently target Na⁺ and Ca²⁺ channels and may cause excessive fatigue (Manion et al., 2019). One more specific target that shows some promise due to its peripheral specificity for pain pathways is NaV 1.7. Evidence from people carrying a loss-of-function mutation in the gene for NaV 1.7 showed that this channel seems to be important for pain perception but does not appear to contribute to other functions. Such a specific target is a rare opportunity in analgesic development, however it has been quite challenging to develop NaV 1.7-specific blockers for therapeutic use. Recently, some pharmaceutical companies have attempted to find NaV 1.7-specific blockers in nature by deriving them from tarantula venom, but the long-term efficacy of these compounds is yet to be seen (Kingwell, 2019). One final challenge in the development of NaV 1.7 blockage is the potential for nerve damage, or neuropathy, with long-term blockade of pain signaling. As exemplified by individuals with loss-of-function mutations in NaV 1.7, complete loss of pain signaling allows for the potential of extensive tissue damage. Therefore, a balance must be struck between alleviating debilitating chronic pain and getting rid of pain signaling entirely (Manion et al., 2019).

Other biologic approaches, such as genetic interventions, cell transplants, and antibodies are also being explored as potential alternative therapies for chronic pain. (Manion et al., 2019) Frequently, the distinction between inflammatory pain (due to tissue injury and accumulation of inflammatory factors) and neuropathic pain (due to neuronal damage) is accounted for in developing these treatments (Xu & Yaksh, 2011). However, these treatments must focus even more specifically on certain pathologies, as within the categories of inflammatory and neuropathic pain there can be many different types of underlying biological causes. For example,

one of the newest class of antibody therapies for chronic pain is anti-calcitonin gene-related peptide receptor (α -CGRPR) therapy. (Manion et al., 2019; Mohanty & Lippmann, 2020) CGRP is known to cause dilation of blood vessels within the brain, which is a key part in the induction of migraines. Therefore, blocking of CGRP signaling through α -CGRPR therapy has provided alleviation of migraine for many patients. However, there are still many patients who do not respond to α -CGRPR therapy, and response is often incomplete. Therefore, even within the context of a condition like migraine, there are likely several underlying pathologies (Woo, 2020).

Development of nonopioid analgesics does not mean that the journey is over for opioids in pain treatment. Many patients respond to opioids well in the acute term, and some can even use them long term and retain some beneficial effect (Matthias et al., 2018). Further, opioid links to emotional circuits and the importance of emotion in pain processing should not be overlooked. However, perhaps the time has come for more studies of augmenting the endogenous opioid system in individuals with chronic pain. There is some evidence showing that β -endorphin is decreased in certain chronic pain states, and certain non-pharmaceutical interventions, such as exercise, have been shown to increase β -endorphin (Bonifácio de Assis et al., 2021; Misra et al., 2017; Nijs et al., 2012; Yonehara et al., 1983). Further, our findings that POMC neurons send projections to pain-related areas at the exclusion of reward-related areas could inform future attempts to increase β -endorphin concentrations in analgesic areas. This would likely depend upon the identification of specific biomarkers for this subgroup of neurons or identification of certain behavioral states that activate these subgroups.

Overall, the results described within the preceding chapters showcase the complexity of the opioid system from how receptors move in the membrane to how POMC circuitry is set up as subpopulations that project to individual downstream targets. While our attempt to alter

endogenous opioid system tone with LDN did not appear to be very effective, the finding that POMC neurons exhibit subpopulation-specific afferent projections lends promise towards enhancing the function of POMC-related pathways in the future. The complexity of the opioid system makes it difficult to create treatments with no side effects, but perhaps capitalizing upon the beneficial emotional effects of opioids and focusing on enhancing activation of the endogenous system would help to improve opioid treatment.

References

- Bagley, E. E., & Ingram, S. L. (2020). Endogenous opioid peptides in the descending pain modulatory circuit. *Neuropharmacology*, 173, 108131. doi:10.1016/j.neuropharm.2020.108131
- Bonifácio de Assis, E., Dias de Carvalho, C., Martins, C., & Andrade, S. (2021). Beta-Endorphin as a Biomarker in the Treatment of Chronic Pain with Non-Invasive Brain Stimulation: A Systematic Scoping Review. *J Pain Res*, 14, 2191-2200. doi:10.2147/jpr.S301447
- Busse, J. W., Wang, L., Kamaleldin, M., Craigie, S., Riva, J. J., Montoya, L., . . . Guyatt, G. H. (2018). Opioids for Chronic Noncancer Pain: A Systematic Review and Meta-analysis. *JAMA*, 320(23), 2448-2460. doi:10.1001/jama.2018.18472
- Díaz, A., Pazos, A., Flórez, J., Ayesta, F. J., Santana, V., & Hurlé, M. A. (2002). Regulation of mu-opioid receptors, G-protein-coupled receptor kinases and beta-arrestin 2 in the rat brain after chronic opioid receptor antagonism. *Neuroscience*, 112(2), 345-353. doi:10.1016/s0306-4522(02)00073-8
- Djurendić-Brenesel, M., Pilija, V., Mimica-Dukic, N., Budakov, B., & Cvjeticanin, S. (2012). Distribution of opiate alkaloids in brain tissue of experimental animals. *Interdiscip Toxicol*, 5(4), 173-178. doi:10.2478/v10102-012-0029-y
- FDA. (2021, July 2, 2021). Timeline of Selected FDA Activities and Significant Events Addressing Opioid Misuse and Abuse. Retrieved from <https://www.fda.gov/drugs/information-drug-class/timeline-selected-fda-activities-and-significant-events-addressing-opioid-misuse-and-abuse>
- Gianoulakis, C., Drouin, J. N., Seidah, N. G., Kalant, H., & Chrétien, M. (1981). Effect of chronic morphine treatment on beta-endorphin biosynthesis by the rat neurointermediate lobe. *Eur J Pharmacol*, 72(4), 313-321. doi:10.1016/0014-2999(81)90569-0
- Göktalay, G., Cavun, S., Levendusky, M. C., Resch, G. E., Veno, P. A., & Millington, W. R. (2006). Hemorrhage activates proopiomelanocortin neurons in the rat hypothalamus. *Brain Res*, 1070(1), 45-55. doi:10.1016/j.brainres.2005.11.076
- Holdgate, A., & Pollock, T. (2005). Nonsteroidal anti-inflammatory drugs (NSAIDs) versus opioids for acute renal colic. *The Cochrane database of systematic reviews*, 2004(2), CD004137-CD004137. doi:10.1002/14651858.CD004137.pub3
- Huang, R., Jiang, L., Cao, Y., Liu, H., Ping, M., Li, W., . . . Wang, X. (2019). Comparative Efficacy of Therapeutics for Chronic Cancer Pain: A Bayesian Network Meta-Analysis. *J Clin Oncol*, 37(20), 1742-1752. doi:10.1200/jco.18.01567

- Iyengar, S., Woller, S. A., Hommer, R., Beierlein, J., Wright, C. B., Tamiz, A. P., & Karp, B. I. (2020). Critical NIH Resources to Advance Therapies for Pain: Preclinical Screening Program and Phase II Human Clinical Trial Network. *Neurotherapeutics : the journal of the American Society for Experimental NeuroTherapeutics*, 17(3), 932-934. doi:10.1007/s13311-020-00918-2
- Izquierdo, I., & Netto, C. A. (1985). Role of beta-endorphin in behavioral regulation. *Ann N Y Acad Sci*, 444, 162-177. doi:10.1111/j.1749-6632.1985.tb37587.x
- Kingwell, K. (2019). Nav1.7 withholds its pain potential. *Nat Rev Drug Discov*. doi:10.1038/d41573-019-00065-0
- Krebs, E. E., Gravely, A., Nugent, S., Jensen, A. C., DeRonne, B., Goldsmith, E. S., . . . Noorbaloochi, S. (2018). Effect of Opioid vs Nonopioid Medications on Pain-Related Function in Patients With Chronic Back Pain or Hip or Knee Osteoarthritis Pain: The SPACE Randomized Clinical Trial. *JAMA*, 319(9), 872-882. doi:10.1001/jama.2018.0899
- Le Merrer, J., Becker, J. A., Befort, K., & Kieffer, B. L. (2009). Reward processing by the opioid system in the brain. *Physiol Rev*, 89(4), 1379-1412. doi:10.1152/physrev.00005.2009
- Liu, J., Garza, J. C., Truong, H. V., Henschel, J., Zhang, W., & Lu, X. Y. (2007). The melanocortinergic pathway is rapidly recruited by emotional stress and contributes to stress-induced anorexia and anxiety-like behavior. *Endocrinology*, 148(11), 5531-5540. doi:10.1210/en.2007-0745
- Manion, J., Waller, M. A., Clark, T., Massingham, J. N., & Neely, G. G. (2019). Developing Modern Pain Therapies. *Front Neurosci*, 13, 1370. doi:10.3389/fnins.2019.01370
- Markowitz, C. E., Berkowitz, K. M., Jaffe, S. B., & Wardlaw, S. L. (1992). Effect of opioid receptor antagonism on proopiomelanocortin peptide levels and gene expression in the hypothalamus. *Mol Cell Neurosci*, 3(3), 184-190. doi:10.1016/1044-7431(92)90037-3
- Matsumura, S., Eguchi, A., Okafuji, Y., Tatsu, S., Mizushige, T., Tsuzuki, S., . . . Fushiki, T. (2012). Dietary fat ingestion activates β -endorphin neurons in the hypothalamus. *FEBS Lett*, 586(8), 1231-1235. doi:10.1016/j.febslet.2012.03.028
- Matthias, M. S., Donaldson, M. T., Jensen, A. C., & Krebs, E. E. (2018). "I Was a Little Surprised": Qualitative Insights From Patients Enrolled in a 12-Month Trial Comparing Opioids With Nonopioid Medications for Chronic Musculoskeletal Pain. *J Pain*, 19(9), 1082-1090. doi:10.1016/j.jpain.2018.04.008
- Metz, M. J., Daimon, C. M., & Hentges, S. T. (2021). Reported Benefits of Low-Dose Naltrexone Appear to Be Independent of the Endogenous Opioid System Involving Proopiomelanocortin Neurons and β -Endorphin. *eNeuro*, 8(3). doi:10.1523/eneuro.0087-21.2021
- Metz, M. J., Pennock, R. L., Krapf, D., & Hentges, S. T. (2019). Temporal dependence of shifts in mu opioid receptor mobility at the cell surface after agonist binding observed by single-particle tracking. *Sci Rep*, 9(1), 7297. doi:10.1038/s41598-019-43657-x
- Misra, U. K., Kalita, J., Tripathi, G., & Bhoi, S. K. (2017). Role of β endorphin in pain relief following high rate repetitive transcranial magnetic stimulation in migraine. *Brain Stimul*, 10(3), 618-623. doi:10.1016/j.brs.2017.02.006
- Mohanty, D., & Lippmann, S. (2020). CGRP Inhibitors for Migraine. *Innovations in clinical neuroscience*, 17(4-6), 39-40. Retrieved from <https://pubmed.ncbi.nlm.nih.gov/32802591>
<https://www.ncbi.nlm.nih.gov/pmc/articles/PMC7413335/>

- Nalamachu, S. (2013). An overview of pain management: the clinical efficacy and value of treatment. *Am J Manag Care*, 19(14 Suppl), s261-266.
- Navratilova, E., & Porreca, F. (2014). Reward and motivation in pain and pain relief. *Nat Neurosci*, 17(10), 1304-1312. doi:10.1038/nn.3811
- Nijs, J., Kosek, E., Van Oosterwijck, J., & Meeus, M. (2012). Dysfunctional endogenous analgesia during exercise in patients with chronic pain: to exercise or not to exercise? *Pain Physician*, 15(3 Suppl), Es205-213.
- Olszewski, P. K., Wirth, M. M., Shaw, T. J., Grace, M. K., Billington, C. J., Giraudo, S. Q., & Levine, A. S. (2001). Role of alpha-MSH in the regulation of consummatory behavior: immunohistochemical evidence. *Am J Physiol Regul Integr Comp Physiol*, 281(2), R673-680. doi:10.1152/ajpregu.2001.281.2.R673
- Panigrahi, S. K., Meece, K., & Wardlaw, S. L. (2019). Effects of Naltrexone on Energy Balance and Hypothalamic Melanocortin Peptides in Male Mice Fed a High-Fat Diet. *J Endocr Soc*, 3(3), 590-601. doi:10.1210/js.2018-00379
- Pathan, S. A., Mitra, B., & Cameron, P. A. (2018). A Systematic Review and Meta-analysis Comparing the Efficacy of Nonsteroidal Anti-inflammatory Drugs, Opioids, and Paracetamol in the Treatment of Acute Renal Colic. *European Urology*, 73(4), 583-595. doi:https://doi.org/10.1016/j.eururo.2017.11.001
- Porreca, F., & Navratilova, E. (2017). Reward, motivation, and emotion of pain and its relief. *Pain*, 158 Suppl 1(Suppl 1), S43-s49. doi:10.1097/j.pain.0000000000000798
- Rodríguez, E. M., Blázquez, J. L., & Guerra, M. (2010). The design of barriers in the hypothalamus allows the median eminence and the arcuate nucleus to enjoy private milieus: the former opens to the portal blood and the latter to the cerebrospinal fluid. *Peptides*, 31(4), 757-776. doi:10.1016/j.peptides.2010.01.003
- Schüchen, R. H., Mücke, M., Marinova, M., Kravchenko, D., Häuser, W., Radbruch, L., & Conrad, R. (2018). Systematic review and meta-analysis on non-opioid analgesics in palliative medicine. *J Cachexia Sarcopenia Muscle*, 9(7), 1235-1254. doi:10.1002/jesm.12352
- Sobieraj, D. M., Martinez, B. K., Miao, B., Cicero, M. X., Kamin, R. A., Hernandez, A. V., . . . Baker, W. L. (2020). Comparative Effectiveness of Analgesics to Reduce Acute Pain in the Prehospital Setting. *Prehosp Emerg Care*, 24(2), 163-174. doi:10.1080/10903127.2019.1657213
- Stott, D. G., & Pleuvry, B. J. (1991). Relationship between analgesia and respiratory depression for mu opioid receptor agonists in mice. *Br J Anaesth*, 67(5), 603-607. doi:10.1093/bja/67.5.603
- Tempel, A., Gardner, E. L., & Zukin, R. S. (1984). Visualization of opiate receptor upregulation by light microscopy autoradiography. *Proc Natl Acad Sci U S A*, 81(12), 3893-3897. doi:10.1073/pnas.81.12.3893
- Unterwald, E. M., Anton, B., To, T., Lam, H., & Evans, C. J. (1998). Quantitative immunolocalization of mu opioid receptors: regulation by naltrexone. *Neuroscience*, 85(3), 897-905. doi:10.1016/s0306-4522(97)00659-3
- Unterwald, E. M., Rubinfeld, J. M., Imai, Y., Wang, J. B., Uhl, G. R., & Kreek, M. J. (1995). Chronic opioid antagonist administration upregulates mu opioid receptor binding without altering mu opioid receptor mRNA levels. *Brain Res Mol Brain Res*, 33(2), 351-355. doi:10.1016/0169-328x(95)00143-g

- Varga, A. G., Reid, B. T., Kieffer, B. L., & Levitt, E. S. (2020). Differential impact of two critical respiratory centres in opioid-induced respiratory depression in awake mice. *J Physiol*, 598(1), 189-205. doi:10.1113/jp278612
- Veening, J. G., Gerrits, P. O., & Barendregt, H. P. (2012). Volume transmission of beta-endorphin via the cerebrospinal fluid; a review. *Fluids Barriers CNS*, 9(1), 16. doi:10.1186/2045-8118-9-16
- Vowles, K. E., McEntee, M. L., Julnes, P. S., Frohe, T., Ney, J. P., & van der Goes, D. N. (2015). Rates of opioid misuse, abuse, and addiction in chronic pain: a systematic review and data synthesis. *Pain*, 156(4), 569-576. doi:10.1097/01.j.pain.0000460357.01998.fl
- Vuong, C., Van Uum, S. H., O'Dell, L. E., Lutfy, K., & Friedman, T. C. (2010). The effects of opioids and opioid analogs on animal and human endocrine systems. *Endocr Rev*, 31(1), 98-132. doi:10.1210/er.2009-0009
- Wan, R. Q., Wiegant, V. M., de Jong, W., & de Wied, D. (1996). Alterations of beta-endorphin-like immunoreactivity in CSF following behavioral training using a passive avoidance procedure. *Psychoneuroendocrinology*, 21(6), 503-513. doi:10.1016/s0306-4530(96)00013-3
- Woo, M. (2020). A new generation of headache drugs. *Nat Outlook*, 586, S4-S6. doi:10.1038/d41586-020-02862-9
- Wu, Q., Lemus, M. B., Stark, R., Bayliss, J. A., Reichenbach, A., Lockie, S. H., & Andrews, Z. B. (2014). The temporal pattern of cfos activation in hypothalamic, cortical, and brainstem nuclei in response to fasting and refeeding in male mice. *Endocrinology*, 155(3), 840-853. doi:10.1210/en.2013-1831
- Xu, Q., & Yaksh, T. L. (2011). A brief comparison of the pathophysiology of inflammatory versus neuropathic pain. *Current opinion in anaesthesiology*, 24(4), 400-407. doi:10.1097/ACO.0b013e32834871df
- Yonehara, N., Kudo, T., Iwatsubo, K., Maeda, S., Saito, K., & Inoki, R. (1983). A possible involvement of the central endorphin system in the autoanalgesia induced by chronic administration of Freund's adjuvant solution in rats. *Pain*, 17(1), 91-98. doi:10.1016/0304-3959(83)90131-8

APPENDIX

Supplementary information for: Temporal dependence of shifts in mu opioid receptor mobility at the cell surface after agonist binding observed by single-particle tracking (Metz et al., 2019)

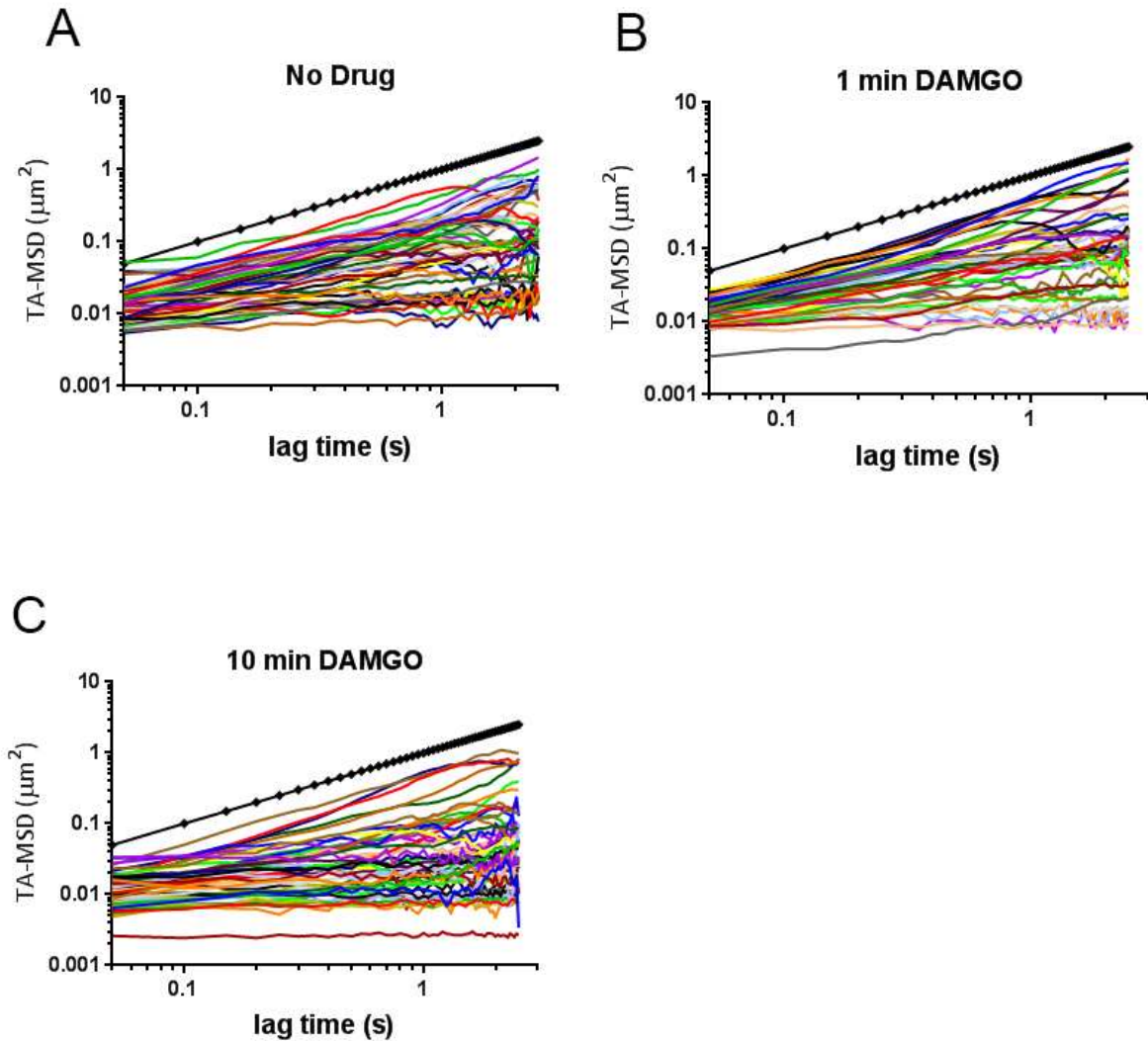


Figure 21. Individual MSDs of randomly chosen trajectories. Log-log plots of time averaged MSDs from individual tracks in the **A)** no drug, **B)** 1 min DAMGO, and **C)** 10 min DAMGO experimental conditions. Most trajectories are subdiffusive, as they lie below the slope of a simulated track of $\alpha = 1$ (black dotted line).

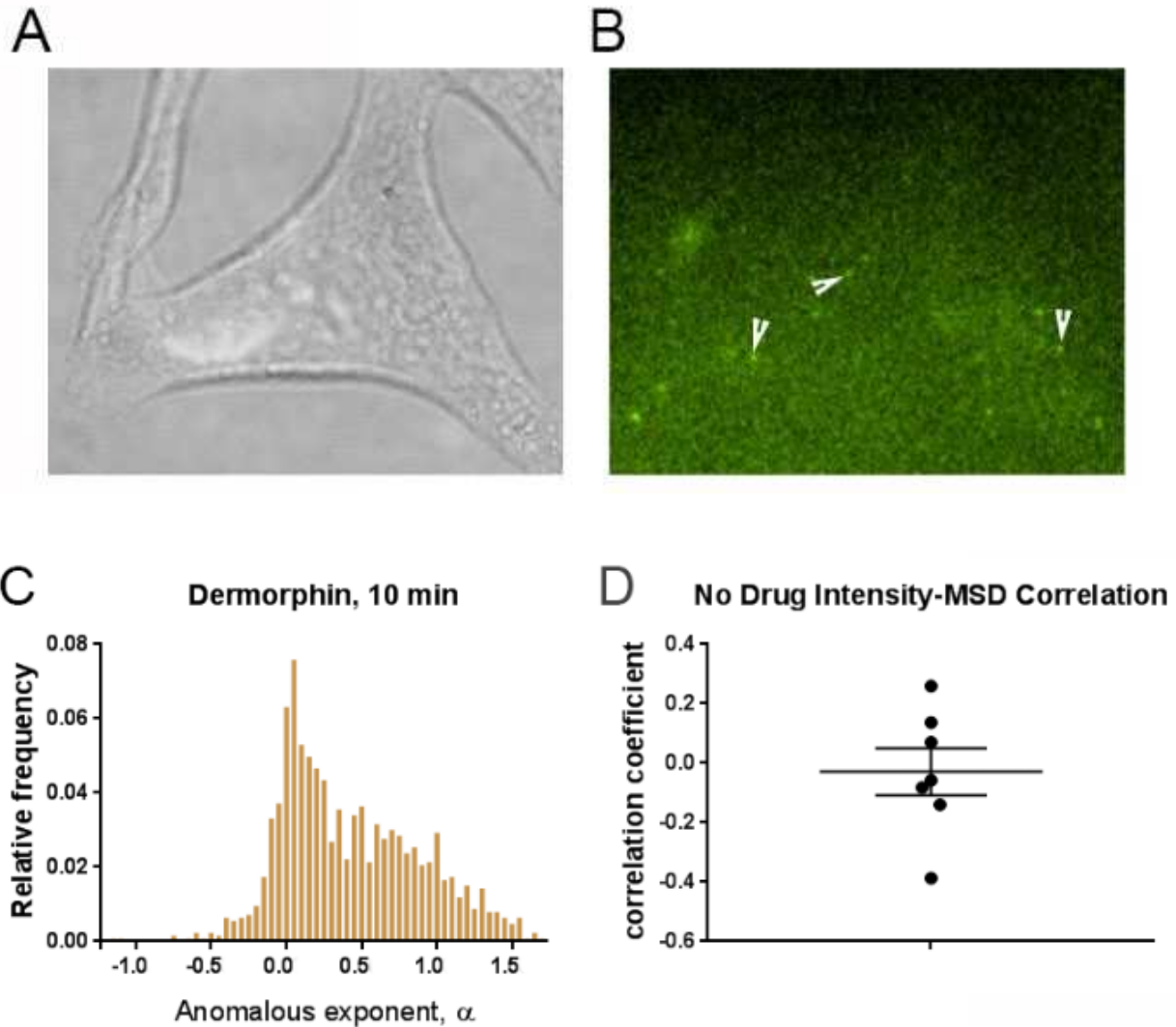
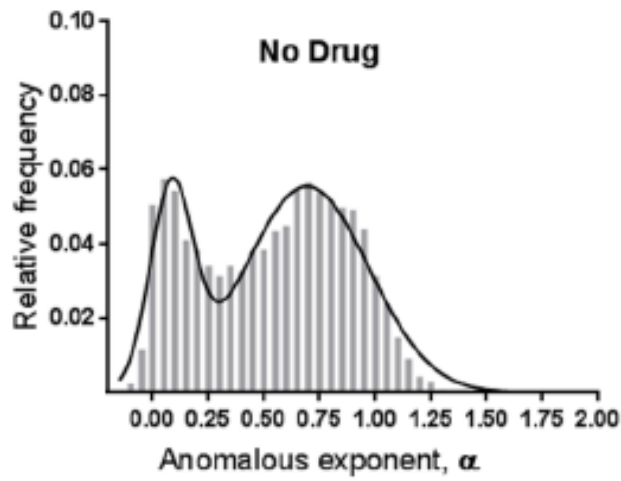
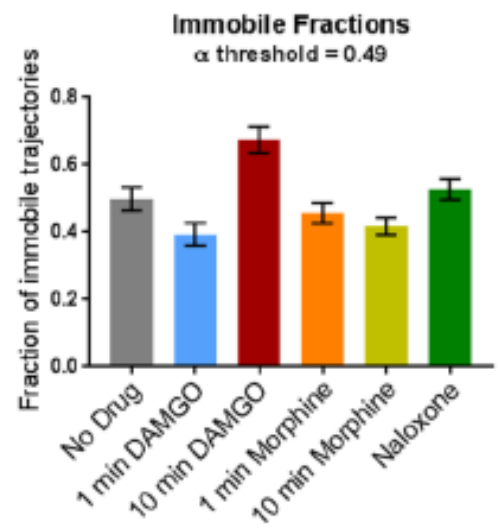
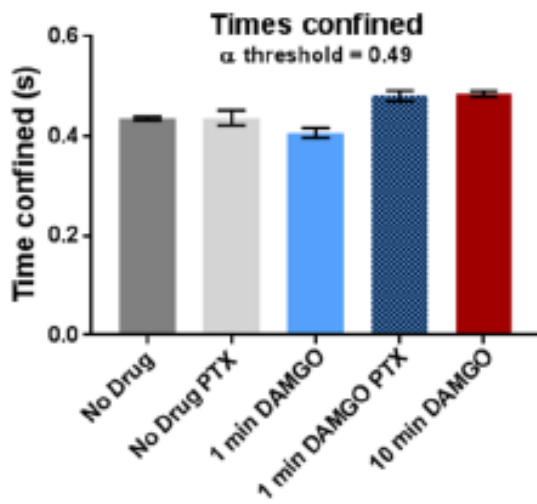
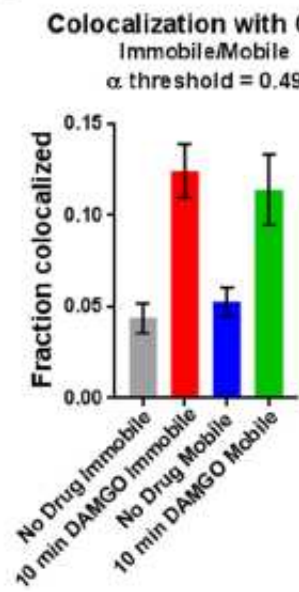


Figure 22. Single particle tracking after 10 min of Dermorphin-488 (60 pM) application reveals that the immobile population of MORs is not due to antibody-mediated crosslinking or Qdot hindering of mobility. A. DIC image of an AtT20 cell labeled with Dermorphin-488. B) The same cell is shown under fluorescence, and arrows indicate MORs labeled with a single Dermorphin-488 conjugate. C) Distribution of α values after tracking of MOR-Dermorphin-488 conjugates ($n = 5$ cells, 1266 tracks) incubated for 10 min in the presence of 60 pM Dermorphin-488. The distribution of α values is similar to those observed with Qdot tracking, and the fraction of $\alpha < 0.27$ is 0.44 ± 0.08 , similar to MOR-Qdots in the 10 min DAMGO condition (0.45 ± 0.12). Values below 0 are likely due to errors made during tracking caused by the low signal to noise ratio with this labeling approach. D) Distribution of MSD vs. fluorescence intensity correlation coefficients for individual cells in the no drug condition, with a mean correlation coefficient of -0.03 ± 0.08 .

A**B****C****D**

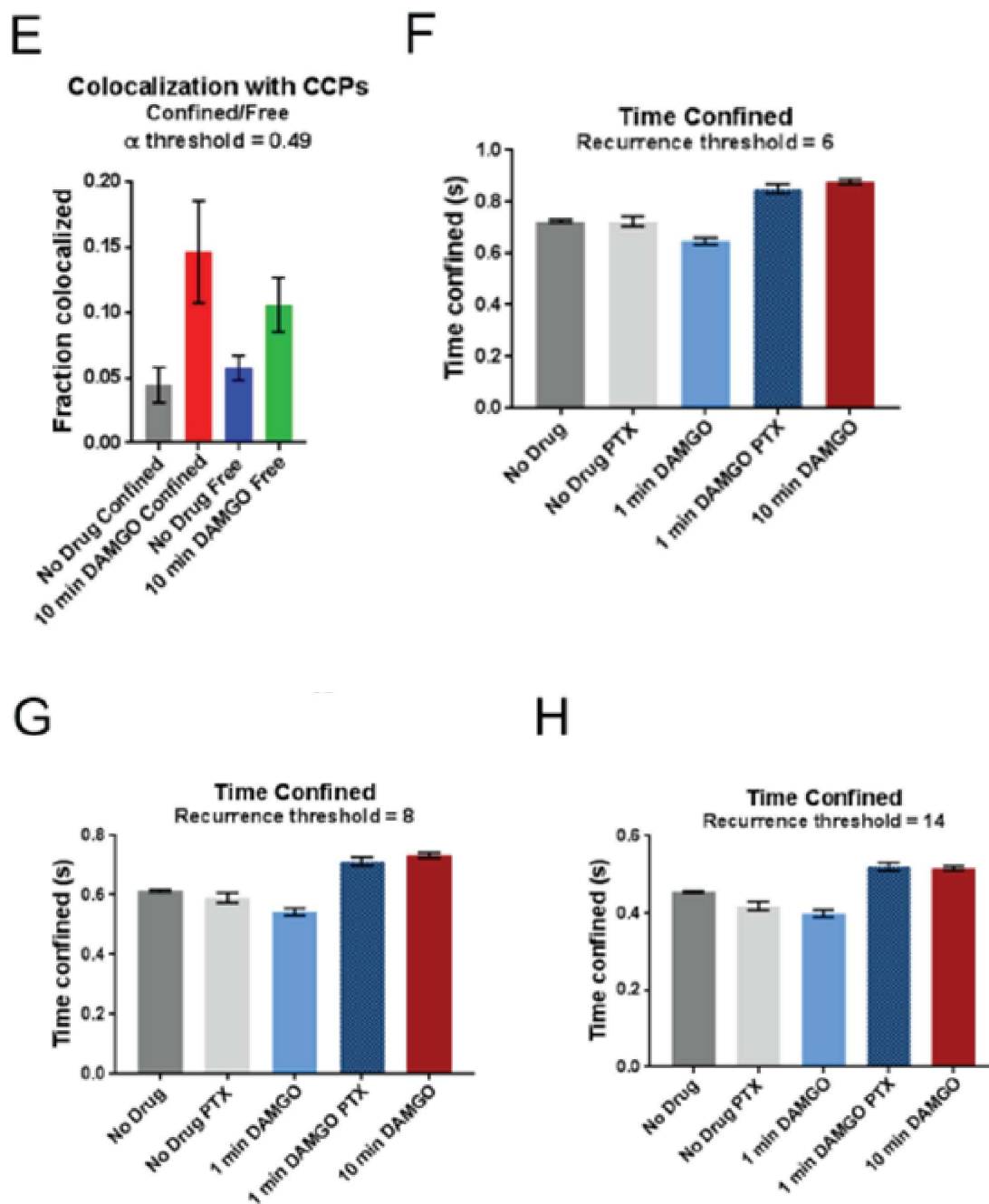


Figure 23. Reported results are robust to changes in mobile/immobile and confined/free thresholds. A) Two Gaussian fitting results in a threshold near our chosen threshold of $\alpha = 0.27$. B) The pattern for fraction of immobile trajectories does not change when using the threshold of $\alpha = 0.49$ determined using k-means for most experimental conditions, with the exception of 10 min Morphine. C) The pattern of confined times does not change at an $\alpha = 0.49$ threshold. D) The pattern of colocalization with CCPs does not change when comparing immobile and mobile trajectories or E) confined and free trajectories. F) Changing the recurrence threshold during recurrence analysis does not change the time confined when the recurrence threshold is 6, G) 8, H) or 14.

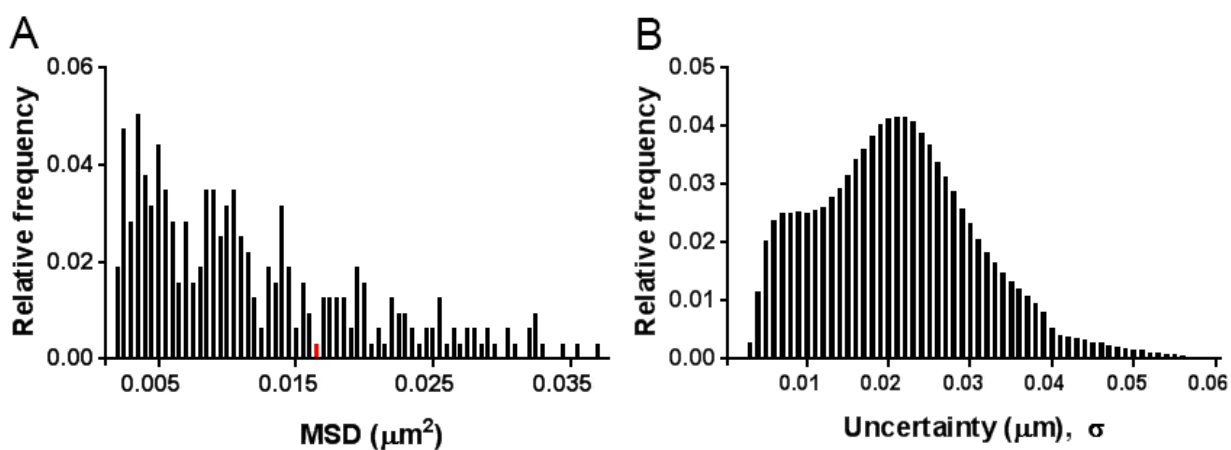


Figure 24. Data for trajectory corrections. **A)** Frequency histogram of MSD for glass-stuck Qdot-655 tracked without cells on the coverslip. The cutoff of 0.0165 μm^2 is highlighted in red. Most MSDs are less than this cutoff. **B)** Histogram of localization uncertainties, σ , for each detected particle of a representative subset in the no drug condition. An average σ of 0.02 μm was used for uncertainty correction of tracks.